The Dissertation Committee for Daniel Allen Mitchell
certifies that this is the approved version of the following dissertation:

Computational Methods for Stochastic Control Problems with Applications in Finance

Committee:

Kumar Muthuraman, Supervisor

Svetlana Boyarchenko

Patrick Brockett

Rafael Mendoza-Arriaga

Sheridan Titman

Efstathios Tompaidis

Computational Methods for Stochastic Control Problems with Applications in Finance

by

Daniel Allen Mitchell, B.S.Math.; M.S.I.R.O.M.; M.S.

DISSERTATION

Presented to the Faculty of the Graduate School of

The University of Texas at Austin

in Partial Fulfillment

of the Requirements

for the Degree of

DOCTOR OF PHILOSOPHY

THE UNIVERSITY OF TEXAS AT AUSTIN

May 2014

Dedicated to the years 2003-2014.

Acknowledgments

I would firstly like to thank my family for supporting me throughout my academic career, especially my wife Lauren who knows first hand the difficulties of pursuing a PhD. She has been a constant source of support during my time in graduate school and has encouraged me to work as hard as she does. My parents, Ann and Don, have also been a great source of support even when they were never quite sure what I was actually doing.

I am extremely thankful for the guidance my advisor, Dr. Kumar Muthuraman, has given me along my path through graduate school. Not only has he helped me write better papers, he has also taught me what it truly means to be an academic. His support has been essential to my success and I hope to count him as a collaborator and friend for many years to come.

I extend a special thanks to Dr. Stathis Tompaidis and Dr. Rafael Mendoza-Arriaga who have acted as co-mentors during my time at the University of Texas. They have each approached me for collaborations which have served to make me a much more well-rounded researcher.

I would also like to thank Dr. Svetlana Boyarchenko, Dr. Patrick Brockett and Dr. Sheridan Titman who have graciously agreed to serve on my dissertation committee and have given me great feedback on my work. I would like to thank my co-authors who are not on my dissertation committee, Dr.

Jonathan Goodman and Dr. Haolin Feng, who have been very helpful with their input and feedback on our joint work.

Last, but certainly not least, I thank my fellow PhD students at McCombs who have been great sources of ideas and friendship for the past five years. Our periodic happy hours have been great for getting to know each other and taking short breaks from the otherwise hectic life of doctoral candidacy.

Computational Methods for Stochastic Control Problems with Applications in Finance

Publication No. _____

Daniel Allen Mitchell, Ph.D.
The University of Texas at Austin, 2014

Supervisor: Kumar Muthuraman

Stochastic control is a broad tool with applications in several areas of academic interest. The financial literature is full of examples of decisions made under uncertainty and stochastic control is a natural framework to deal with these problems. Problems such as optimal trading, option pricing and economic policy all fall under the purview of stochastic control. These problems often face nonlinearities that make analytical solutions infeasible and thus numerical methods must be employed to find approximate solutions. In this dissertation three types of stochastic control formulations are used to model applications in finance and numerical methods are developed to solve the resulting nonlinear problems. To begin with, optimal stopping is applied to option pricing. Next, impulse control is used to study the problem of interest rate control faced by a nation's central bank, and finally a new type of hybrid control is developed and applied to an investment decision faced by money managers.

Table of Contents

List of Tables

List of Figures

Chapter 1

Introduction

This dissertation focuses on developing numerical methods to solve stochastic optimal control problems, specifically applied to three problems related to finance. Firstly, we consider the problem of finding optimal exercise policies for American options, both under constant and stochastic volatility settings. Rather than work with the usual equations that characterize the price exclusively, we derive and use boundary evolution equations that characterize the evolution of the optimal exercise boundary. Using these boundary evolution equations we show how one can construct very efficient computational methods for pricing American options that avoid common sources of error. Finally we compare runtime and accuracy to other popular numerical methods. The ideas and methodology presented herein can easily be extended to other optimal stopping problems. This work was completed together with Jonathan Goodman and Kumar Muthuraman and a version is forthcoming in Mitchell et al. (2014b).

Next, we examine the effect that a central bank's interventions have on longer term interest rate securities by examining a stochastic short rate process that can be controlled by the central bank. Rather than investigate the

motivations for the intervention, we assume that the bank is able to quantify its preferences and tolerances for various rates. We allow for a very general class of stochastic processes for the short rate and most of the popular models in literature fall within this class. Interventions are best modeled as Impulse controls which are very difficult to handle, even computationally, except in very special cases. Allowing interventions to be modeled by Impulse controls, we develop a computational method and provide relevant convergence results. We also derive error bounds for intermediate iterations. Using this method we solve for the central bank's optimal control policy and also study the effect of this on longer term interest rate securities using a change of measure. The method developed here can easily be applied to a very wide range of impulse control problems beyond the realm of interest rate models. This work was completed together with Haolin Feng and Kumar Muthuraman and a version is forthcoming in Mitchell et al. (2014a).

Finally we study the problem of hedge fund contracts, which are generally characterized by a flat fee, a performance fee and what are known as high-water-mark provisions. We describe and characterize these contract features and analyzes how they influence the hedge fund's risk choices. We model the hedge fund's portfolio choice as a stochastic control problem with hybrid discrete and continuous controls. We develop a computational method to solve this widely applicable class of problems and prove its convergence. This work was completed together with Kumar Muthuraman and Sheridan Titman.

Chapter 2

Boundary Evolution Equations for American Options

2.1 Introduction

This chapter develops numerical methods to solve the optimal stopping problem associated with pricing American style options. American options provide the holder the right (but not the obligation) to trade an underlying asset for a specified strike price anytime before a specified expiry time. Pricing and finding the optimal exercise policy, which is known to be a surface that partitions the domain into exercise and hold regions, are interrelated and are solved for by transforming them to differential equation problems. The resulting differential equation, along with boundary conditions, formulate a free-boundary problem and characterize the price of the option. An accurate computation of the solution to the free-boundary problem relies on an accurate representation of the boundary and an accurate treatment of its dynamics. Rather than work with the equation that characterizes the price evolution of an American security exclusively, one could potentially derive and use the equations that characterize the evolution of the free-boundary for computational purposes. This however has not been seen as a valuable method because the boundary evolution equation also depends implicitly on the price, which

seemed to be challenging to handle efficiently.

In this paper we consider American options, in the Black-Scholes setting and in a stochastic volatility setting, and derive boundary evolution equations. We show how one can construct computational procedures that efficiently utilize these evolution equations to compute both the price and the optimal exercise policy of American options. The evolution equations tell us exactly how fast the exercise boundary should move in time. This speed is dependent on both the current level of the boundary and a mixed derivative of the price function at the boundary, resulting in a system of differential equations. By solving these equations simultaneously we can track both the optimal exercise policy and the price function.

A challenge in constructing a boundary evolution equation based computational procedure, apart from that posed by the implicit dependence of the equation on the price, is in taming the errors that arise from having to choose amongst points on a predefined grid to represent the boundary. Hence, we first construct a computational procedure that works on the standard rectangular cartesian grid by allowing a boundary to float between grid points. Though the performance of this first step is very encouraging, one could potentially eliminate any error due to the grid and boundary mismatch by allowing the grid to adapt to the boundary rather than pre-define it. To this extent we next construct an improved methodology that dynamically builds a non-linear grid while solving the boundary evolution equations. Such a dynamic evolution while being a relatively complicated implementation, performs significantly

better and becomes essential under stochastic volatility. For cases where an integral representation of the option price is available, as is the case for the Black-Scholes model, we could potentially use the representation for further efficiency in solving the boundary evolution equation. We demonstrate how this can be done too for the Black-Scholes case. We also provide numerical evidence that the methods constructed in this paper are faster and more accurate than other relevant numerical methods. More work could potentially be done to extend this to existing integral representations of American options with stochastic volatility.

The primary objective of the paper is to show that it is possible to construct efficient numerical methods that take advantage of boundary evolution equations to avoid common sources of error. The expressions for the dynamics of the boundary in the Black-Scholes setting was found in van Moerbeke (1975) then rediscovered, independently, in Goodman and Ostrov (2002), and they were extended to some multi-factor models in Hayes (2006). The corresponding equations for the stochastic volatility case have been derived in this paper. American option pricing is probably the most popular example amongst a larger class of very similar problems known as optimal stopping problems. Although this paper focuses exclusively on American options, the arguments for deriving the boundary evolution equations and the computational methods that solve these equations can readily be extended to other optimal stopping problems.

In Section 2.2 we consider the classical Black-Scholes setting of con-

stant volatility and present three methods which leverage on the boundary equation. We then compare these methods to other numerical methods and find that all three methods constructed perform better. Section 2.3 considers the stochastic volatility case with a setting that is general enough to encompass several popular stochastic volatility models. For numerical comparisons, we only consider the most popular Heston model and describe the dynamic grid based method in this context. We then compare the method to other existing numerical methods and find improved performance. A version of this work is forthcoming in Mitchell et al. (2014b).

2.1.1 Background and Previous Literature

A put option is a contingent claim that gives the owner the right, but not the obligation, to sell a share of stock (or any other asset) at a pre-specified price. Throughout the paper we restrict discussion to the put option only because almost the same arguments and equations will hold for the call option, wherein the owner has the right to buy a share of stock at a pre-specified price. Put options come in two main flavors, "European," where the owner can only exercise this right at one pre-specified time (expiration), and "American," where the owner can exercise this right anytime before expiration. When valuing an American put option the crucial step is to find the optimal early exercise boundary, which indicates the circumstances under which the option should be exercised before it expires. While a closed form solution for the value of a European option with constant volatility was found in the classical paper

Black and Scholes (1973) and for one particular stochastic volatility model in the paper in Heston (1993), there is no known closed form solution for the value of an American option with constant or stochastic volatility.

For constant volatility there are two main classes of numerical methods that approximate the price of American options. The first class computes the expected value of the American's payoff under the risk neutral measure. This class usually consists of Monte Carlo and binomial methods, and these methods only find the price of the option for one particular price and time to expiration and are typically unable to compute the early exercise boundary efficiently. The second class rephrases the expected value as the solution to a free-boundary partial differential equation, and methods in this class find the entire pricing function and the early exercise boundary. It can be difficult to compare methods in different classes because PDE methods give much more information than the first class.

The most well known numerical method for solving the free-boundary problem was developed in Brennan and Schwartz (1977) but there have been several numerical methods developed since then. Muthuraman (2008) uses an iterative method to convert the free-boundary problem into a sequence of fixed boundary problems. Also Goodman and Ostrov (2002) find a differential equation that governs the early exercise boundary, which will be used heavily in this paper, and use it to derive a short time asymptotic expansion of the boundary.

There are other methods that do not solve the free-boundary problem;

rather they evaluate the risk neutral expected value of the option's payoff. Two common methods in practice that solve this problem are the binomial and trinomial tree methods. The binomial method was first seen in Cox et al. (1979). Also, there has been much success in solving this problem using Monte-Carlo simulation, most notably in Tilley (1993), Broadie and Glasserman (1997) and Longstaff and Schwartz (2001). Other methods that solve this problem partition the price as a European option's price plus an early exercise premium which results in an integral equation (Kim (1990); Jacka (1991); Carr et al. (1992)).

Recently there has been some work that exploits asymptotic analysis of the early exercise boundary to find approximate closed form solutions to the American option problem in the Black-Scholes setting. In Bunch and Johnson (2002) the authors find an implicit equation that can approximate the boundary at any time and then use numerical integration to find the price of the option. In Stamicar et al. (1999) the authors find an approximate explicit formula for the early exercise boundary. In Chen and Chadam (2007) the authors provide a detailed mathematical analysis of the early exercise boundary and provide an implicit ODE that governs the boundary. Evans et al. (2002) provides results for American options on dividend paying stocks. A more comprehensive comparison of numerical methods can be found in AitSahlia and Carr (1997).

In the years since the seminal work of Black and Scholes there have been many empirical studies that suggest that simple Geometric Brownian Motion

does not capture enough of the dynamics of a stock price to give an accurate price for derivative securities. As a result people have studied the case when the volatility of the stock follows a stochastic process. There have been several models that incorporate this but most work has focused on European options. As in the Black-Scholes setting, there is no known closed form solution for American options under any model.

Despite the vast research in American options with constant volatility there has been relatively less work exploring stochastic volatility. While some of the methods mentioned above can be extended to handle stochastic volatility, namely the PDE and Monte-Carlo methods, there are also many methods that cannot handle stochastic volatility. Given the limitations of the above methods there has been some work looking for fast methods to price American options with stochastic volatility, including the multigrid method in Clarke and Parrott (1999) and a moving boundary method in Chockalingam and Muthuraman (2011). Ikonen and Toivanen (2007) uses a componentwise splitting method to create three simple linear complementarity problems which they solve using the Brennan-Schwartz method. Also Wilmott (1998) describes how to use projected successive over relaxation (PSOR) to solve the free-boundary problem. In Detemple and Tian (2002) the authors present an integral representation for American options with stochastic volatility and interest rates that can be recursively solved to find the early exercise boundary. Broadie et al. (2000) uses non-parametric techniques to investigate properties of the early exercise boundary under stochastic dividends and volatility. In

Ikonen and Toivanen (2008) the authors present a more exhaustive review of other computational methods for American options with stochastic volatility.

2.2 Constant Volatility

In this section we generalize a boundary evolution equation, for the Black-Scholes setting, found in Goodman and Ostrov (2002) to a more general setting than non-dividend paying stocks that includes assets such as futures, dividend paying stocks and options on foreign currency. We then develop three numerical methods that leverage on the boundary evolution equation to obtain fast and accurate approximations of the price of an American option with constant volatility. For the rest of the paper we use the notation of Karatzas and Shreve (1998).

2.2.1 The Boundary Equation

We start with the classical Black-Scholes partial differential equation for valuing an American put option, $p(x, \tau)$, where x is the price of the underlying asset and τ is the time until expiry. An American put option can be exercised at any time before it expires with payoff of $q - x$, where q is the strike price of the option. This suggests that we should partition the domain into two distinct regions separated by the early exercise boundary, $c(\tau)$. If at time τ, $x \leq c(\tau)$ the option should be exercised immediately with a payoff of $q-x$, and if $x > c(\tau)$ the option should be held. The optimal choice of $c(\tau)$ is decided by comparing the intrinsic value of the option to its tradable value; if it is

worth more on the open market than its intrinsic value, then it should not be exercised. In the constant volatility case if $x > c(\tau)$ then $p(x, \tau)$ is governed by the classical Black-Scholes PDE,

$$\frac{\partial p}{\partial \tau} = \tfrac{1}{2}\sigma^2 x^2 \frac{\partial^2 p}{\partial x^2} + bx\frac{\partial p}{\partial x} - rp. \tag{2.1}$$

Here r is the risk-free interest rate, σ is the volatility of the underlying asset and b is the instantaneous cost of carrying the underlying asset, as in Huang et al. (1996). Using this notation for b allows us to price several financial instruments. For example, for non-dividend paying stocks, $b = r$; for stocks with constant dividend yield δ, $b = r - \delta$; for futures, $b = 0$; and for options on foreign currency with foreign risk-free rate r_f, $b = r - r_f$.

We know that at $\tau = 0$ the option expires, thus it must be exercised or abandoned and therefore $c(0) = q$, if $b \geq 0$, otherwise $c(0) = \frac{r}{r-b}q$. The last thing we need to know about this option is the smooth pasting condition, which states that on the boundary p must be differentiable as shown in Merton (1992). With this information we can establish initial and boundary conditions for p; which are

$$\begin{aligned} p(x,0) &= \max(q - x, 0), \\ p(c(\tau),\tau) &= q - c(\tau), && (2.2) \\ \tfrac{\partial p(c(\tau),\tau)}{\partial x} &= -1. \quad \text{and} && (2.3) \\ \lim_{x\to\infty} p(x,\tau) &= 0 && (2.4) \end{aligned}$$

Equation (2.4) implies that

$$\lim_{x\to\infty} \frac{\partial p}{\partial x} = 0, \tag{2.5}$$

because p is convex and decreasing, as seen in Karatzas and Shreve (1998). It is more convenient, numerically, to use Equation (2.5) as a boundary condition for large x, so we will not use Equation (2.4) in numerical experiments.

Now that we have the boundary conditions we would like a differential equation that governs $c(\tau)$. We find this using higher order derivatives that are continuous up to the early exercise boundary from the continuation region, but not across into the exercise region (see, for example, Lawrence and Salsa (2009) for a proof of this in several multi-asset cases). We use these expressions to treat the price and boundary as a coupled system to be solved simultaneously.

Theorem 2.1. The differential equation that governs $c(\tau)$ is

$$\frac{\partial c(\tau)}{\partial \tau} = -\frac{\partial^2 p(c(\tau), \tau)}{\partial x \partial \tau} \frac{\sigma^2 c^2(\tau)}{2qr - 2(r-b)c(\tau)}. \tag{2.6}$$

The proof can be found in the appendix.

Even with this equation, finding the price of the American put is still a hard problem. We see in Equation (2.6) that the boundary's evolution depends on both a mixed derivative of the price function and the current boundary level, which creates a system of non-linear differential equations. The price of the put option depends on the boundary and the boundary depends on the price of the put. In order to solve these equations we must find a way to evolve them simultaneously.

Figure 2.1 shows the state space partitioned into the exercise region and the continuation region. The two regions are separated by the early exercise

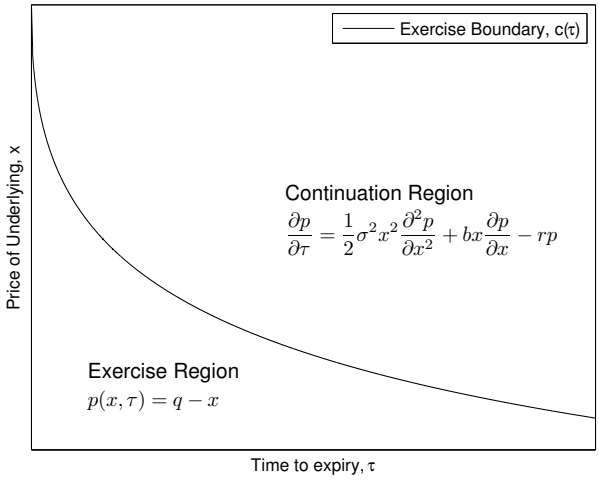

Figure 2.1: Partitioned State Space

boundary. In the exercise region the price of the put is equal to its intrinsic value. In the continuation region the price of the put is governed by Equation (2.1).

2.2.2 Numerical Method on a Static Grid

This section constructs a numerical method that uses Equation (2.6) to compute the early exercise boundary and the price function of an American put option. The basic idea is to step forward in time to expiry discretely, evolving p and c at each step using finite difference approximations to Equations (2.1) and (2.6). In this process several intricacies need to be addressed so we describe the algorithm with a three step iterative procedure.

Step 1: Initialize p and c at a small time before expiration

To begin evolution using Equations (2.1) and (2.6) we need an initial value of p and c. We know that at $\tau = 0$ the boundary is located at $c(0) = \min(q, \frac{r}{r-b}q)$, and at every value of x such that $x \geq q$ we have $p(x, 0) = 0$. In this numerical method we only consider the domain where $x \geq c(\tau)$ because when $x > c(\tau)$ we know that p is governed by Equation (2.1) and when $x = c(\tau)$, p must obey the boundary conditions so any value of $x < c(\tau)$ cannot be used. Using this information as an initial value we will see that all finite difference approximations to derivatives in the x variable will be zero if $b \geq 0$. This happens because we do not consider the domain such that $x < c(0)$, the only place where $p(x, 0) \neq 0$, so any place that we calculate a derivative in x will result in a linear combination of zeros, which is zero. For example, if $q = 100$ and $b > 0$ then $c(0) = q$. Now if we try to approximate the derivative of p at $x = 101$, using a finite difference approximation, we will find that $p(101 + \Delta x, 0) = p(101 - \Delta x, 0) = 0$, and $\frac{\partial p}{\partial x} \approx \frac{p(101+\Delta x,0)-p(101-\Delta x,0)}{2\Delta x} = \frac{0-0}{2\Delta x} = 0$.

This fact together with Equation (2.1) tells us also that the numerical approximation of $\frac{\partial p}{\partial \tau}$ must also be zero. This means the price of the put cannot change in one step, and thus the location of the boundary cannot change in one step, if we start with the initial data at $\tau = 0$. If they do not move in the first step then they will not move in any subsequent step and the price of the put will stay at zero for all times to expiry, which is clearly incorrect. However, if $b < 0$ we do not have a problem.

In order to overcome this problem we approximate the put, at a short

time before expiration, as a European option, as in Broadie and Detemple (1996), and with this we can take advantage of the closed form Black-Scholes equation for European options. On a discrete set of equally spaced grid points in x between zero and some $\hat{x}$, where $\hat{x}$ is the maximal value in the computational domain, we find the value of a European put, $f(x, \tau_o)$, a short time before expiration, τ_o. The choice of $\hat{x}$ is not entirely trivial here, we need to pick $\hat{x}$ so that Equation (2.5) is approximately true for all times to expiry that we consider. Since f is a European option it must satisfy $f(x, \tau_o) = qe^{-r\tau_o}N(-d_2) - xe^{-(r-b)\tau_o}N(-d_1)$, where $d_1 = \frac{\log(x/q)+(b+\frac{1}{2}\sigma^2)\tau_o}{\sigma\sqrt{\tau_o}}$ and $d_2 = d_1 - \sigma\sqrt{\tau_o}$. Here N is the standard normal cumulative distribution function. We initialize p for a short time as $p(x, \tau_o) = \max(f(x, \tau_o), q - x)$.

In order to find the initial value for the boundary, $c(\tau_o)$, we use a binary search to find the place where $f(x, \tau_o)$ intersects the line $q - x$. Here we will almost certainly find that $c(\tau_o)$ is not located at one of the grid points chosen above, but this is not a problem; we will evolve p on the fixed grid and let c move between the grid points.

In Figure 2.2 we illustrate how to initialize p and c. In the figure the dashed line represents the intrinsic value of the put and the solid line represents the value of a European option. We say that to the left of the intersection the American is equal to the dashed line, to the right of the intersection the American is equal to the solid line and the boundary is located at the intersection of the two lines. However we only work in the domain such that $x \geq c(\tau)$ so we only need the location of the intersection and the solid line

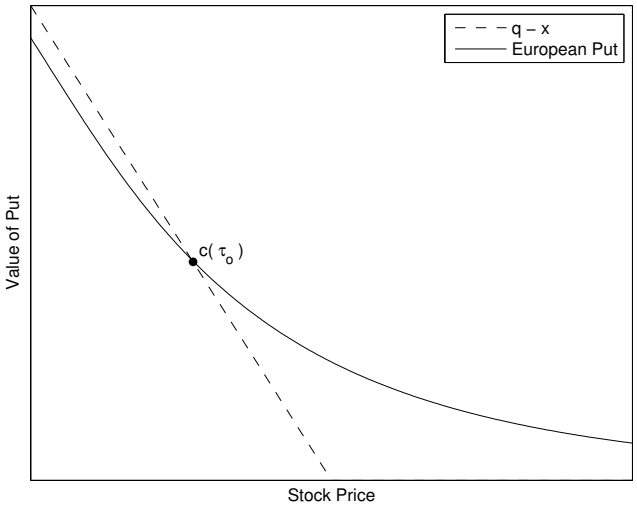

Figure 2.2: Initialization of $p(x, \tau_o)$ and $c(\tau_o)$

to the right for initialization. Figure 2.2 exaggerates the initialization procedure for illustrative purposes. In the numerical experiments we run in Section 2.2.5 we find that the slope of the European option at the initial approximate boundary ranges between -0.999 and -0.975 when we initialize at half a trading day before expiration, $\tau_0 = \frac{1}{2}\frac{1}{252}$.

Step 2: Evolve p one step in time to expiry and approximate the mixed derivative

The next step is to evolve p one step backwards in time, holding $c(\tau)$ fixed. This, however, presents a problem because the values of p are not exactly uniform and we want to use a finite difference method. The grid points where we know p are uniformly spaced, but we also know the value of p at the

boundary, which does not fit on this uniform spacing. In order to use a finite difference method we need to approximate all derivatives using the value of the price function at discrete grid points. For most of the grid points we can use standard central difference methods however at the first grid point to the right of the boundary, call this point x_0, we cannot use these standard central difference formulae. To find the derivatives of p at x_0 we use Taylor series expansion to derive non-central finite difference approximations involving x_0, $x_0 + h$ and $x_0 - h_2$.

Here h_2 is the distance between x_0 and $c(\tau)$, and $p(x_0 - h_2) = q - c(\tau)$ because $x_0 - h_2 = c(\tau)$. One advantage of using this method to compute the derivatives of p at x_0 is that we can insert these equations directly into any discrete time stepping finite difference algorithm, like the Crank-Nicolson algorithm(Crank and Nicolson (1947)), which we use.

In the evolution of p we do not need to calculate any derivatives at $c(\tau)$ or $\hat{x}$ because we can use Equations (2.2) and (2.5) as boundary conditions. Equation (2.2) means that in one time step the value of the put at $c(\tau)$ does not change. Equation (2.5) means that the value of the put at $\hat{x}$ is equal to the value of the put at the grid point just before $\hat{x}$. Both of these boundary conditions can easily be satisfied implicitly using the Crank-Nicolson algorithm.

After we evolve p we need to approximate the x derivative of the price function at the early exercise boundary so that we can use it to calculate $\frac{\partial^2 p(c(\tau),\tau)}{\partial x \partial \tau}$. In order to calculate this derivative we need to use the location of

the boundary, $c(\tau)$, the value of the put at the boundary, $q - c(\tau)$, and a few grid points to the right of the boundary. In this calculation we cannot simply use standard one sided finite difference formulae because the boundary is not located at a grid point. This means that the places where we know the value of the put to the right of the boundary are not equally spaced; if the distance between grid points is h then the space between the boundary and the first grid point to the right of the boundary must be less than h. To overcome this problem we fit a spline through the boundary and a few grid points to the right of the boundary. Using the coefficients of this spline we can analytically approximate the derivative of the price function at the boundary.

With this value for the x derivative we can approximate $\frac{\partial^2 p(c(\tau),\tau)}{\partial x \partial \tau}$ using a first order finite difference method in time. If we say the value of the x derivative at the boundary before we evolved p is $p_x^{\text{old}} = -1$ and the value after we evolved p is p_x^{new} then $\frac{\partial^2 p(c(\tau),\tau)}{\partial x \partial \tau} \approx \frac{p_x^{\text{new}}+1}{\Delta \tau}$, where $\Delta \tau$ is the step size in time to expiry.

Step 3: Evolve c one step in time to expiry

Now that we have evolved p and calculated the mixed derivative at the boundary we need to evolve $c(\tau)$ one step in time to expiry to catch up with p. For this we hold $\frac{\partial^2 p(c(\tau),\tau)}{\partial x \partial \tau}$ fixed and use Equation (2.6) and an explicit Runge-Kutta method to evolve c, we use the second order Runge-Kutta method in numerical experiments; see Iserles (2008) for details on Runge-Kutta methods.

There is one last problem we face: what happens when the boundary

crosses from one side of a grid point to the other? For example, if at time τ, $c(\tau)$ is located between the 99^{th} and 100^{th} grid points and at time $\tau + \Delta\tau$, $c(\tau)$ is located between the 98^{th} and 99^{th} grid points, what do we do? Here there are a few options as well. In Chen et al. (1997) the authors suggest using a spline to interpolate the value of p, however we find that simply leaving p at this point as its intrinsic value, $q - x$, does not lead to any significant reduction in accuracy, and thus using a spline is not worth the added complexity. We then repeat steps **2** and **3** until we reach the desired time before expiration.

2.2.3 Numerical Method on a Dynamic Grid

In the previous section we allowed the optimal early exercise boundary to move between fixed grid points in the computational domain, however this can lead to some error when the boundary is very close to the next grid point and h_2 is very small when compared to h. In order to overcome this error we use numerical grid generation to force the grid points to conform to the boundary at every time step by using a change of variables. This forces the grid points we use, to approximate p, to move over time, and the space between the boundary and the closest grid point remains a constant. This has the advantage of allowing us to use standard high-order finite difference approximations when calculating the mixed derivative at the boundary and the standard difference methods at the first grid point greater than the boundary.

Numerical grid generation is used to transform complicated computational domains, through a change of variables, to much simpler domains that

allow the use of standard finite difference methods. In our case we wish to transform the domain $\{(x,\tau) : \forall\tau \geq 0, x \geq c(\tau)\}$ to $\mathbb{R}^2_+$. For details of numerical grid generation see Thompson et al. (1985). The front fixing methods in Nielsen et al. (2002) and Wu and Kwok (1997) also use a change of variables to eliminate the moving boundary, however this does not translate to a computational advantage because they do not use the boundary evolution equation considered here. The change of variable we use to transform our domain is

$$\begin{aligned} \omega &= x - c(\tau), \\ g(\omega,\tau) &= p(x,\tau). \end{aligned} \tag{2.7}$$

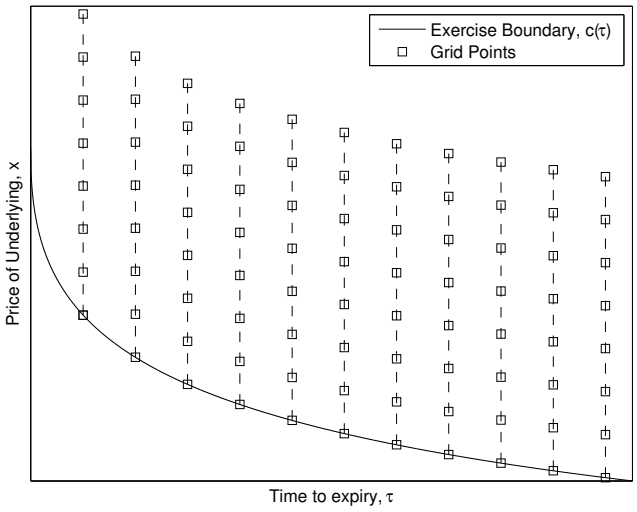

Figure 2.3: Computational grid in x at different times τ

Here ω can be interpreted as distance to the boundary. Given this change in variable we discretize ω uniformly from zero to some $\hat{\omega}$, which is

equivalent to re-discretizing x at every time step uniformly from $c(\tau)$ to some $\hat{x}$, where $\hat{x}$ changes at each step to $c(\tau) + \hat{\omega}$. Figure 2.3 shows the computational grid in the (x, p) space for different values of τ. As τ increases $c(\tau)$ decreases and the grid points align with the boundary for every value of τ. After transformation to the (ω, g) space the computational grid is a standard rectangular region.

Using the chain rule we find the PDE that governs the evolution of g and c to be

$$\frac{\partial g}{\partial \tau} = \tfrac{1}{2}\sigma^2(\omega + c(\tau))^2 \frac{\partial^2 g}{\partial \omega^2} + b(\omega + c(\tau))\frac{\partial g}{\partial \omega} - rg + \frac{\partial g}{\partial \omega}\frac{\partial c}{\partial \tau}, \quad (2.8)$$

$$\frac{\partial c(\tau)}{\partial \tau} = -\frac{\partial^2 g(0,\tau)}{\partial \omega \partial \tau}\frac{\sigma^2 c^2(\tau)}{2qr - 2(r-b)c(\tau)}. \quad (2.9)$$

The main difference between Equations (2.8) and (2.1) is the addition of the final non-linear term which comes from using the chain rule to differentiate g with respect to time. Known as the grid speed, this term allows us to find the value of p at the new grid points without the need for any sort of interpolation. Here, however, it is not as easy to estimate the mixed derivative at the boundary and we must come up with a new method of approximation. As the grid speed term in Equation (2.8) also depends on the boundary evolution equation we cannot simply evolve g one step and use that to calculate the boundary evolution. The numerical method presented here can be described by a three step iterative procedure as well.

Step 1: Initialization

We initialize p for a small time before expiry, τ_0, the same way we did in Section 2.2.2. However in this case we first find $c(\tau_0)$ and then initialize p uniformly between $c(\tau_0)$ and $\hat{x}$. Then we assign these values to ω and g according to the change of variables (2.7).

Step 2: Calculate $\frac{\partial^2 g(0,\tau)}{\partial\omega\partial\tau}$

Here, again, the calculation of the mixed derivative at the boundary can be difficult. In order to approximate this we simply evolve a few grid points greater than the boundary using Equation (2.8) with out the last term, the grid speed, and calculate the ω derivative after this evolution to use in a time finite difference method. Omitting the grid speed term has the effect of freezing the grid points for one small step in time and telling us how much the price of the put would change on those fixed grid points. For example if we use a 4 point finite difference approximation for the ω derivative and a second order Runge-Kutta method for the time derivative, we only need to evolve six grid points larger than the boundary, so that we do not need to worry about right boundary conditions, which is not computationally expensive so we use this in numerical experiments.

Figure 2.4 shows how we calculate $\frac{\partial^2 g(0,\tau)}{\partial\omega\partial\tau}$ in the (ω, g) space. We see that all grid points are equally spaced and the grid points on the solid and dashed lines correspond the the same horizontal values because we dropped the grid speed term to get the dashed line. We also see that we only have the value of the put on the dashed line for a few grid points. Using the grid points on the dashed line and a standard one sided finite difference equation

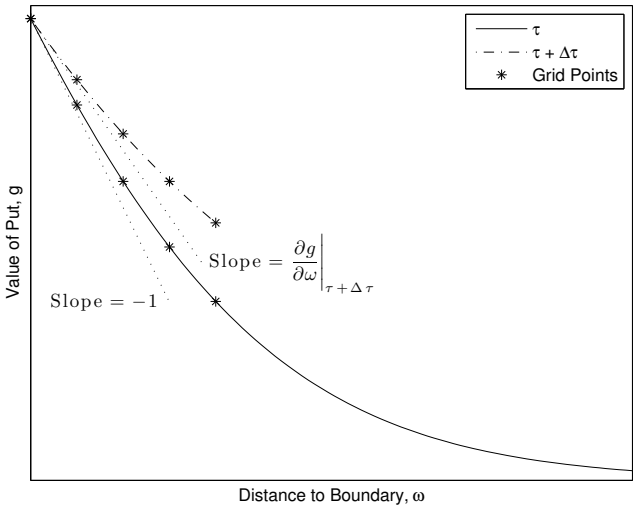

Figure 2.4: Difference in slopes, to calculate $\frac{\partial^2 g}{\partial \omega \partial \tau}$

we calculate the ω derivative. Using these two values with Equation (2.3) we can approximate $\frac{\partial^2 g(0,\tau)}{\partial \omega \partial \tau}$.

Step 3: Evolve g and c simultaneously one step

Once we have calculated the mixed derivative we hold it constant while we evolve Equations (2.8) and (2.9). Since we hold this constant we can use a coupled Runge-Kutta method to evolve g and c; in numerical experiments we use the second order coupled Runge-Kutta method. Also for this method we use the same boundary condition for large ω as we did in Section 2.2.2. However to increase accuracy we add an extra grid point to the end of the computational domain every time $c(\tau) + \hat{\omega} < \hat{x}$. When this extra grid point is brought into the computational domain it is introduced according to Equation

(2.5). We repeat steps **2** and **3** until we reach the desired time and then change the variables back to x and p.

We could potentially evolve the system implicitly but Equations (2.8) and (2.9) are both non-linear. This means we either need to linearize the equations or use a non-linear solver to evolve the system, however we do not want to rely on the speed of any specific non-linear solver to determine the computational time of the algorithm. When we consider stochastic volatility we will have non-linear PDEs similar to these and we apply a linearization to the system. However in constant volatility the linearization is not beneficial on a fine mesh so we only use an explicit method.

In this method we cannot evolve g one step, calculate the mixed derivative and then evolve c one step as we did in the previous section because the grid is moving. Considering the (x, p) space in the evolution of the price with the grid speed term, the grid points used to calculate the space derivative before the price evolution and the grid points used after the evolution are not the same. Therefore we cannot combine these values to calculate the mixed derivative. Also, the value of the grid speed term is partially determined by the mixed derivative. If we do not know the value of the mixed derivative, then we do not know the value of the grid speed term and we cannot evolve g through time.

Figure 2.5 shows the evolution of the value of the put and the grid points used to calculate its value over a step in time to expiry. The solid line represents the value of the put in the (x, p) space and the corresponding grid

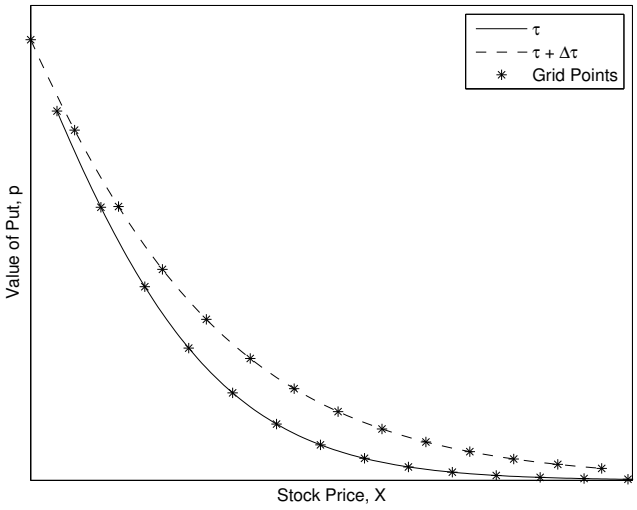

Figure 2.5: Illustrating different grid points used at two different times

points in x before the price and boundary are evolved one step. The dashed line shows the value of the put and the corresponding grid points after the price and boundary are evolved in step **3**. We can see that the grid points on the solid and dashed curves do not coincide because they have moved over the course of a step in time to expiry. The first grid point on each line corresponds to the early exercise boundary at that time.

There are a couple minor drawbacks to this algorithm. The first problem is that we will almost always have to use a spline to compute the price of the put at some x value after the algorithm is finished because we cannot pick the grid to include that value like we could in the method presented in Section 2.2.2. For example, if we wish to know the price of the option when

the underlying stock costs $100 the method in Section 2.2.2 lets us pick 100 to be a grid point since the grid is static. However if we choose the grid spacing so that 100 is a grid point when we initialize we will almost certainly find that 100 is not a grid point when the algorithm is finished because the grid has moved. Therefore we must interpolate to find the value of the option when the underlying costs $100. The next problem is that since we include the non-linear term to the end of Equation (2.8) the CFL condition forces us to use a smaller time step size than that required in Section 2.2.2. We will see however that despite these problems this method compares favorably in speed and accuracy to the static grid method.

2.2.4 Modified Integral Method

In the previous sections we needed to evolve the boundary and the value function simultaneously because the boundary evolution equation requires a mixed derivative of the value function evaluated at the boundary. In this section we present a numerical method that does not require the value function to be explicitly evolved with the boundary. This is achieved by using the integral representation of the American put option, as in Kim (1990). Although we do not directly extend this to American options with stochastic volatility, this method gives a good example of how to use boundary evolution equations to improve other numerical methods besides PDE methods.

The integral representation of the American put option states that the value of an American put is equal to the value of a European put, plus an early

exercise premium. The early exercise premium is an integral of a function of the boundary. The value of an American put is

$$p(x,\tau) = f(x,\tau) + \int_0^\tau \left[rqe^{-r(\tau-u)}N(-d_2^*) - (r-b)xe^{-(r-b)(\tau-u)}N(-d_1^*)\right] \mathrm{d}u, \tag{2.10}$$

where

$$d_1^* = \frac{\log(x/c(u)) + (b + \frac{1}{2}\sigma^2)(\tau - u)}{\sigma\sqrt{\tau - u}} \quad \text{and} \quad d_2^* = d_1^* - \sigma\sqrt{\tau - u}.$$

Here $f(x,\tau)$ is the value of a European put, N is the standard normal cumulative distribution function, and we see that d_1^* and d_2^* are functions of the boundary.

Using this representation, if we know the value of the boundary between $\tau = 0$ and some time to expiry, τ_1, then we would like to express the value of the mixed derivative at τ_1 as some integral of the known boundary, which we can approximate using numerical integration. If this is possible we can then calculate the value of the boundary at $\tau_1 + \Delta\tau$ using Equation (2.6), and an ODE solver. This is exactly what we will do, however there are a few subtleties that arise that make this process complicated so we describe the process in four steps below.

Step 1: Initialization

In order to start this algorithm we must know the value of the boundary at a small time to expiry, as we did in the previous sections, because in order to calculate the mixed derivative using Equation (2.10) we need something to

integrate. To initialize this method we tried two different approaches. First we tried the asymptotic expansions for small τ, found in several papers mentioned in Section 2.1.1. We also tried the method we have used in previous sections: find the intersection of the European option with the intrinsic value of the put. It is somewhat surprising, but in numerical experiments we find that the method of finding the intersection is about five times more accurate than the asymptotic expansions that we tried, so we initialize with the binary search method. Once we know the boundary, we do not need to calculate the price function as we did in the previous sections because we will evaluate the mixed derivative as an integral of the boundary.

Step 2: Calculate $\frac{\partial^2 p}{\partial x \partial \tau}$

In order to calculate the mixed derivative we differentiate Equation (2.10) first with respect to x and then τ. The derivative with respect to x is

$$\frac{\partial p}{\partial x} = \frac{\partial f}{\partial x} - \int_0^\tau \left[\frac{rq}{x\sigma\sqrt{\tau-u}} e^{-r(\tau-u)} N'(d_2^*) - \frac{r-b}{\sigma\sqrt{\tau-u}} e^{-(r-b)(\tau-u)} N'(d_1^*) + (r-b) e^{-(r-b)(\tau-u)} N(-d_1^*) \right] \mathrm{d}u. \tag{2.11}$$

When we differentiate Equation (2.11) with respect to τ, using the Liebniz rule, and evaluate at $x = c(\tau)$ we find that $\frac{\partial^2 p}{\partial x \partial \tau} = \frac{\partial^2 f}{\partial x \partial \tau} + \infty - \infty$.

This does not mean that the derivative does not exist, rather it means that there is no analytical expression for the derivative, because there is no analytical expression for the integral in Equation (2.11). This happens because the integrand in Equation (2.11) blows up when $u = \tau$, even though it is still integrable.

In order to overcome this problem we employ numerical integration to calculate $\frac{\partial p}{\partial x}$, using Equation (2.11), evaluated at $(c(\tau - \Delta\tau), \tau)$ and assume that $\lim_{u\to\tau} d^*_{1,2} = 0$. Then we can approximate the mixed derivative as

$$\left.\frac{\partial^2 p}{\partial x \partial \tau}\right|_{(c(\tau),\tau)} \approx \left(\left.\frac{\partial p}{\partial x}\right|_{(c(\tau-\Delta\tau),\tau)} + 1\right)/\Delta\tau.$$

Here the "plus one" comes from the assumption that $\left.\frac{\partial p}{\partial x}\right|_{(c(\tau-\Delta\tau),\tau-\Delta\tau)} = -1$.

The approximation of the integral in Equation (2.11) is also not entirely straightforward because the integrand blows up when $u = \tau$, so any standard numerical approximation will undervalue the integral. To fix this we split the integral into two parts, first the integral from 0 to $\tau - \Delta\tau$ and then the integral from $\tau - \Delta\tau$ to τ. The first part of the integral can easily be approximated using any numerical integration technique and the second part of the integral can be approximated in closed form if we assume that $d^*_{1,2} = 0$ on the interval $[\tau - \Delta\tau, \tau]$. In fact, $d^*_{1,2} = 0$ when $u = \tau$ only if we evaluate at $x = c(\tau)$. Since we are trying to approximate the derivative at a value close to $c(\tau)$ we use $d^*_{1,2} = 0$ as an approximation. If $d^*_{1,2} = 0$ on the interval then $N'(d^*_{1,2}) = \frac{1}{\sqrt{2\pi}}$ and $N(d^*_{1,2}) = \frac{1}{2}$. This together with the fact that $\int \frac{e^{-\beta(\tau-u)}}{\sqrt{\tau-u}}\mathrm{d}u = -\sqrt{\frac{\pi}{\beta}}\mathrm{erf}\left(\sqrt{\beta(\tau-u)}\right)$, where erf is the error function, we can approximate the second part of the integral, and the mixed derivative quite accurately.

Step 3: Evolve $c(\tau)$

After the mixed derivative is calculated we hold it constant for one step and evolve the boundary one step using Equation (2.6). Since we hold

the mixed derivative constant for one step we see that Equation (2.6) becomes an ODE and we can evolve it using any ODE solver. Once we evolve the boundary one step we repeat steps **2** and **3** until we know the boundary at the desired time to expiration.

Step 4: Calculate the price of the put

Once we know the boundary for all values between 0 and τ we can use Equation (2.10) to find the value of an American put at any value of x. Again we need to use numerical integration but this time the integral is very simple because the integrand does not blow up, so we can use any standard numerical integration technique. Numerical results are presented in the next section.

2.2.5 Numerical Results

In order to compare the speed and accuracy we compute the (long-dated) option values over the set of parameters presented on Table 3a in AitSahlia and Carr (1997). Here we assume that the underlying asset is a constant dividend paying stock and thus $b = r - \delta$, where δ is the dividend yield and we use $\hat{x} = 6.5q$. The value of the put is calculated when $x = 80, 85, 90, 95, 100, 105, 110, 115, 120$ for the parameter values $q = 100$, $\tau = 3$, $\sigma = 0.4$, $r = 0.06$ and $\delta = 0.02$. Then holding all other parameters fixed at this level we evaluate the at-the-money put with the parameters $r = 0.02, 0.04, 0.08, 0.1$, $\delta = 0, 0.04$, $\sigma = 0.3, 0.35, 0.45, 0.5$ and $\tau = 0.5, 1, 1.5, 2, 2.5, 3.5, 4, 4.5, 5, 5.5$. This leads to 21 sets of parameters where we evaluate the American put.

We compare these values to the values calculated using the very accurate, yet very slow, binomial tree method. We then compare this accuracy measure to the accuracy of four other computational methods: the finite difference moving boundary method in Muthuraman (2008), the Brennan-Schwartz method, the front fixing method in Nielsen et al. (2002) and the standard integral method in Carr et al. (1992). A more comprehensive comparison of other numerical methods can be found in Muthuraman (2008). The Brennan-Schwartz and the moving boundary method have some similarity to the static grid and dynamic grid methods since they find the boundary and evolve the price by time stepping. However in these methods the boundary is always considered to be at a grid point and the way it is found, by evolving Equation (2.1) over a large domain several times, is much slower than our method, evolving an ODE. We compare to the standard integral method because we have created a modified integral method that uses the boundary evolution equation and we would like to see if this is advantageous. The front fixing method is considered too, because it also removes the moving boundary by a change of variables similar to the one considered here, however this method is very slow and inaccurate because it must solve a large system of nonlinear equations at each time step.

The measure of accuracy here is the same as the one used in Broadie and Detemple (1997), root mean squared relative error, RMSE, and we consider the "exact" price to be the average of a 10,000 and a 10,001 step binomial tree approximation, as in AitSahlia and Carr (1997). RMSE is defined as

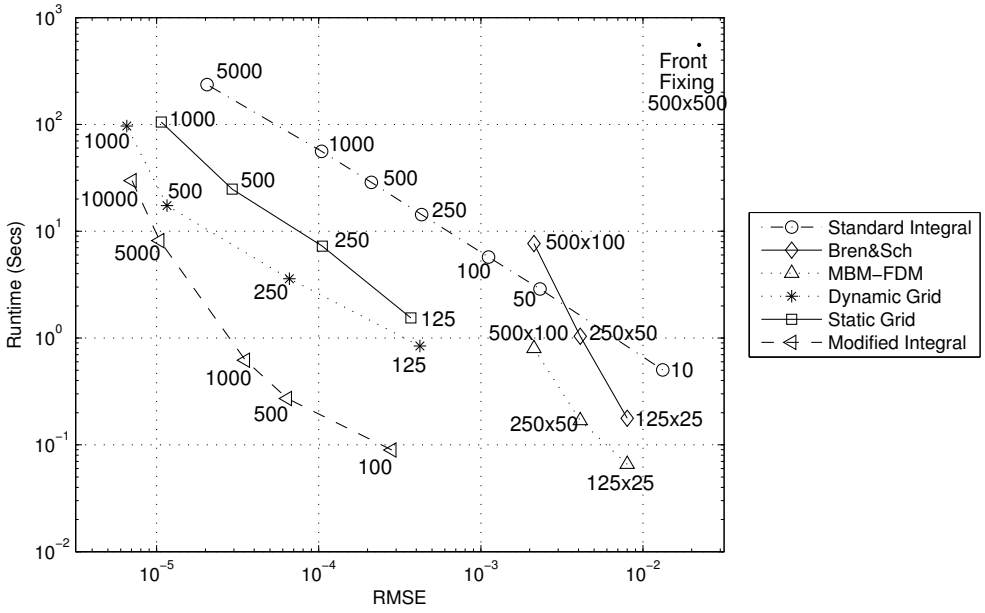

Figure 2.6: RMSE vs Runtime for Constant Volatility

$\text{RMSE} = \sqrt{\frac{1}{n}\sum_{i=1}^{n}\left(\frac{\text{approx}_i - \text{exact}_i}{\text{exact}_i}\right)^2}$ where the sum is taken over all numerical experiments, approx_i is the value of the i^{th} put found by the approximate numerical method, and exact_i is the "exact" value of the put.

The measure of speed is simply average total computational time. We calculate the speed and error of these methods over several grid sizes and show the results in Figure 2.6. For the dynamic and static grid methods the labels refer to the number of spacial grid points; the number of grid points in time to expiry is determined by the CFL condition: the step size in τ is proportional to the square of the step size in x, which guarantees that the matrices used for evolution are positive definite. It is important that the evolution matrices

be positive definite because if values on the main diagonal are negative then roundoff error can accumulate quickly, see Courant et al. (1967). For the modified and standard integral methods the labels refer to the number of time grid points, and for the Brennan-Schwartz, moving boundary and front fixing methods the labels refer to the number of space and time grid points. All computations were performed in Matlab on a PC with a 3.06 GHz processor and 4GB of RAM running Ubuntu Linux 10.10.

All analysis here was performed with $0 \leq \delta \leq r$. Unfortunately, when $r < \delta$ it can happen that our initial approximation of $c(\tau_o)$ is greater than $\frac{r}{\delta}q$. This means that the denominator of Equation (2.6) is negative and the whole equation is positive, indicating that the boundary is increasing in time-to-expiry, which is clearly incorrect. To overcome this problem we can use other methods to initialize the American put, such as a few steps in the integral method or any variety of short time asymptotic approximations. It seems that using a few steps in the integral method is favorable to short time asymptotic approximations because the time required to initialize with the integral method does not increase total computational time by much and it typically results in less error than short time asymptotic approximations. Alternatively if $\delta < 0$, (i.e. $b > r$), there is no change to the method and speed and accuracy are comparable to the existing results.

We can see that the static and dynamic grid methods perform better than the standard integral method in both computational time and accuracy. They also provide better accuracy than the Brennan and Schwartz method

and the moving boundary method. We also see that the front fixing method is the worst method considered, as is also seen in Muthuraman (2008).

The dynamic grid method is faster than the static grid method despite requiring more time steps because one time step of an explicit method, used in the dynamic grid method, can be faster than one time step of an implicit method, used in a static grid method. The dynamic grid method forces us to use an explicit method because of the non-linearities. Each step in this explicit method results in a few matrix multiplications (depending on the order of the Runge-Kutta method) whereas the Crank-Nicolson method requires matrix multiplication and factorization, to solve a system of equations, at each time step. It is not possible to pre-store the matrix factorization before evolving the system because at each step the matrix changes and thus the factorization changes as well. Even though the dynamic grid method takes more time steps than the static grid method, each step in the dynamic grid method is faster than a step in the static grid method and this trade off comes out in favor of the dynamic grid method for most mesh sizes.

Even more impressive than the static and dynamic grid methods is the modified integral method. The modified integral method offers a huge improvement over the standard integral method in both computational time and accuracy. It also out performs the static and dynamic grid methods, especially on a coarse grid. We do not directly extend the modified integral method to stochastic volatility but this would be an interesting direction for future research following Detemple and Tian (2002).

We would also like to know how error in these methods depend on grid size. In order to do this we will perform two convergence studies where we systematically decrease the step size in the x and τ variables. The first study will be performed on the Fixed Grid and Dynamic Grid methods. In this study when we reduce the step size in x (or ω) linearly, we reduce the step size in τ quadratically, to maintain the CFL condition. We then calculate the L^2 error and find the slope of the log step size versus the log error, this gives us the order of accuracy of the method.

In order to approximate the L^2 error we compute the price of the put for $x \in [80, 120]$ at $\tau = 3$ for the first parameter set described above. When we perform this regression we find the slope is 1.985 for the dynamic grid method and 1.419 for the fixed grid method, suggesting that the dynamic grid method is second order accurate. The most likely reason that the fixed grid method loses some accuracy is the non-uniform grid spacing at the boundary; the small distance between the boundary and the first grid point can dominate finite difference calculations.

In the second study we examine the effect of $\Delta\tau$ on error. We perform this test only on the modified integral method. Here we systematically decrease the step size in τ, there is no step size in x, and again approximate the L^2 error over the same domain as in the previous example. When we perform this regression we find the slope is 0.949. This method is only first order accurate, despite using what seemed to be a second order finite difference method for $c(\tau)$, because the calculation of the mixed derivative at the boundary, which

is only first order accurate in time, dominates the error.

2.3 Stochastic Volatility

In this section we seek the boundary evolution equation that characterizes the early exercise boundary when the dynamics of the underlying asset are modeled by a stochastic volatility process. We will also leverage on the derived equation to create a fast and accurate numerical method to approximate the price of an American option. This time however we will only be able to implement the numerical method on a dynamic grid due to grid effects that will be explained later.

Working with stochastic volatility makes pricing options challenging since there are two space dimensions and one time dimension. The space dimensions are x, which represents the price of the underlying asset, and y, which represents the volatility, or some function of the volatility, of the underlying asset.

Unlike the constant volatility case, when we consider stochastic volatility there are several models in literature for the underlying dynamics of the asset's volatility. The popular models are the Heston model (Heston (1993)), the Hull and White model (Hull and White (1987)), the Scott model (Scott (1987)) and the Stein and Stein model (Stein and Stein (1991)). As each model uses a different stochastic process for volatility the PDE describing the risk neutral expectation is different for each model. In each of these the authors have worked on pricing European style derivatives. Of the above models, the

Heston model is the most popular and in the next sections we focus mostly on this model but also present some results for the other models above.

2.3.1 The Boundary Equation

As in the constant volatility case we must partition the computational domain into two distinct regions separated by the early exercise boundary. Now, however, the early exercise boundary is not just a function of time, but also the volatility level because different levels of volatility will lead to different optimal exercise policies. Before we can derive a PDE for the early exercise boundary we must first understand stochastic volatility models. We will begin working with a set of stochastic differential equations that are sufficiently general to accommodate the popular stochastic volatility models. The SDEs are

$$\begin{aligned} dX_t &= \mu X_t dt + f(Y_t) X_t dW_1, \\ dY_t &= \eta(Y_t) dt + \lambda(Y_t) dW_2, \\ \langle dW_1, dW_2 \rangle &= \rho dt. \end{aligned}$$

Here X_t is the stochastic process representing the price of the underlying asset, Y_t represents the volatility of the underlying asset, f, η, and λ are model specific functions and ρ is the correlation between the two Brownian motions, W_1 and W_2. With these SDE's we can use a dynamic programming argument with Itô calculus and the no-arbitrage argument to write a PDE and boundary conditions that the value of the American put must satisfy in the

non-exercise region of the domain, $\{(x, y, \tau) : \forall y, \tau \geq 0, x > c(y, \tau)\}$. Here we do not consider dividends for simplicity. The differential equation is

$$\frac{\partial p}{\partial \tau} = \tfrac{1}{2}x^2 f(y)^2 \frac{\partial^2 p}{\partial x^2} + \tfrac{1}{2}\lambda(y)^2 \frac{\partial^2 p}{\partial y^2} + \rho\lambda(y) f(y) x \frac{\partial^2 p}{\partial x \partial y} + rx\frac{\partial p}{\partial x} + \eta(y)\frac{\partial p}{\partial y} - rp, \tag{2.12}$$

with boundary conditions

$$\begin{aligned} p(c(y,\tau), y, \tau) &= q - c(y,\tau), & (2.13)\\ \frac{\partial}{\partial x} p(c(y,\tau), y, \tau) &= -1, & (2.14)\\ \frac{\partial}{\partial y} p(c(y,\tau), y, \tau) &= 0, \quad \text{and} & (2.15)\\ p(x, y, 0) &= \max(q - x, 0). \end{aligned}$$

We also assume

$$\lim_{y\to\infty} \frac{\partial p}{\partial y} = 0, \tag{2.16}$$

which implies that $\lim_{y\to\infty} \frac{\partial c}{\partial y} = 0$. And for large x we use the same boundary condition as Equation (2.5). Equations (2.14) and (2.15) are the smooth pasting conditions for stochastic volatility, as found in Fouque et al. (2000). Now that we have the boundary conditions we next seek a differential equation that governs $c(y, \tau)$. We give the proof for the general formulation and later present the results for several specific models.

Theorem 2.2. If $\frac{\partial c}{\partial \tau} \neq 0$ and $c(y, \tau)$ is sufficiently smooth, the differential equation that governs $c(y, \tau)$ is

$$\frac{\partial c}{\partial \tau} = -\frac{\partial^2 p(c, y, \tau)}{\partial x \partial \tau} \frac{1}{2rq} \left(f(y)^2 c^2 - 2\rho\lambda(y) f(y) c \frac{\partial c}{\partial y} + \lambda(y)^2 \left(\frac{\partial c}{\partial y} \right)^2 \right). \tag{2.17}$$

The proof can be found in the appendix.

Now that we have the formula for the general stochastic volatility formulation we plug in the model specific functions, f, η and λ, and describe the boundary equations for the four models above in Table 2.1. In all of these models the market price of risk is assumed to be zero but it could be inserted into the differential equations without much effort because the coefficient of the first derivative in y, which is where the market price of risk enters the system, is not present in the boundary evolution equation.

In the statement of Theorem 2.2 we only derive the boundary evolution equation when $\frac{\partial c}{\partial \tau} \neq 0$ for all values of y. This guarantees that we do not divide by zero when plugging Equation (A.7) into (A.10). If this is not true, then the boundary just does not move at that point. It seems however for the Heston model and the Hull and White model that as $y \to 0$ we also have $\frac{\partial c}{\partial \tau} \to 0$ for all values of τ. This would mean that $c(0, \tau) = q$ and $p(x, 0, \tau) = 0$ for all τ and $x \geq q$. For the Hull and White model this is not surprising because the variance in this model follows a Geometric Brownian Motion, which stays at zero forever if the process is ever zero, almost surely. This means that the value of the underlying becomes deterministic and thus an out-of-the-money put can have no value when $y = 0$, which can be used as a boundary condition for the Hull and White model.

This point is subtle because even though a Geometric Brownian Motion can never reach zero, if it starts at a positive value, the PDE for the value function needs a boundary condition. The boundary condition chosen

Model	Stochastic Process	Boundary Equation
Heston $\rho \neq 0$	$dX_t = \mu X_t dt + \sqrt{Y_t} X_t dW_1$ $dY_t = \kappa(m' - Y_t)dt + v\sqrt{Y_t} dW_2$	$\frac{\partial c}{\partial \tau} = -\frac{\partial^2 p(c,y,\tau)}{\partial x \partial \tau} \frac{1}{2rq} \left(yc^2 - 2\rho v y c \frac{\partial c}{\partial y} + v^2 y \left(\frac{\partial c}{\partial y} \right)^2 \right)$
Hull & White $\rho = 0$	$dX_t = \mu X_t dt + \sqrt{Y_t} X_t dW_1$ $dY_t = \alpha_1 Y_t dt + \alpha_2 Y_t dW_2$	$\frac{\partial c}{\partial \tau} = -\frac{\partial^2 p(c,y,\tau)}{\partial x \partial \tau} \frac{1}{2rq} \left(yc^2 + \alpha_2^2 y^2 \left(\frac{\partial c}{\partial y} \right)^2 \right)$
Scott $\rho = 0$	$dX_t = \mu X_t dt + e^{Y_t} X_t dW_1$ $dY_t = \alpha(m - Y_t)dt + \beta dW_2$	$\frac{\partial c}{\partial \tau} = -\frac{\partial^2 p(c,y,\tau)}{\partial x \partial \tau} \frac{1}{2rq} \left(e^{2y} c^2 + \beta^2 \left(\frac{\partial c}{\partial y} \right)^2 \right)$
Stein & Stein $\rho = 0$	$dX_t = \mu X_t dt + \lvert Y_t \rvert X_t dW_1$ $dY_t = \alpha(m - Y_t)dt + \beta dW_2$	$\frac{\partial c}{\partial \tau} = -\frac{\partial^2 p(c,y,\tau)}{\partial x \partial \tau} \frac{1}{2rq} \left(y^2 c^2 + \beta^2 \left(\frac{\partial c}{\partial y} \right)^2 \right)$

Table 2.1: Boundary evolution equations for several popular stochastic volatility models

here needs to agree with the dynamics of the stochastic process, and since a Geometric Brownian Motion that starts at zero must stay at zero, this is the boundary condition that we must use.

The above economic reasoning, however, does not make sense for the Heston model because the variance follows a square root process which becomes positive immediately after hitting zero, almost surely (for certain parameter values satisfying the Feller Condition, zero is inaccessible to the variance process, like Geometric Brownian Motion, but we still need a boundary condition.) This means that the value of the underlying cannot be deterministic and thus an out of the money put must have positive value when $y = 0$, implying that $\lim_{y\to 0^+} \frac{\partial c}{\partial y} = -\infty$.

In this case the rate that the derivative explodes must be very specific. It must go to infinity like $\frac{-1}{\sqrt{y}}$. If it goes to infinity any faster then the last term in the Heston boundary equation will go to infinity and so will the whole boundary equation. If it goes to infinity any slower then the last term will go to zero and so will the whole boundary equation. If the derivative does go to infinity at the right speed then the last term becomes indeterminate, which makes

$$\frac{\partial c(0,\tau)}{\partial \tau} = -\frac{\partial^2 p(c,y,\tau)}{\partial x \partial \tau}\frac{v^2}{2rq}\gamma. \tag{2.18}$$

Although the above constant, γ, is unknown we can interpret this as a boundary condition for the Heston model, which will be explained in further detail in the next section.

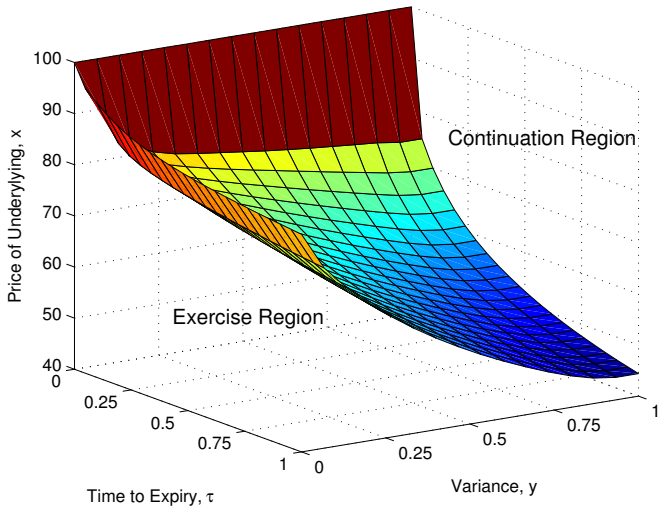

Figure 2.7: Partitioned State Space for Heston Model

Figure 2.7 shows the state space partitioned to the exercise region and the continuation region for the Heston model. The two regions are separated by the early exercise surface. The exercise region is below the surface and the price of the put is equal to its intrinsic value there. The continuation region is above the surface and there the price of the put is is governed by Equation (2.12).

2.3.2 Numerical Method on a Dynamic Grid

In this section we will focus only on the Heston model of stochastic volatility. We want to transform the no exercise region to a simpler domain that allows for standard finite difference methods. We transform the domain $\{(x, y, \tau) : \forall y, \tau \geq 0, x > c(y, \tau)\}$ to $\mathbb{R}^3_+$. The change of variable we use to

transform our domain is

$$\begin{aligned} \omega &= x - c(y,\tau) \\ g(\omega, y, \tau) &= p(x, y, \tau). \end{aligned} \tag{2.19}$$

This change of variable involves derivatives in the y variable. The second derivative and the mixed derivative lead to several nonlinear terms in the resulting PDE. Equation (2.12) for the Heston model is

$$\frac{\partial p}{\partial \tau} = \tfrac{1}{2} y x^2 \frac{\partial^2 p}{\partial x^2} + \tfrac{1}{2} v^2 y \frac{\partial^2 p}{\partial y^2} + \rho v y x \frac{\partial^2 p}{\partial x \partial y} + r x \frac{\partial p}{\partial x} + \kappa(m' - y)\frac{\partial p}{\partial y} - rp. \tag{2.20}$$

We use the chain rule to find the pricing equation for the g function and the corresponding boundary equation, which are

$$\begin{aligned} \frac{\partial g}{\partial \tau} &= \tfrac{1}{2} y(\omega + c(y,\tau))^2 \frac{\partial^2 g}{\partial \omega^2} + \tfrac{1}{2} v^2 y \left(\frac{\partial^2 g}{\partial \omega^2} \left(\frac{\partial c}{\partial y} \right)^2 - \frac{\partial g}{\partial \omega} \frac{\partial^2 c}{\partial y^2} \right. \\ &\quad \left. - 2 \frac{\partial c}{\partial y} \frac{\partial^2 g}{\partial \omega \partial y} + \frac{\partial^2 g}{\partial y^2} \right) + \rho v y (\omega + c(y,\tau)) \left(\frac{\partial^2 g}{\partial \omega \partial y} - \frac{\partial c}{\partial y} \frac{\partial^2 g}{\partial \omega^2} \right) \\ &\quad + r(\omega + c(y,\tau)) \frac{\partial g}{\partial \omega} + \kappa(m' - y) \left(\frac{\partial g}{\partial y} - \frac{\partial g}{\partial \omega} \frac{\partial c}{\partial y} \right) - rg + \frac{\partial g}{\partial \omega} \frac{\partial c}{\partial \tau}, \end{aligned} \tag{2.21}$$

$$\frac{\partial c}{\partial \tau} = -\frac{\partial^2 g(0, y, \tau)}{\partial \omega \partial \tau} \frac{1}{2rq} \left(y c^2 - 2\rho v y c \frac{\partial c}{\partial y} + v^2 y \left(\frac{\partial c}{\partial y} \right)^2 \right). \tag{2.22}$$

Given this change of variables we seek a numerical method that exploits the equations for boundary and price evolution. The method presented here can be summarized in a three step process.

Step 1: Initialization

Similar to the constant volatility case, we cannot start the numerical method with the initial conditions when $\tau = 0$, and as such we need to approximate the value of the American option a short time before expiry as a European option. There are two ways to approximate the value of the European option. First we could use the semi closed form solution to European options under the Heston model to find the price of the European a short time before expiry, the details of which can be found in Heston (1993) or Gatheral (2006). Alternatively we could use the constant volatility Black-Scholes equation to find the value of the put a short time before expiration. It might seem that this simplistic method would lead to large error, but it turns out that the two methods have comparable accuracy and the second is significantly faster than the first. The reason is that the functions being integrated in the solution to the European put under the Heston model are highly oscillatory and are dampened very slowly for small values of τ. This makes approximating this integral a very slow process because a large integration domain is required with a fine integration mesh, and so for numerical tests we simply use the Black-Scholes equation to initialize p.

In order to initialize we need to divide the y domain uniformly between 0 and $\hat{y}$, where $\hat{y}$ is the maximal value of the computational domain. Here again the value of $\hat{y}$ needs to be large enough so that the boundary condition in Equation (2.16) is approximately true for all values of x. At each grid point in y we perform a binary search to find the intersection of the value of the European option and the intrinsic value of the option as in Figure 2.2. If we

use the Black-Scholes formula to get the value of the European then we need to set the variance equal to the y grid value. We initialize the boundary at each y grid point as the location of the intersection. Then for each value of y we find the value of the European at n equally spaced grid points, in x, larger than the boundary, where n is chosen large enough so that the boundary condition (2.5) is satisfied. We find that the initial boundary is deceasing in y and as such the maximal value of x for each value of y is also decreasing. After we find the price of the European at all of these grid points we transform the domain using Equation (2.19). Figure 2.8 shows how the computational domain looks before the transformation.

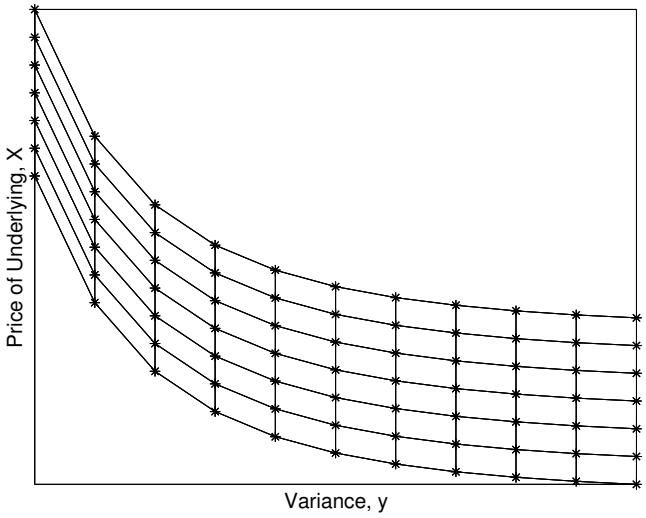

Figure 2.8: Computational grid before transformation.

Step 2: Calculate $\frac{\partial^2 g(0,y,\tau)}{\partial \omega \partial \tau}$

As in the constant volatility case the hardest part of the algorithm is finding the mixed derivative at the boundary. In the constant volatility case we discussed two ways to calculate this derivative; one in the fixed grid method and one in the dynamic grid method. Here since we only work on a dynamic grid we simply evolve a few grid points greater than the boundary for every value of y according to Equation (2.21) without the last term, the grid speed term, using an explicit Runge-Kutta method. We use a standard one sided finite difference method to calculate the value of the x derivative at the boundary for every value of y after this partial evolution. Then using this value with Equation (2.14) we can approximate the value of the mixed derivative by using a first order finite difference method.

Step 3: Evolve c and g in time to expiry

As opposed to the method used for constant volatility, we linearize Equation (2.21) so that we can use an implicit method to step backwards in time, which dramatically reduces the number of steps required in time to expiry when compared to an explicit method. In constant volatility we could have also linearized the price evolution equation in the dynamic grid section to use an implicit method. However on a fine grid linearization accounts for a large portion of the numerical error and so we only use an explicit method. In stochastic volatility it is not practical to use a fine grid because there are two space dimensions which greatly increases the total number of grid points and therefore we linearize Equation (2.21).

We see that in Equation (2.21) all the non-linearities come from mul-

tiplying derivatives of g with derivatives of c. This means that if we can approximate the derivatives of c then we can use them to linearize the evolution equation for g. In order to linearize this equation we must get the first and second order derivatives of the boundary with respect to y. To do this we simply evolve the boundary one step using a Runge-Kutta method and compute the derivatives for the boundary at the τ and $(\tau+1)^{\text{st}}$ steps using standard finite difference methods. Then using the values computed here we plug them into Crank-Nicolson matrices A and B, where A and B are block tridiagonal matrices satisfying the equation $A \cdot g^{\tau} = B \cdot g^{\tau+1}$. Here we plug the values of the derivatives before the evolution into the A matrix and the values of the derivatives after the evolution into the B matrix. One important fact to remember is that at each step the matrices A and B must be recalculated because the boundary and the derivatives of the boundary have changed. After we evolve the price function we let the boundary be equal to the value at the $(\tau+1)^{\text{st}}$ step.

There is still a boundary condition we need to address; the boundary when y goes to 0. For this we simply assume that the constant in Equation (2.18) is attained at the second y grid point and that the value of p evolves with the standard PDE when 0 is inserted for y, which eliminates several terms. After we evolve g one step we repeat steps **2** and **3** until we reach the desired time to expiration and change the variables back to x and p.

We cannot adopt this method onto a fixed grid, as we did with constant volatility, because the boundary is decreasing in y. Say for a specific y value

the boundary is be between the 99^{th} and 100^{th} x grid values and for the next y value the boundary is between the 98^{th} and 99^{th} x grid values. We will then get a discontinuity in the calculation of the mixed derivative when this happens. This discontinuity in the mixed derivative leads to a discontinuous boundary which in turn leads to large error in the price of the put and as such we need a dynamical grid method. The boundary is also decreasing in time to expiry and so this phenomenon could also occur in the τ variable. The effect, however, is less drastic in τ than in y because at each discrete step in τ we numerically approximate derivatives in y, whereas we relate derivatives in τ to derivatives in y using Equation (2.21) removing the need for continuous derivatives in τ. This relationship is why we were able to use a static grid for constant volatility.

Also, as in the constant volatility case we add extra grid points to each value of y every time that the boundary decreases below a certain value. This again has the benefit of maintaining accuracy for options that are out of the money.

2.3.3 Numerical Results

Numerical comparison of speed and accuracy is more challenging for stochastic volatility than for constant volatility because finding a "true" price for the option is not clear. In this section we only compute the price of the put for eight set of parameters, the "true" values were calculated by Jari Toivanen using his component wise splitting method on a very fine mesh. The value of

the put is calculated when $x = 8, 9, 10, 11, 12$, $y = 0.0625, 0.25$ and $\tau = 0.25$ for the parameter values $r = 0.1$, $v = 0.9$, $\kappa = 5$, $m' = 0.16$ and $\rho = 0.1$. Then holding all other parameters fixed we evaluate the puts with the parameters $r = 0.08, 0.12$, $v = 0.7, 1.1$, $\kappa = 2.5$ and $\rho = 0.05, 0.15$.

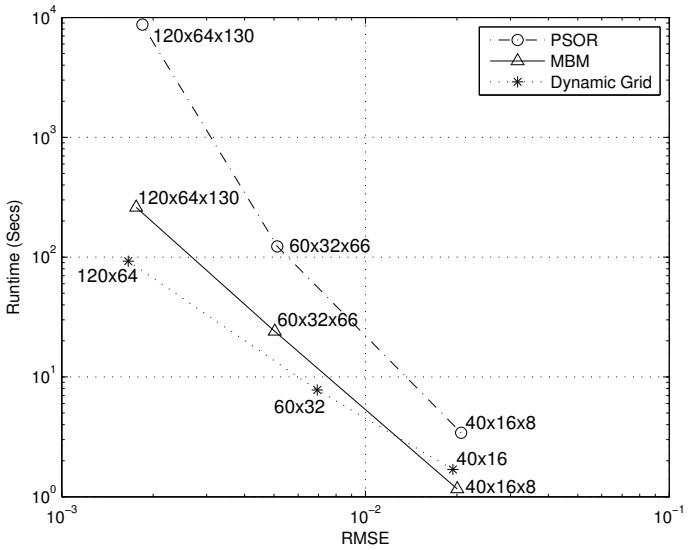

Figure 2.9: RMSE vs Runtime for Stochastic Volatility

We compare our method to two existing methods, the PSOR and the moving boundary method, MBM, presented in Choklingham and Muthuraman (2011), in Figure 2.9. We only compare our method against these methods because although the PSOR method is quite slow, Ikonen and Toivanen (2008) finds that it is the simplest to implement, and in Chockalingam and Muthuraman (2011) the authors find that the moving boundary method was the fastest method tested. As in the constant volatility case we plot the root

mean squared error of the methods versus the total computational time. For the moving boundary method and the PSOR the labels refer to the number of x, y and τ grid points. For the dynamic grid method the labels refer to the number of x and y grid points, and the number of time grid points is determined by the CFL condition.

The non-linearities of the dynamic grid method unfortunately cause the necessary number of steps in time to expiry to be quite large, despite the linearization of Equation (2.21), this however is offset by the speed with which each time step is executed versus the moving boundary method and the PSOR. Both of these methods must search for the early exercise boundary while our method knows exactly where it is. We see that for the coarsest grid the moving boundary method is slightly better than our method, however on finer grids our method performs significantly better. For the finest grid our method is almost three times faster than the moving boundary method.

2.4 Concluding Remarks

Boundary evolution equations have significant computational benefit when one relies on dynamic grids that are evolved with the boundary during the solution process. The key insight into the construction of efficient numerical methods is that we do not have to iteratively guess the location of the boundary at each step, rather the boundary evolution equation tells us its location. Moreover, by evolving the grid along with the boundary one gets the added benefit of minimizing the error in approximating the boundaries with a

predefined grid structure.

The American option pricing problems studied here belong to the much larger class of optimal stopping problems in stochastic control. Most optimal stopping problems do not have analytical solutions and are difficult to solve, especially when the complexity of the state evolution equation increases. In many cases the location of the boundary that separates the stopping and continuation regions is of primary interest. As such boundary evolution equations can provide insight into the structure and nature of these boundaries. The derivation of the boundary evolution equations rely on the smooth pasting condition at the interface between the stopping and continuation regions. Similar smooth pasting conditions are also common in several derivative securities and other optimal stopping problems, such as simultaneous hypothesis testing and earliest detection problems. See Peskir and Shiryaev (2006) for examples of other optimal stopping problems.

In the Black-Scholes setting we presented a modified integral method for pricing American options that relied on an integral representation of the price of the American option. This method proved to be extremely fast and accurate in the simple case of Black-Scholes. An extension to multi-factor models of the integral representation has been presented in Detemple and Tian (2002) and an interesting direction of future research would be to apply the boundary evolution equations for stochastic volatility found in this paper to a modified integral method for multi-factor models.

Two other classes of stochastic control problems whose solutions are

characterized by free-boundary problems are singular and impulse control. In these problems the state process is not terminated at the boundary, but a control is applied to it. Both deriving boundary evolution equations and constructing computational methods for these would be interesting future work. The ideas in this paper cannot be immediately extended to optimal stopping problems with multiple boundaries and this would be interesting future work as well.

Chapter 3

Impulse Control of Interest Rates

3.1 Introduction

This chapter develops a numerical method to solve a general class of Impulse control problems and uses the solution to study the yield curve of interest rates when a nation's central bank intervenes, via an Impulse control, in the short-term interest rate market. Interest rate securities make up a huge portion of the global financial markets. McKinsey and Company (2011) estimates that the size of the global interest rate securities market in 2011 was $157 trillion, while the global equities market was only $54 trillion. The dynamics of interest rates have been heavily studied in the financial literature. Most of these studies have made the assumption that interest rates move freely in an open market. Relatively, much less attention has been given to studies that consider the optimal control of interest rates by a nation's central bank that has the power to intervene in the interest rate market. This ability to intervene in the interest rate market is seen, for example, in the United States through the Federal Reserve's open market operations (Freund and Guttentag (1969)). Here the Federal Reserve (Fed) periodically sets a target short term interest rate (Fed funds target rate) and trades various securities in large quantities to keep the short term rate close to this target. This is a common

practice in many other countries as well. The Fed issued large interventions in the short term interest rate market 41 times between 2000–2012[1] and in each of these instances there were large jumps in the interest rate market indicating that it is important to investigate the Fed's intervention policy and the way this policy affects longer term interest rates.

A central bank may want to intervene in the interest rate market for several reasons; it may wish to limit inflation to a certain level or it may want to maintain a certain exchange rate with another country. Rather than investigating the motivations for the bank's interventions, we assume that the bank is able to precisely quantify its preferences and tolerances. Specifically this means that the bank is able to quantify its relative tolerances for various rates above and below its preferred rate level. Also motivated by the frequency and size of observed interest rate interventions, we assume that the central bank's aversion to intervening too often can be captured by a 'cost' of intervention that the bank can quantify as fixed cost with an optional proportional component. The Fed's objective is then to find the best intervention strategy. Our goal is to compute and examine the implications that these interventions have on the term structure of interest rates. In doing this we find that the model is able to replicate the market's current yield curve. We can therefore replicate the current state of the interest rate market while assuming that in the future the central bank may intervene. This possibility has not yet been seen in the

[1]Data from the Federal Reserve Bank of New York.
www.newyorkfed.org/markets/omo/dmm/historical/fedfunds/index.cfm

interest rate literature.

This paper considers a model in which a country's central bank can intervene in the domestic short term interest rate market. The model allows for many popular stochastic short rate models in literature. Given the costs of deviating from the target rate and the costs of control, the objective of the central bank is to find the optimal policy that strikes the best balance between frequent intervention and large deviations from the target rate. This yields a stochastic control problem and more specifically a stochastic 'impulse' control problem due to the generality of the cost structure. We model the central banks intervention policy as an impulse control because of the frequency and size of the Fed's interventions. A classical control model is only appropriate when the Fed can make changes to the rate-of-change of short rate rather than bring about an instantaneous change to the short rate directly. Moreover the size of short rate jumps are rather significant and hence a singular control model would be inappropriate as well. Of the 41 times the Fed intervened between 2000 – 2012 the average magnitude of intervention was about 14% of the Fed funds rate.

Such impulse control problems, where the controller has the ability to bring about a discontinuity in the state (the short rate) dynamics, are notoriously hard to solve. Impulse controls are natural ways to model the large economic decisions that are made infrequently but are often approximated with controls that do not bring about such discontinuity (for example by only allowing proportional costs of control), to foster solvability. There is absolutely

no hope of finding closed form solutions of impulse control problems and all solution methods that are available are numerical. While one can discretize the problem and then brute force the solution using value or policy iteration, these methods are very inefficient even for singular control problems. For impulse control problems, these inefficiencies are even worse. Moreover since there are several short rate models, this paper also develops an iterative method that can solve a very general class of impulse control problems and can hence easily be applied to a very wide range of impulse control problems beyond the realm of interest rate models. We provide relevant convergence results and derive error bounds for intermediate iterations. A version of this work is forthcoming in Mitchell et al. (2014a).

3.1.1 Related literature and outline

Two main streams of literature are relevant; interest rate models and impulse control. In following the overview of the interest rate literature we focus mostly on short rate models. We concentrate on short rate models because the Fed's main avenue for intervention is in the Fed Funds market, which is an extremely short term, overnight, interest rate market. Additionally short rate models are mathematically tractable and guarantee the absence of arbitrage, see for example Chapter 6.5 in Shreve (2004).

In a popular paper, Vasicek (1977) finds a closed form expression for bond prices when the short rate follows a simple mean reverting Ornstein-Uhlenbeck process. Cox et al. (1996) presents a more robust model for the

short rate that includes state dependent volatility and again finds a closed form solution for bond prices. Hull and White (1987) generalizes these models and also finds closed form solutions to bond prices that are able to match any existing yield curve and Black and Karasinski (1991) considers a model for the log of the short rate. Chan et al. (1992) makes an empirical comparison of several short rate models and Chapman and Pearson (2000) investigates nonlinearities in short rate models. Piazzesi (2005) examines the yield curve when the Fed funds target rate follows a compound Poisson process, Balduzzi et al. (1997) looks at the effect of policy changes by the Fed on the yield curve, and Rudebusch (1995) models the behavior of the Federal Reserve's intervention behavior and examines the effect of this on the yield curve.

We model the central bank's ability to intervene in the interest rate market as an impulse control problem. Impulse control problems are seen, for example, in Constantinides and Richard (1978) to model a cash management problem and in Sulem (1986) to model an inventory management problem. Harrison et al. (1983) study impulse control in a canonical setting and Feng and Muthuraman (2010) present a computational method for solving an impulse control problem in the case of a Brownian motion. Dai and Yao (2012a) proves a general property of impulse control strategies under Brownian motion. Additionally, there has been some work at the interface of these two areas. In particular Cadenillas and Zapatero (1999) presents a model in which the central bank wishes to keep exchange rates at a certain level. To achieve this goal the bank issues an impulse control on the exchange rate and in Cadenillas

and Zapatero (2000) the bank also has the ability to exactly set the interest rate. The stochastic dynamics in Constantinides and Richard (1978), Sulem (1986), Feng and Muthuraman (2010) and Dai and Yao (2012a) are restricted to a Brownian motion. The dynamics in Cadenillas and Zapatero (2000) and Cadenillas et al. (2010) are restricted to geometric Brownian motion and an Ornstein-Uhlenbeck process, respectively.

The computational method developed in this paper is a generalization of the method presented in Feng and Muthuraman (2010) which works only for the impulse control of a Brownian motion. Feng and Muthuraman (2010) leverages heavily on the restriction on Brownian motions and also on the past results that were known for the Brownian case. Popular interest rate models will not fall within the scope of Feng and Muthuraman (2010) and a generalization is needed. While it is exciting to see that the idea of transforming a free boundary problem to a sequence of fixed boundary problems can be helpful in solving a very general class of stochastic processes, establishing the necessary convergence results in this general case is a significant challenge and more involved. Apart from the required proofs of convergence, we also present an ϵ-optimality result. Since all numerical algorithms have to be stopped after convergence within a tolerance, the ϵ-optimality result is extremely critical as it maps the tolerance to bounds on the objective value.

The rest of the paper is organized as follows. In Section 3.2 we present the stochastic model for the evolution of interest rates and describe the central bank's possible intervention strategies. Section 3.3 describes the equation for

the expected cost of control and presents an algorithm that minimizes this cost by solving a free boundary problem for a large class of stochastic processes. Then using this optimal control policy in Section 3.4 we find the price of a zero coupon bond and show that the model is able to capture interesting term structures with a change of measure. Section 3.5 shows a few examples and highlights the differences between controlled and uncontrolled short rate processes. Finally, Section 3.6 concludes.

3.2 The Short Rate Model

Following the convention in Vasicek (1977) we start with a market in which the federal government issues default-free zero-coupon bonds that are traded in an open market. A zero-coupon bond is a bond which pays some known quantity, say \$1, when it matures with no intermediate payments, or coupons, before maturity. At time t, we say the price of such a bond that matures at time $T > t$ is $B(t, T)$, also called the discount factor. The yield to maturity of this bond is the value, $R(t, T)$, that satisfies

$$B(t, T) = e^{-R(t,T)\cdot(T-t)}. \tag{3.1}$$

The short rate, r_t, the instantaneous rate of interest is given by

$$r_t = \lim_{T \downarrow t} R(t, T). \tag{3.2}$$

As in Vasicek (1977) and Cox et al. (1996) we assume that the short rate follows a stochastic process, however we incorporate a very general model for

the stochastic process and we allow the central bank to control it. We model the uncontrolled short rate as a general stochastic process, under the physical measure, described by

$$d\hat{r}_t = \mu(\hat{r}_t)dt + \sigma(\hat{r}_t)dW_t. \tag{3.3}$$

This general form allows for several common stochastic processes. For example, if $\mu(r) = a - b \cdot r$ and $\sigma(r) = \sigma_0\sqrt{r}$ then Equation (3.3) is the familiar mean reverting square root model used to model the short rate in Cox et al. (1996). Additionally, if $\sigma(r) = \sigma_0$ then Equation (3.3) is an Ornstein-Uhlenbeck process used to model the short rate in Vasicek (1977). Arithmetic and geometric Brownian motion are also both possible in this framework.

The central bank is then able to apply an impulse control to the short rate, which allows them to instantaneously move the short rate up or down by some non-zero amount. An impulse control, ν, is defined as a sequence of non-decreasing stopping times $\{\tau_i\}_{i=1}^{\infty}$ associated with the corresponding amounts of control $\{\xi_i\}_{i=1}^{\infty}$. Given an impulse control $\nu = (\tau_1, \xi_1; \cdots; \tau_i, \xi_i; \cdots)$, the controlled short rate becomes

$$\begin{cases} dr_t = \mu(r_t)dt + \sigma(r_t)dW_t & \tau_i \leq t < \tau_{i+1} \\ r_{0-} = r \\ r_{\tau_i} = r_{\tau_i -} + \xi_i. \end{cases} \tag{3.4}$$

As mentioned earlier, we assume that the central bank has the ability to quantify its preferences and tolerances for the level of the short rate. Specifically, this implies that the central bank is able to quantify its desire for the short rate to remain at a target rate with a running cost function and its aversion

to intervention through fixed and proportional costs. These costs do not necessarily represent money paid by the central bank, rather the running cost reflects the bank's desire for the short rate to be at a certain target level, and the control costs represent the bank's aversion from intervening in the interest rate market, similar to the policy maker's objective in Lohmann (1992) and Cadenillas and Zapatero (1999). The central bank must weigh these two goals and make a decision about how to best control the interest rate market. The central bank's goal is to find the optimal control policy, ν, to minimize these costs but in order to do this we must first define the cost structure that encompasses running costs and control costs.

At each moment, t, we say the economy with short rate r_t incurs a running cost at a rate of $h(r_t) \geq 0$, where h is designed to penalize the bank for deviations from the target short rate; for example if the central bank's target short rate is 1% then h could be increasing above and decreasing below 1% to represent the desire for the rate to stay at 1%. The central bank also incurs a cost, $G(\xi)$, each time it applies a control of size ξ to the short rate. This represents the central bank's desire to avoid intervening too often in the market. The cost of control has two components, a fixed component and an optional proportional component. This means that each time the government increases or decreases the short rate they suffer a fixed cost, as well as a cost proportional to the amount by which they move the short rate. It is apparent that central banks do not want to intervene in the interest rate market often, and for this reason it makes sense that there is a perceived fixed cost for each

time the bank exerts control. We define the cost of control as

$$G(\xi) = \begin{cases} K + k \cdot \xi & if \quad \xi \geq 0, \\ L - l \cdot \xi & if \quad \xi < 0. \end{cases} \tag{3.5}$$

where $K, L, k, l > 0$. Here we can see that the cost of control is an asymmetric function of ξ; the fixed cost of increasing or decreasing the short rate are K and L, respectively, and the proportional cost of increasing or decreasing the short rate by ξ are k and l, respectively. We consider an infinite planning horizon and we discount future costs at a rate $\beta > 0$. Putting all this together the central bank's objective is to pick a control policy to minimize the expected value of future discounted costs. The total expected cost of using control ν is given by

$$\mathcal{J}_r(\nu) = \mathbb{E}\left[\int_0^\infty e^{-\beta t} h(r_t)dt + \sum_n e^{-\beta \tau_n} G(\xi_n) \middle| r_0 = r\right]. \tag{3.6}$$

In order for this to be a well defined problem we only consider those impulse controls, ν, such that $\forall r < \infty,\ \mathcal{J}_r(\nu) < \infty$ as in Harrison et al. (1983). We also place some technical restrictions on h to avoid trivial solutions. The restrictions on h are detailed in the following assumption.

Assumption 3.1. The function $h(\cdot)$ is a non-negative function, and it is continuously differentiable with the only possible exceptions at a finite set N_h, and there exist a point x_0 such that

- $h(r)$ is non-increasing for all $r < x_0$
- $h(r)$ is non-decreasing for all $r > x_0$

Also, there exist some points z_1 and z_2 such that

- $h'(r) > (\beta - \mu'(r)) \cdot l$ for all $r > z_2$ and
- $h'(r) < -(\beta - \mu'(r)) \cdot k$ for all $r < z_1$.

Furthermore,

- $h'(r) \geq (\beta - \mu'(r)) \cdot l$ implies $h'(z) \geq (\beta - \mu'(r)) \cdot l$ for all $z > r$ and
- $h'(r) \leq -(\beta - \mu'(r)) \cdot k$ implies $h'(z) \leq -(\beta - \mu'(r)) \cdot k$ for all $z < r$.

The intuition of Assumption 3.1 is that, when the short rate becomes too large or too small the running cost h will grow fast enough that it is better to intervene in the short rate. Assumptions on h made in Constantinides and Richard (1978), Feng and Muthuraman (2010) and Dai and Yao (2012b) are special cases of Assumption 3.1.

Definition 3.1. An impulse control $\nu = (\tau_1, \xi_1; \cdots; \tau_i, \xi_i; \cdots)$ is called *admissible* if the following conditions are satisfied,

- $|\xi_i| > 0, \tau_i < \tau_{i+1}$, and ξ_i is $\mathcal{F}_{\tau_i}$ measurable for every i;
- $\mathcal{J}_r(\nu) < \infty \ \forall r < \infty$;
- The controlled state process r_t satisfies the growth conditions

$$\lim_{t\to\infty} e^{-\beta t}\mathbb{E}\left[\left|r_t\right|\right] = 0, \tag{3.7}$$

$$\mathbb{E}\left[\int_0^\infty e^{-2\beta t}\sigma^2(r_t)dt\right] < \infty. \tag{3.8}$$

The collection of all the admissible impulse controls is denoted $\mathbb{A}$.

Equation (3.7) and (3.8) guarantee that the controlled short rate does not grow uncontrollably and are essentially mild technical conditions similar to the ones in Korn (1997).

3.3 The Value Function

The bank's objective is to find a control, ν , such that the associated cost function $\mathcal{J}_r(\nu)$ is minimized. We call the cost optimal function corresponding to such a control the value function,

$$V(r) = \min_{\nu \in \mathbb{A}} \mathcal{J}_r(\nu). \tag{3.9}$$

Bensoussan and Lions (1973) use Quasi-Variational-Inequalities (QVI) to study stochastic impulse control problems. Thereafter, QVIs have become a standard way of formulating impulse control problems. The main goal of QVI is to adopt dynamic programming arguments with Itô's formula to characterize the value function and the optimal control using a differential equation problem. The QVI is derived using the idea that if at time zero we use some control for an infinitesimal amount of time, and then immediately switch to the optimal control, the resulting cost cannot be less than the cost function associated with the optimal control applied since the very beginning. We now develop the QVI for the problem considered here with a brief explanation.

First, let $\mathcal{A}$ be the infinitesimal generator of the uncontrolled process,

so that

$$\mathcal{A}v(r) = \frac{1}{2}\sigma^2(r)v''(r) + \mu(r)v'(r).$$

Then, assuming enough smoothness, we have $\mathcal{A}V(r) - \beta \cdot V(r) + h(r) \geq 0$ (a.e.). This is the result of the aforementioned dynamic programming argument, no intervention is placed during $t \in [0, \Delta t)$ for some small $\Delta t > 0$ and then we switch to the optimal policy thereafter, the resulting cost function will be no better than the optimal; letting Δt go to zero and appling Itô's formula gives us this result.

Also due to the dynamic programming argument, for any given r and ξ we have $V(r+\xi) + G(\xi) - V(r) \geq 0$. This means, if at time zero we place some intervention (to increase or reduce the short rate process) and then switch to the optimal control policy, the resulting cost function will be at best equal to the optimal one. Taking infimum over all possible ξ yields $\inf_\xi V(r+\xi) + G(\xi) - V(r) \equiv \mathcal{Q}V(r) \geq 0$. The dynamic programming argument implies that one of these inequalities should be tight for each value of r, depending upon what is optimal. Putting all this together we have the following Quasi-Variational-Inequalities

$$\begin{cases} \mathcal{A}V(r) - \beta \cdot V(r) + h(r) & \geq 0 \ \text{ a.e. } r, \\ \inf_\xi V(r+\xi) + G(\xi) - V(r) \equiv \mathcal{Q}V(r) & \geq 0 \ \forall\ r, \\ \mathcal{Q}V(r) \cdot [\mathcal{A}V(r) - \beta \cdot V(r) + h(r)] & = 0 \ \forall\ r. \end{cases} \tag{3.10}$$

Hereafter, we refer to (3.10) as the QVI for the impulse control problem considered. Theorem 3.1 says that, if a cost function v associated with an

admissible impulse control policy $\hat{\nu}$ satisfies the QVI (3.10) together with some technical conditions, then v coincides with the value function V.

Theorem 3.1 (Verification Theorem). Suppose $v(r)$, the cost function associated with an admissible impulse control policy $\hat{\nu}$, satisfies the QVI (3.10). If the following are satisfied

1. v is linear for $r \leq d$ and $r \geq u$ for some $d < u$,
2. $v \in C^1(\mathbb{R}) \cap C^2(\mathbb{R} \setminus \{d, u\})$,

then v coincides with the value function V.

The proof can be found in the appendix.

Due to the dynamic programming argument, in the region $\mathcal{C} = \{r : \mathcal{A}V(r) - \beta \cdot V(r) + h(r) = 0\}$, the optimal decision is not to intervene. Such a region, $\mathcal{C}$, is called the continuation region. As soon as the process leaves the continuation region we have $\mathcal{Q}V(r) = 0$, and thus the control implied by the QVI chooses to intervene by increasing or decreasing the short rate by the appropriate amount. We next describe the differential equation problem that will enable us to find the continuation region as well as the value function.

3.3.1 The free boundary problem

The value function, V, which solves the QVI, partitions $\mathbb{R}$ into two disjoint sets, the continuation region and the intervention region. To search for the optimal policy is essentially to search for boundaries of the continuation

region and the size of the intervention when the short rate hits the boundaries of the continuation region. Such a problem, wherein the boundaries must be computed as part of the solution, is called a free boundary problem.

A control band policy is a policy that can be characterized by four points, d, D, U and u with $d < D \leq U < u$. The corresponding strategy is to exert intervention if the short rate attempts to exit (d, u) and the process is left uncontrolled when in (d, u). When the short rate strikes or is below d, the control policy instantaneously increases it to D and similarly when the rate strikes or is above u the policy instantaneously decreases it to U. This policy is illustrated in Figure 3.1. In this paper we will focus exclusively on control band policies and we will show, by construction, that the optimal policy is a control band policy.

Now given any admissible impulse control policy, ν, characterized by a control band $(d,\ D,\ U,\ u)$, Theorem 3.2 shows that we obtain its cost function $\mathcal{J}_r(\nu)$ by solving the following second-order differential equation problem with fixed boundary

$$0 = \mathcal{A}v(r) - \beta \cdot v(r) + h(r),\ \forall r \in (d, u), \tag{3.11}$$

$$v(d) = v(D) + K + k \cdot (D - d), \tag{3.12}$$

$$v(u) = v(U) + L + l \cdot (u - U). \tag{3.13}$$

Theorem 3.2. Suppose ν is an admissible impulse control characterized by $(d,\ D,\ U,\ u)$. If $v(r) \in C^2(d, u)$ solves the differential equation problem

Figure 3.1: Evolution of r_t under a (d, D, U, u) policy

(3.11)-(3.13) in $[d, u]$, then $v(r)$ is equal to the cost function $\mathcal{J}_r(\nu)$ associated with ν for $r \in [d, u]$.

The proof can be found in the appendix.

By the definition of the $(d,\ D,\ U,\ u)$ policy, we can see that

$$\mathcal{J}_r(\nu) = \begin{cases} v(D) + K + k \cdot (D - r) = v(d) + k \cdot (d - r) & if \quad r \leq d \\ v(U) + L + l \cdot (r - U) = v(u) + l \cdot (r - u) & if \quad r \geq u. \end{cases} \tag{3.14}$$

This enables us to obtain the cost function associated with $(d,\ D,\ U,\ u)$ for every possible r by extending v from (d,u) to the whole real line. Hereafter we denote v as the solution to Equations (3.11)-(3.13) together with the extension in Equation (3.14).

Now, given a control policy, ν described by $(d,\ D,\ U,\ u)$ we solve the boundary value problem described in Equations (3.11)-(3.13) to compute v

and extend it with (3.14). We then use Theorem 3.2 to verify that this is equal to $\mathcal{J}_r(\nu)$. This means that finding the optimal control policy is the same as finding the $(d,\ D,\ U,\ u)$ such that the resulting v satisfies the optimality conditions in Equation (3.10), meaning V is the solution to a free boundary problem.

In the next section we describe an efficient method to find the optimal policy corresponding to the solution to the free boundary problem.

3.3.2 Finding the free boundary

In order to solve the free boundary problem from the previous section, we now describe an iterative algorithm that converts the free boundary problem into a sequence of fixed boundary problems and we restrict our attention to control band policies. For some given control band policy characterized by (d_n, D_n, U_n, u_n) we find the associated cost function as the solution to Equations (3.11) - (3.14), and call this V_n. Then with this policy and cost function the algorithm finds a new policy and cost function, $(d_{n+1}, D_{n+1}, U_{n+1}, u_{n+1})$ and V_{n+1}, that is closer to the optimal control policy and value function. Upon iteration we find that this algorithm monotonically converges to the optimal control policy and value function.

To begin the algorithm we start with an initial guess policy (d_0, D_0, U_0, u_0) with $d_0 < D_0 \leq U_0 < u_0$. We obtain the associated cost function by solving the fixed boundary problem (3.11)–(3.14) and denote it V_0. The choice of this initial guess is not entirely trivial because we must be sure that the optimal

continuation region is contained within (d_0, u_0). We can check this property with the following condition,

$$\lim_{r \downarrow d_0} V_0'(r) + k \geq 0 \tag{3.15}$$

$$\lim_{r \uparrow u_0} V_0'(r) - l \leq 0. \tag{3.16}$$

We say that an initial guess satisfies the *superset condition* if the above inequalities hold. An initial guess can be found easily by, for example, increasing the length of (d_0, u_0), by say 50%, repeatedly until the superset condition is satisfied. Intuitively, if the superset condition is not satisfied, say $\lim_{r \downarrow d_0} V_0'(r) + k < 0$, then it indicates that in the neighborhood above d_0, the cost function decreases faster than the cost of control. However, when r is sufficiently small, by assumption the running cost grows fast enough to justify the exertion of control to increase the short rate. This means, when d_0 is small enough, the proportional control cost decreases faster than the cost function in the neighborhood of d_0, which will make the superset condition at d_0 satisfied. An analogous argument holds for sufficiently large u_0. A similar explanation of the assumptions made on the running cost function, h, can be found in Constantinides and Richard (1978), Feng and Muthuraman (2010), and Dai and Yao (2012b). Once such an initial guess of (d_0, D_0, U_0, u_0) and V_0 are found we begin our iteration by setting $n = 0$.

The next step of the algorithm is to find new values of d and u. We

define these new values as

$$d_{n+1} = \sup\left\{y \in [d_n, D_n) : \forall r \in [d_n, y],\ V_n'(r) + k \geq 0\right\}, \tag{3.17}$$

$$u_{n+1} = \inf\left\{y \in (U_n, u_n] : \forall r \in [y, u_n], V_n'(r) - l \leq 0\right\}. \tag{3.18}$$

We illustrate the update procedure for d in Figure 3.2. The solid black line in the figure represents the cost function on an iteration. We see that between d_n and d_{n+1} we have $V_n'(r) + k \geq 0$ and that the slope at d_{n+1} is equal to $-k$. We also illustrate the boundary condition from Equation (3.12) here which relates the values of the cost function at d_n and D_n.

We select d_{n+1} in this way because in a region above d_n if we have $V_n' \geq -k$ then the proportional cost decreases at least as fast as the value function, suggesting it would be beneficial to increase d. Also, we know that at convergence we want the first derivative to be continuous across d, as required by Theorem 3.1, so we pick d_{n+1} to help satisfy that constraint. Similar reasoning holds for u_{n+1} also. We can see in this figure that the slope of V_n at d_{n+1} is equal to $-k$. This helps us see that at convergence the value function should have a continuous first derivative, otherwise known as the smooth pasting principle.

After we find the new values d_{n+1} and u_{n+1} we find the cost function associated with the control band policy characterized by $(d_{n+1}, D_n, U_n, u_{n+1})$ by re-solving Equations (3.11) - (3.13). We call this cost function $\bar{V}_n(r)$. With

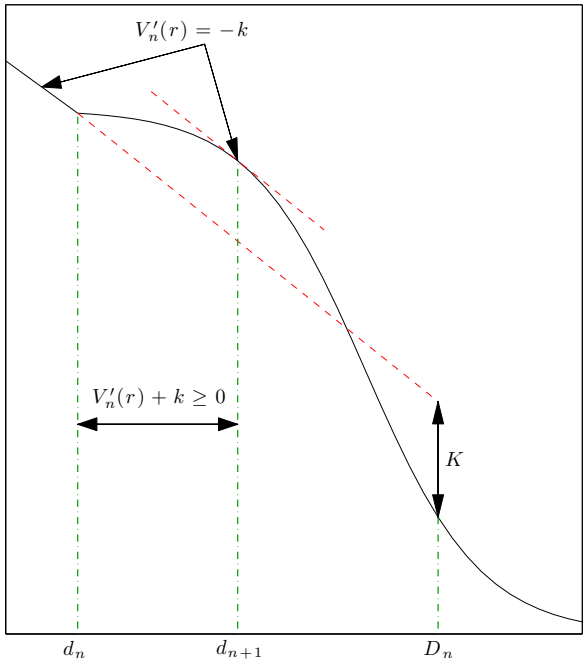

Figure 3.2: An illustration of updating d and Equation (3.12)

this new cost function, $\bar{V}_n(r)$, we define new values of D and U as

$$D_{n+1} = \underset{r\in(d_{n+1},u_{n+1})}{\arg\min} \left\{\bar{V}_n(r) + k \cdot r\right\}, \tag{3.19}$$

$$U_{n+1} = \underset{r\in(d_{n+1},u_{n+1})}{\arg\min} \left\{\bar{V}_n(r) - l \cdot r\right\}. \tag{3.20}$$

Later we will show that $D_{n+1} \leq U_{n+1}$. D_{n+1} and U_{n+1} are chosen to be the most efficient 'jump to' points for the given associated cost function. With $(d_{n+1}, D_{n+1}, U_{n+1}, u_{n+1})$ we can finally find $V_{n+1}(r)$ by solving Equations (3.11) - (3.13) with these new boundary locations, and then iterate this until convergence. We present a flowchart that illustrates this algorithm in Figure 3.3.

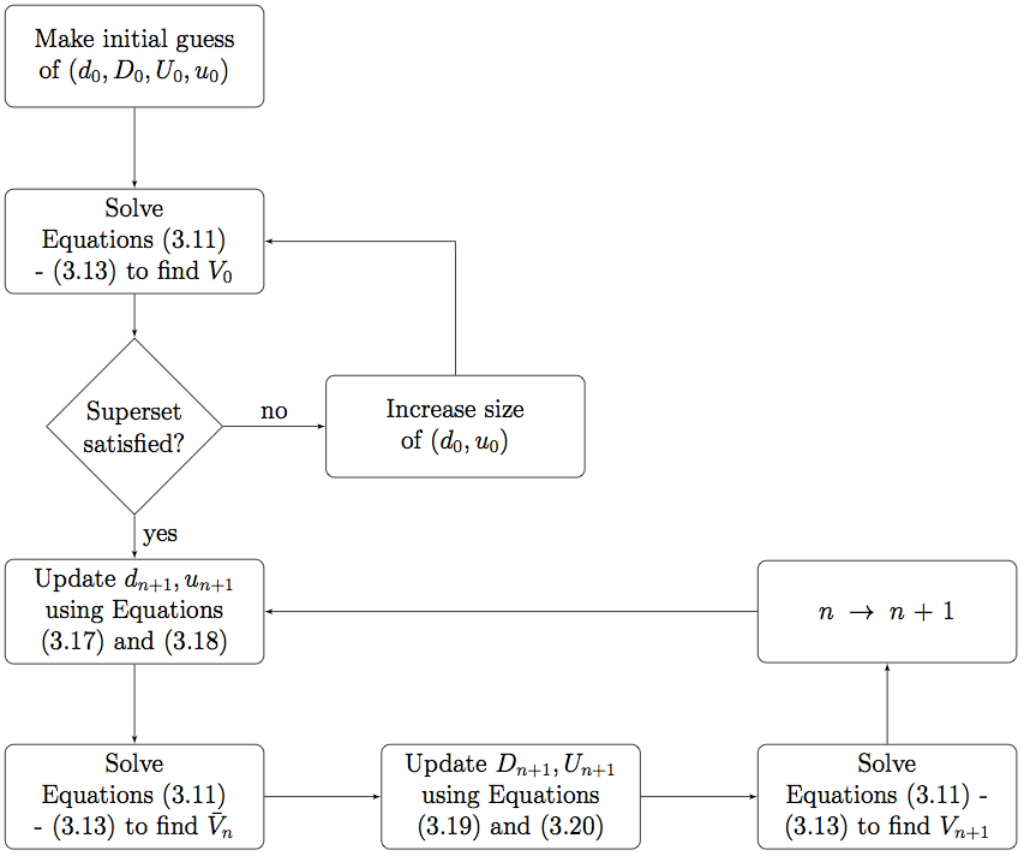

Figure 3.3: Description of boundary update algorithm

Theorem 3.3 shows that for any r we have $V_{n+1}(r) \leq V_n(r)$ and the superset condition holds with the new V_{n+1}, d_{n+1} and u_{n+1}. These conditions warrant the repetitive improvement on the cost function as well as a sequence of shrinking continuations regions, (d_n, u_n).

Theorem 3.3. Given an admissible impulse control policy characterized by $(d_n,\ D_n,\ U_n,\ u_n)$, let $V_n(r)$ be defined by the solution to Equations (3.11)-(3.14). If V_n and $(d_n,\ D_n,\ U_n,\ u_n)$ satisfy the superset condition, let d_{n+1},

u_{n+1}, $\bar{V}_n$, D_{n+1}, U_{n+1} and V_{n+1} be as in the above algorithm, then we have

1. $\bar{V}_n(r) \leq V_n(r), \quad \forall r$
2. $\lim_{r \downarrow d_{n+1}} \bar{V}_n'(r) + k \geq 0$, $\lim_{r \uparrow u_{n+1}} \bar{V}_n'(r) - l \leq 0$
3. $D_{n+1} \leq U_{n+1}$
4. $V_{n+1}(r) \leq \bar{V}_n(r), \quad \forall r$
5. V_{n+1} satisfies the superset condition with d_{n+1} and u_{n+1}, which means $\lim_{r \downarrow d_{n+1}} V_{n+1}'(r) + k \geq 0$ and $\lim_{r \uparrow u_{n+1}} V_{n+1}'(r) - l \leq 0$.

The proof of this theorem can be found in the appendix.

Theorem 3.3 establishes that the boundary update procedure can be iteratively used to improve the cost function monotonically and to shrink the continuation region, thus the scheme is guaranteed to converge. Figure 3.4 gives an illustration of a sequence of V_n. The sequence is monotonically decreasing and the dots on each curve represent (d_n, D_n, U_n, u_n). Each V_n in the sequence is not expected to be in C^1 over the whole space, however the v associated with the converged (d, D, U, u) policy is expected to have a continuous derivative everywhere due to the smooth pasting nature of the boundary update equations (3.17) and (3.18). The following theorem provides the conditions that guarantee the optimality of the cost function obtained at convergence, given that it is C^1.

Theorem 3.4. Suppose that $h(r)$ satisfies Assumption 3.1 and let (d, D, U, u) be the policy obtained at convergence with v, its associated cost function. This implies that $v(r)$ solves (3.11)–(3.14) and that v is C^1. If $\beta - \mu'(r) \geq 0 \; \forall r$ then it is identical to the optimal value function V. If, however, $\beta - \mu'(r) < 0$ for some r, and if $h'(d) + (\beta - \mu'(d)) \cdot k \leq 0$, $-k < v'(r) < l$ in (D, U), $v'(r) + k \leq 0$ in $[d, D]$, $-v'(r) + l \leq 0$ in $[U, u]$, and $h'(u) + (\mu'(u) - \beta) \cdot l \geq 0$ then $v(r)$ is identical to the value function $V(r)$, and $(d,\ D,\ U,\ u)$ is the corresponding optimal control policy.

The proof is given in the appendix.

We can see that popular short rate models such as the Vasicek and the CIR model have $\mu'(r) < 0$ which falls into the case $\beta - \mu'(r) \geq 0$. Therefore, the optimality of the solution obtained by the monotone improvement scheme is warranted. For general diffusion process with drift that does not necessarily satisfy $\beta - \mu'(r) \geq 0 \; \forall r$ we have provided additional conditions for optimality in Theorem 3.4.

Since any computational iteration must be stopped when a specific tolerance is reached, the question of how the tolerance relates to deviations from optimality is important. The following theorem and corollary provide an upper bound on the difference between the optimal value function and the cost function associated with the (d, D, U, u) policy obtained in any step of the scheme. It is also important to note that while the convergence to optimality established in Theorem 3.4 requires some conditions on $\beta - \mu'(r)$, the ϵ-optimality result that follows does not make any assumptions on $\mu'(r)$.

Theorem 3.5 ($\epsilon-$Optimality). Suppose $v(r)$ is the cost function associated with some admissible impulse control characterized by $d < D \leq U < u$. If $v(r)$ satisfies the following conditions for some $\epsilon_1,\ \epsilon_2,\ \epsilon_3 > 0$

$$\begin{cases} \mathcal{A}v(r) - \beta \cdot v(r) + h(r) & \geq -\epsilon_1 \text{ a.e. } r \\ \inf_{\xi>0} \left\{ v(r+\xi) + K + k \cdot \xi \right\} - v(r) & \geq -\epsilon_2 \\ \inf_{\xi>0} \left\{ v(r-\xi) + L \ + l \cdot \xi \right\} - v(r) & \geq -\epsilon_3 \end{cases}$$

$$\begin{aligned} v'(d+) + k &\geq 0 \\ -v'(u-) + l &\geq 0 \end{aligned}$$

then we have

$$v(r) \leq (1 + \frac{\epsilon_2}{K} + \frac{\epsilon_3}{L}) \cdot V(r) + \frac{\epsilon_1}{\beta}.$$

in which $V(r)$ is the value function.

The detailed proof is found in the appendix.

Corollary 3.1. Suppose $v(r)$ is the cost function associated with some admissible impulse control characterized by $d < D \leq U < u$. If $v(r)$ satisfies the following conditions for some $\epsilon > 0$

$$\begin{cases} \mathcal{A}v(r) - \beta \cdot v(r) + h(r) & \geq -\epsilon \text{ a.e. } r \\ \mathcal{Q}v(r) & \geq -\epsilon \end{cases}$$

$$\begin{aligned} v'(d+) + k &\geq 0 \\ -v'(u-) + l &\geq 0 \end{aligned}$$

then we have

$$v(r) \leq (1 + \frac{\epsilon}{\bar{K}}) \cdot V(r) + \frac{\epsilon}{\beta},$$

in which $\bar{K} \equiv \min\{K, L\}$

The detailed proof can be found in the appendix.

3.4 Bond Prices

This section focuses on pricing a bond whose short rate follows the optimally controlled dynamics. In the previous sections all computations were performed by the central bank under the physical measure because the bank is concerned with the actual deviations from the target short rate. Now, however, we must abandon this measure and use the risk-neutral measure to find bond prices, as this prevents arbitrage in the market.

We first note that the price of a bond is determined by the bond's tenor and the current short rate, in this way we can rewrite the price of a bond as $B(t, T, r)$. To find the price of the bond we must use the Girsanov theorem to change the physical measure to the risk neutral measure. In doing this we can rewrite the controlled dynamics between the stopping times that correspond to d and u as

$$dr_t = \tilde{\mu}(t, r_t)dt + \sigma(r_t)dW_t^Q, \quad \tau_i \leq t < \tau_{i+1}, \tag{3.21}$$

where $\tilde{\mu}(t, r)$ is determined by the market and W_t^Q is a Brownian motion under the risk-neutral measure. Given this representation the price of a bond is given

by

$$B(t,T,r) = \mathbb{E}^Q \left[e^{-\int_t^T r_s ds} \middle| r_t = r \right], \tag{3.22}$$

where the expectation is taken with respect to the risk-neutral measure, and the short rate process that is being evaluated includes the impulse controls administered by the central bank. This is the typical bond pricing formula however it is not very useful in our setting because we do not know $\tilde{\mu}(t,r)$. We therefore state the following theorem to find the appropriate change of measure and price a bond based on the controlled short rate.

Theorem 3.6 (Price of a Bond). The price of a bond, whose short rate follows the optimally controlled dynamics described in the previous section, satisfies the following PDE with boundary conditions

$$0 = \frac{\partial B}{\partial t} + (\mu(r) + \sigma(r) \cdot q(t,r)) \frac{\partial B}{\partial r} + \frac{1}{2}\sigma^2(r) \frac{\partial^2 B}{\partial r^2} - r \cdot B, \quad t < T,\ r \in (d,u) \tag{3.23}$$

$$B(T,T,r) = 1,\ \forall\ r, \tag{3.24}$$

$$B(t,T,d) = B(t,T,D),\ \forall\ t \leq T, \tag{3.25}$$

$$B(t,T,u) = B(t,T,U),\ \forall\ t \leq T, \tag{3.26}$$

where d, D, U and u describe the optimal control policy and $q(t,r)$ is the so-called market price of risk, and is independent of the bond's tenor.

The proof of this theorem, which relies on an arbitrage argument and closely follows Vasicek (1977), is found in the appendix.

The market price of risk, $q(t,r)$ found in Equation (3.23) represents the instantaneous trade off between the expected return of a bond per unit

of volatility and is to be observed by the market. Given this market price of risk, we can immediately recognize that $\tilde{\mu}(t,r) = \mu(r) + \sigma(r) \cdot q(t,r)$. If we take $\sigma(r)$ to be constant and $q(t,r)$ to be a function of only time, then this can be a variant of the model found in Hull and White (1987). This model has a closed form solution for Equations (3.23) and (3.24) without the boundary conditions (3.25) and (3.26), which is the solution to Equation (3.22) without control. However with these boundary conditions there is no closed form solution and thus any solution to the PDE with boundary conditions must be found numerically.

A convenient property of this model is that given the controlled dynamics of the short rate we can extract the market price of risk from the current yield curve, where the relationship between bond prices and the yield curve is defined in Equation (3.1). In fact, we are able to generate almost any desired yield curve by finding the appropriate market price of risk.

Under this model it is also possible to consider a market price of risk that is a function of both time and the short rate. We can select $\mu(r)$ and $q(t,r)$ in such a way that under the risk-neutral measure the dynamics of the short rate can be represented as

$$dr_t = \big(\bar{a}(t) - \bar{b}(t) r_t\big) dt + \sigma(r_t) dW_t^Q.$$

This means that we can represent the short rate as a mean reverting process with time varying mean and mean reversion rate, if $\bar{b}(t) > 0$. In this model we can still perfectly replicate the market's yield curve and we can also replicate

the interest rate derivative market as in Hull and White (1987).

3.5 Analysis of Results

In the previous sections we described how to find the optimal intervention policy and the yield curve based on that intervention policy. We now present a few examples that use these results to highlight the differences between a controlled and an uncontrolled short rate process. In our first example we take the uncontrolled short rate process to be a mean reverting square root process, as in Cox et al. (1996), described by $d\hat{r}_t = \lambda(\theta - \hat{r}_t)dt + \sigma\sqrt{\hat{r}_t}dW_t$, where we set $\lambda = 1,\ \theta = 0.07,\ \sigma = 0.12$. Additionally we set the costs of control to be $K = 0.005,\ k = 0.18,\ L = 0.005,\ l = 0.12,\ \beta = 0.01$. For the sake of illustration we take the running cost function to be $h(r) = 0.07\log(r/\theta)^2 + (\theta - r)^2$. This choice of non-linear running cost function is motivated by Cadenillas and Zapatero (2000). It captures the preference to keep rates well above zero and also the central bank's preference to keep the rate close to a target θ. This running cost function also satisfies the technical growth conditions, from Assumption 3.1, to ensure that the formulation is meaningful.

Under this short rate process and cost structure we can find the optimal control policy using the method discussed in Section 3.3.2. In Figure 3.4 we plot the sequence of $V_n(r)$ given an initial guess of $(d_0, D_0, U_0, u_0) = (0.005, 0.08, 0.12, 0.25)$. Here the cost functions, $V_n(r)$, are getting smaller in each iteration and the dots represent the intervention policy associated with each iteration of the algorithm. The algorithm converges to the optimal value

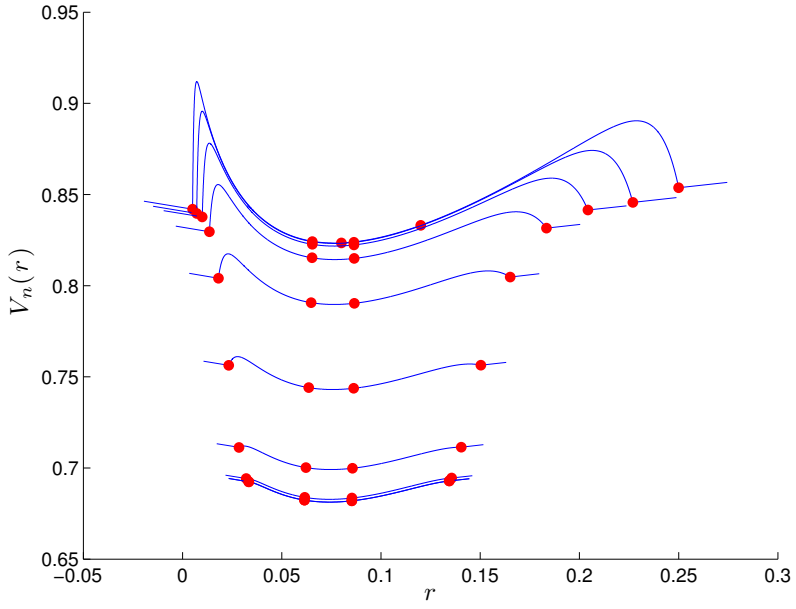

Figure 3.4: Converging sequence of V_n, dots represent (d_n, D_n, U_n, u_n) policy

function at the bottom of Figure 3.4 and the optimal policy is described by $(d, D, U, u) = (0.0334, 0.0614, 0.0853, 0.1343)$. While one can discretize the problem using the finite difference schemes proposed in Kushner (1976) and then brute force the solution using value or policy iteration, this methodology is not expected to perform well on impulse control problems due to the discontinuities in the state evolution that translates to insufficient smoothness in the value function for accelerated convergence. However, for illustration, comparing our method with that of using policy iteration on the discretized Markov chain, our method converges after 22 iterations in 0.176 seconds on a 10,000 point grid, while policy iteration in the controlled Markov chain case

converges after 703 iterations in 1,328 seconds on the same grid. Not only is the number of iterations much larger for the controlled Markov chain, the time spent for each iteration is larger too, resulting in almost 4 orders of magnitude difference.

In order to compute the yield curve we next use the optimal intervention strategy to solve the bond pricing problem found in Theorem 3.6. For this example we take the market price of risk, q, to be zero. With the solution to this problem we can then obtain the yield curve of interest rates based on the controlled short rate model. We plot the resulting yield curves for two initial values of the short rate in Figure 3.5. In this figure we plot the yield curve resulting from both the controlled and uncontrolled short rate process, the solid blue lines represent the yield curve of the controlled short rate process and the dashed green lines represent the yield curve of the uncontrolled short rate. There is a closed form solution to bond prices resulting from this uncontrolled short rate process found in Cox et al. (1996).

Plot (a) in Figure 3.5 shows the two yield curves when the initial value of the short rate is 4.5%. In this scenario the yield curve of the controlled short rate process is above the yield curve of the uncontrolled short rate. This is because when r_t is close to d the probability of the central bank intervening soon is increased. This means we expect the short rate to be elevated to D soon and thus the yield on longer term bonds that are controlled by the bank must have a higher yield than bonds that are not controlled by the bank. Similarly in plot (b) the yield curve of the controlled short rate is below that

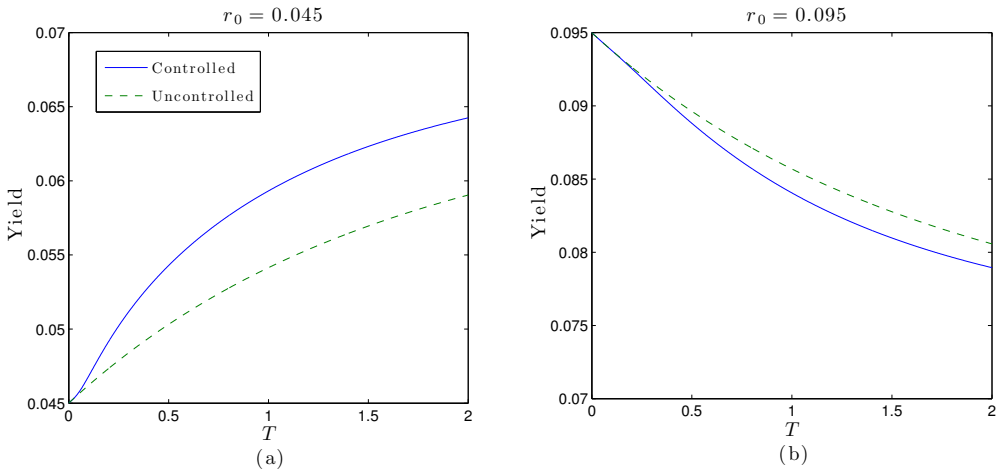

Figure 3.5: Yield curves for two initial values of the short rate

of the uncontrolled short rate, because when r_t is close to u to probability of the central bank pushing the short rate down to U soon is high.

The yield curves in Figure 3.5 consider high and low initial interest rates and in Figure 3.6 we examine the yield curve when the initial rate is equal to θ, the long-term mean of the CIR process. In this figure plot (a) shows the yield curve for the problem described above. In this scenario we see that while the yield curve of the uncontrolled process is decreasing the yield curve of the controlled process is increasing. This is a more drastic difference than the scenarios seen in Figure 3.5 because the shape of the yield curves here is different for the controlled and uncontrolled processes. In general the yield curve for an uncontrolled mean reverting process should be decreasing when the initial value is equal to the long-term mean due to the convexity in Equation (3.22). We find, however, that by issuing control the central bank can

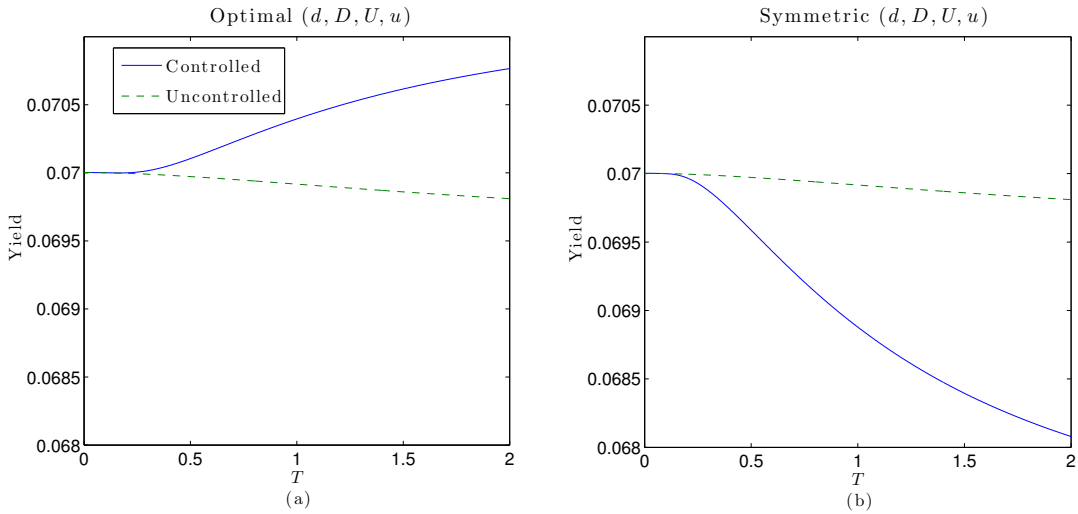

Figure 3.6: Yield curves for two control policies when $r_0 = \theta$

force this yield curve to be increasing. This could be due to the asymmetry in the optimal control band policy. In particular, since the running cost function is steep for small values of r_t the optimal policy issues control quickly when the process goes below the long-term mean. In contrast, the running cost function is less steep larger values of r_t and the optimal policy allows the process to go relatively high before issuing control. With this in mind we can see that the controlled short rate process will spend more time, on average, above θ than below resulting in an increasing yield curve in this case.

To confirm that this increasing yield curve is due to the asymmetry in the control band policy we next consider a control policy where the optimal d and u are symmetric around θ and so are D and U. The resulting yield curve is seen in plot (b) of Figure 3.6. In this plot we see that the yield curve of the controlled process is also decreasing. It is, however, decreasing faster

than the yield curve of the uncontrolled process, again due to the convexity in Equation (3.22) and the asymmetry of the CIR volatility. This example displays an important case where the central bank's intervention can not only change the level of the yield curve, but also the shape.

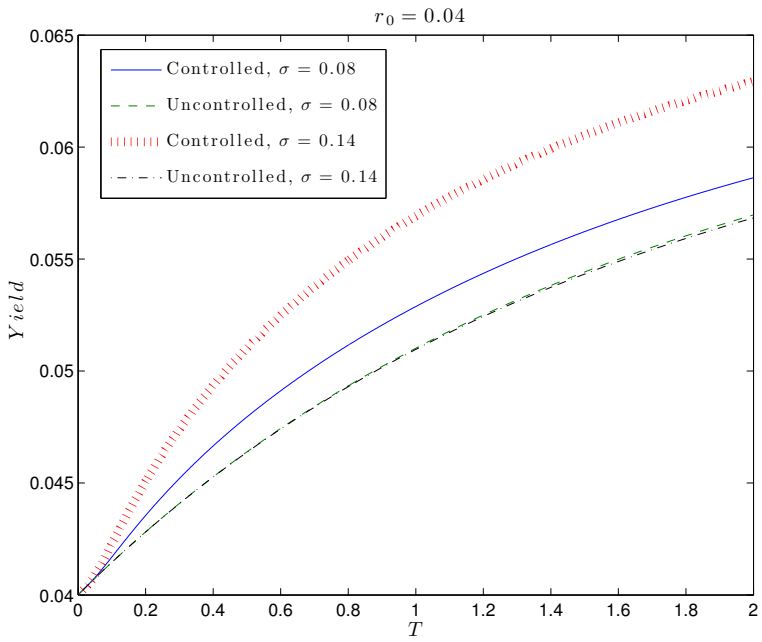

Figure 3.7: Yield curves for two values of σ

With everything else kept the same from the first example we also consider another example with two different values of σ. Figure 3.7 displays the controlled and uncontrolled yield curves when the initial short rate is 4% for the scenarios when $\sigma = 0.08$ and $\sigma = 0.14$.

In Figure 3.7 the yield curves from the uncontrolled short rate processes are close together, indicating that the volatility does not affect the yield curve

very much here. On the other hand the yield curves from the controlled short rate processes differ much more for different values of σ. This is because for the controlled short rate process σ affects the optimal intervention policy and thus the boundary conditions in Equations (3.25) - (3.26). For different control band policies the probabilities of intervention soon can change drastically, and this is seen in the resulting yield curves. In this example the probability of an intervention soon is higher for $\sigma = 0.14$ than for $\sigma = 0.08$ and thus the yield curve is also higher in this case.

In order to understand the model's dependence on volatility better we now examine the optimal control policy for different values of σ. In doing this we look at three popular short rate models, the Vasicek, the CIR, and the model found in Black and Karasinski (1991). The SDE for the uncontrolled short rate process in the Vasicek model is given by $d\hat{r}_t = \lambda(\delta - \hat{r}_t)dt + \phi dW_t$ and the SDE for the Black-Karasinski model is given by $d\hat{r}_t = \lambda(\mu - \log(\hat{r}_t))\hat{r}_t dt + \gamma \hat{r}_t dW_t$. In these two models we select the parameters so that the first two moments of the long-term distribution of the uncontrolled short rate processes are the same as for the uncontrolled CIR model. In each of the three models we use the same mean reversion parameter λ. For the Vasicek model this means we set $\delta = \theta$ and $\phi = \sigma\sqrt{\theta}$ and for the Black-Karasinski model we set

$$\begin{aligned} \mu &= \log(\theta) + \frac{1}{2}\log\left(\frac{\sigma^2}{2\lambda\theta} + 1\right) \\ \gamma &= \sqrt{2\lambda \log\left(\frac{\sigma^2}{2\lambda\theta} + 1\right)} \end{aligned}$$

where θ and σ are from the CIR model. In all three of these models with

parameters chosen this way the long-term mean and variance of the uncontrolled short rate are given by $\mathbb{E}[\hat{r}_t] = \theta$ and $\mathbb{V}\text{ar}[\hat{r}_t] = \frac{1}{2}\sigma^2\theta/\lambda$. We note that although these three models have equal average volatility, in the Vasicek model the instantaneous volatility is equal for all values of $\hat{r}_t$ however for the CIR and Black-Karasinski models the instantaneous volatility is asymmetric in $\hat{r}_t$. In order for these volatilities to average out to the same the CIR and Black-Karasinski models have smaller instantaneous volatilities for small values of the short rate and larger instantaneous volatilities for large values of the short rate. In addition to this asymmetry in volatility the Black-Karasinski model also has asymmetry in its drift term making the Black-Karasinski model the most asymmetric of the three.

In Figure 3.8 we show the optimal intervention policy for these three models, as a function of σ, when λ and θ are the same as in the previous examples. Here we have also changed the cost structure and set $K = L = 0.05$, $k = l = 0.15$, $\lambda = 1$, $\theta = 0.07$, $\beta = 0.01$ and $h(r) = 20(r-\theta)^2$. We have chosen cost functions like this so that the cost of control is completely symmetric about θ; that is it costs the same to issue positive and negative control, and the running cost is a symmetric function about θ. We can see in Figure 3.8 that the control policy for the Vasicek model is symmetric about θ. In plots (a) and (b) we see that the solid black line is the same in both plots, indicating that for the Vasicek model the central bank allows the short rate to deviate equally above and below θ before intervening. Also in plots (c) and (d) the solid black lines are the same, indicating that when the short rate process

hits d or u in the Vasicek model the central bank intervenes equally. This symmetry however is not present for the CIR or the Black-Karasinski model. This is due to the fact that in the Vasicek model the uncontrolled short rate is Gaussian and therefore symmetric, whereas in the CIR model the short rate follows a non-central χ^2 distribution and the Black-Karasinski model follows a Log-Normal distribution. Both of these distributions are asymmetric and therefore the central bank must account for this asymmetry when deciding its optimal control policy for the short rate.

For all three of these models we see that for larger values of σ the short rate must be further away from θ before the central bank intervenes. This can be seen in plots (a) and (b) in Figure 3.8; the curves are increasing with volatility in all cases. The reason that the central bank allows the short rate to deviate further for larger volatilities is that it must weigh the cost of being far away from θ with the cost of frequent intervention. For larger values of σ the cost of frequent intervention is dominant and thus the central bank must allow the short rate more freedom before intervening. We can see in plot (a) of Figure 3.8 that the Vasicek model is allowed the most freedom for smaller values of r, whereas the Black-Karasinski model is the most highly restricted. All three of these models have the same average volatility however for small values of r the Vasicek model has the most instantaneous volatility and the Black-Karasinski model has the least instantaneous volatility. This means that the potential for frequent intervention for small values of r is the most prevalent in the Vasicek model and therefore must be allowed the most

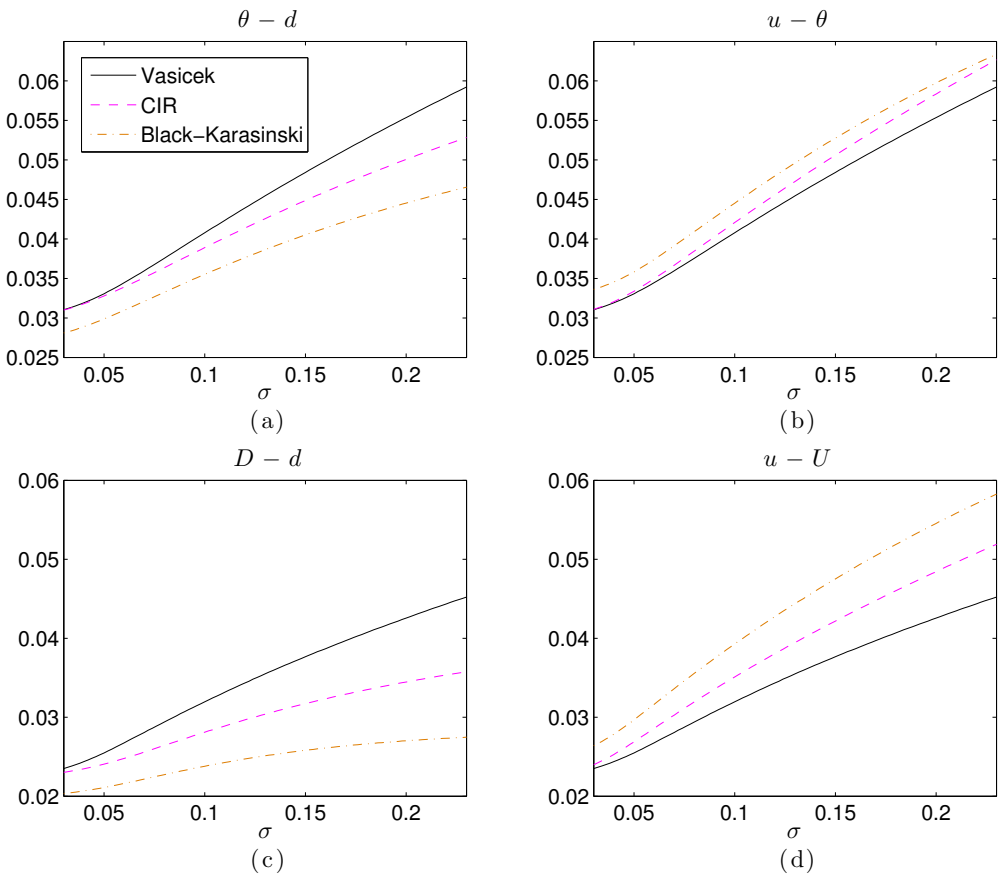

Figure 3.8: Control band policy as a function of σ for three different models, plots (a) and (b) show how far from θ the short rate must be before control is issued, plots (c) and (d) show how much control is issued each time a boundary is hit

freedom of the three models. This balance between running cost and frequent intervention however is exactly opposite for larger values of r, as seen in plot (b) of Figure 3.8. Here the Black-Karasinski model is allowed the most freedom while the Vasicek model is the most restricted. This is due to the fact that for large values of r the Black-Karasinski model has the most instantaneous volatility while the Vasicek model has the least.

In plots (c) and (d) of Figure 3.8 we show the size of the control issued by the central bank when the short rate process hits d or u. We see that for larger values of σ the central bank issues a larger control for each model. This highlights the tradeoff between fixed and proportional costs; in order to minimize costs when volatility is high the central bank avoids paying the fixed cost frequently by issuing larger control and paying larger proportional costs. Furthermore plot (c) shows that the size of control is the largest for the Vasicek model when the short rate hits d and smallest for the Black-Karasinski model. This again is related to the higher instantaneous volatility in the Vasicek model for smaller values for r. As expected, the central bank issues the most control for the Black-Karasinski model when the short rate hits u because of its high local volatility for large values of r relative to the other two models.

In Figure 3.9 we plot the optimal value function for these three models when $\sigma = 0.06$. We see that the symmetry of the Vasicek model also holds for the value function, but again there is no symmetry for the CIR model, due to the asymmetry in volatility, or the Black-Karasinski model due to the asymmetry in both volatility and drift. We also see that the value function

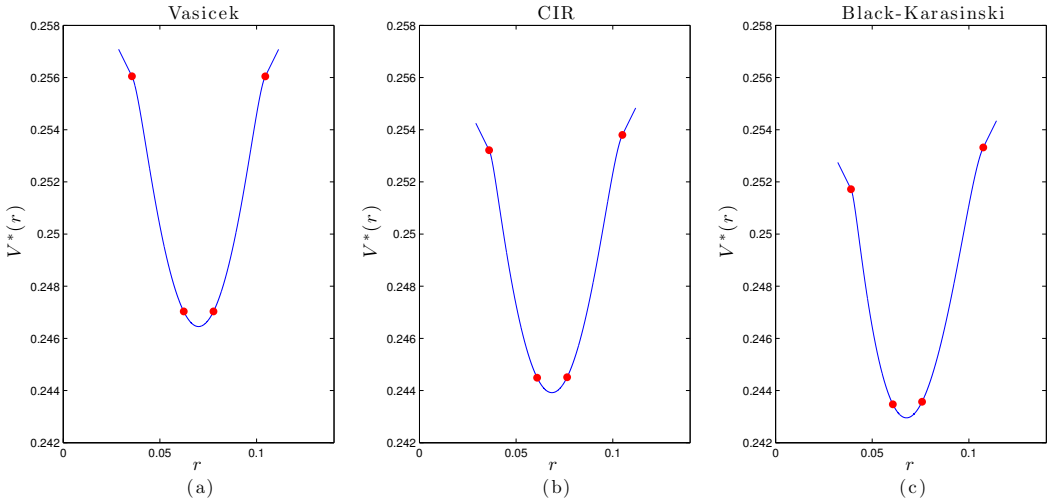

Figure 3.9: Value function for three models when $\sigma = 0.06$, the red dots represent the optimal (d, D, U, u)

for the CIR and Black-Karasinski models are lower than that of the Vasicek model. Although we set the parameters of these models so that the first two moments of the uncontrolled process match we were not able to match higher moments. The CIR and Black-Karasinski models are both leptokurtic and therefore have fatter tails than the Vasicek model. When the central bank imposes a control on the short rate process it is effectively cutting off the tails of the long term distribution. This has the most effect on the most leptokurtic distribution, which is the Log Normal Black-Karasinski model, and therefore the value function for this model is also the lowest.

The examples we have presented here show the rich structure that comes from issuing control on interest rates. We have seen that this control can have drastic and interesting effects on the yield curve in many different

ways. Beyond this the control behaves is rich and interesting way for different interest rate models. Although this is a stylized version of a central bank's intervention methods these examples no doubt shed light on how to best control interest rates in different situations. Perhaps the most interesting insight is that for more volatile interest rates the central bank should wait longer to intervene and when it does finally issue a control it should make a more drastic intervention.

3.6 Concluding Remarks

The focus of this paper was understanding the implications of interventions on the short rate by the Fed on the term structure of interest rates. However to get to this we have had to develop and present a very general solution technique that can solve optimal control problems that have a fixed cost of control (thereby making it optimal to bring about discontinuities in the state dynamics). These problems, usually called impulse control problems, are notoriously hard to solve and only numerical solutions have been available for special cases. We hence hope that the method developed in this paper will be easily leveraged on by researchers in various application areas like inventory management, portfolio selection and healthcare.

Regardless of the federal government's motivations to exert influence in the interest rate markets, whether it be to keep inflation in check or to maintain certain exchange rates, the influence should be exerted in the most rational way possible. This paper presented a model for the government's ability to control

the interest rate market, found the optimal control policy and contrasted the resulting term structure with models that do not incorporate control. We also found that we are able to match the existing yield curves with our model by extracting the market price of risk from bond prices. This freedom provides for a rich model that can approximate the federal governments goals and the free market's response to those goals.

We have abstracted away from modeling the reasons that the federal government issues its control by simply assuming that the government has the ability to quantify its preferences and tolerances precisely. This, however, imposes a static nature to the government's preferences. Allowing for a dynamic change in the governments preferences is more realistic but will require the careful modeling of the motivations for and side effects of intervening. This will undoubtedly yield a multi-dimensional impulse control model that is almost impossible to solve with what is available currently. While this paper, for the first time, looks at the impulse control of these interest rates and the resulting term structures, going forward it is necessary to consider models that capture the complex relationships between the many macro economic variables and the central banks multi-faceted objectives. These goals are important for the entire economy and quantitatively assessing and optimally achieving these goals has the potential to lead to a stronger world market.

Chapter 4

Money Management with Performance Fees

4.1 Introduction

This chapter formulates a new hybrid stochastic control problem, develops a numerical solution to the problem, and applies it to a problem faced by money managers. Starting with Ross (1973) financial economists have studied the agency problems that exist between fund managers and their clients. One of the key implications of this literature is that performance fees, which can incentivize portfolio managers to exert more effort, can also distort the portfolio manager's risk choices. One of the central issues in this context is understanding the manager's investment behavior in the presence of fee collection and comparing this behavior to when the manager is investing his own money. The presence of performance fees (also called incentive fees) for fund managers leads to the common intuition that managers increase risk to maximize fees due to the inherent optionality in performance fees. In their papers Grinblatt and Titman (1989) and Carpenter (2000) find that in some situations a fund manager should take on infinite levels of risk. In these papers, as well as in Basak et al. (2007), the manager tries to maximize a terminal objective collected without considering the effect of their behavior on future fee collection opportunities.

Our primary focus in this paper is in understanding the impact of multiple fee collections under high-water-mark provisions. We specifically contrast our results against some of the previous works and revisit the question of the manager's incentive to take infinite risk. We set up the manager's optimal investment decision as a stochastic control problem and study a fee structure common to money management firms. The money manager seeks to maximize the discounted expected utility of future consumption out of his personal account assuming that fees will be transferred from the fund into his personal account periodically. To achieve this goal the manager must decide how much to invest in risky versus risk-free assets. The fee structure we study considers management fees, charged on assets under management (AUM), and performance (incentive) fees, charged on profits using a high-water-mark. When profits are calculated using a high-water-mark the performance fee is only collected if the current value of the fund is higher than the previous maximal value of the fund.

We investigate manager behavior taking into consideration the fact that a fund manager is not merely trying to optimize fees for one time, but also must look forward to future fee collection opportunities. A manager that only considers the next fee might take on large amounts of leverage with the risk of severely diminishing the value of the fund, however a forward looking manager must consider the impact of this risk on future fee collections. This is especially important in the presence of high-water-marks because the manager has to outperform all pervious fee collection opportunities in order to collect

the performance fee. We also investigate the effect that manager wealth has on the risk he takes with his clients' money and the effect of capital flows in and out of the fund.

The problem faced by the manager implicitly has two distinct time scales; on the one hand the manager must make investment decisions every day through trading, and on the other hand fees are collected periodically, such as quarterly or annually. At the time of fee collection the manager must also decide whether to keep the fund open or not. In order to examine manager behavior when his decisions affect all future fee collections we must formulate an optimization problem that considers both continuous and discrete time events. This type of problem, however, has not been seen in literature and thus does not fall within a class of problems that have standard solution methodologies. This type of problem cannot be meaningfully approximated entirely as a discrete time or continuous time problem. We thus characterize the solution to this new type of problem so that we can develop a methodology to solve it.

Portfolio selection from the point of view of a money manager who collects performance fees is seen in Grinblatt and Titman (1989) where the manager chooses a β and hedges the performance fee using options. Due to the static portfolio and risk-neutrality the authors find that the manager will take on infinite leverage in simple fee structures. Carpenter (2000) studies a similar problem that allows a risk-averse manager to continuously trade. Under this setting the manager choses to take on extremely large risks only when the fund value is below the performance benchmark but takes on much

lower risk when the fund is above the benchmark. We find, however, that the manager does not take on such extreme risk when future fee collections are also important.

Basak et al. (2007) studies a manager's behavior when fund performance influences inflow and outflow of capital to the fund, and finds that, depending on risk tolerance, the manager may increase or decrease leverage when the fund is below the performance benchmark; we will consider a model similar to the one used here to examine the effects of fund flows in the presence of a high-water-mark provision. Ross (2004) investigates different fee contracts to determine when a manager is likely to take on risky portfolios and finds that under certain conditions a manager with performance fees may take on less risk than expected. The primary focus in the above papers is in understanding the risk appetite of the manager when his objective is in maximizing a one time fee. They all find that the manager has incentives to take on extreme risks at certain times and for certain fund values relative to the benchmark. Goetzmann et al. (2003) investigates hedge fund that charges a performance fee calculated using a high-water-mark. The authors examine the effects of high-water-mark contracts on investors and finds the value of the hedge fund to the manager and the investor. Also Panageas and Westerfield (2009) consider a manager who continuously collects performance fees using a high-water-mark and finds that the manager behaves as a constant relative risk averse investor due to the indefinite horizon of the contract.

The paper proceeds as follows. Section 4.2 describes the model setup

and the optimization problem faced by the manager. Section 4.3 characterizes and describes an algorithm to find the optimal solution to the investment problem. Section 4.4 gives examples of manager behavior under a few scenarios. Section 4.5 considers an extension to the model that incorporates capital flows in and out of the fund, and Section 4.6 concludes. All proofs and solution characterizations are included in the appendix.

4.2 The Model

We consider a model in which a fund manager makes investment decisions in continuous time and collects fees, based on the fund's value, at fixed points in time. We assume that the manager has control over investment decisions in a personal account and the fund's account. At the fixed points in time fees are taken out of the fund's account and some proportion of the fees are transferred into the manager's personal account. The remaining fees are used to pay company expenses, such as rent and employee salaries. In the event that the fees collected are not enough to pay company expenses the manager can choose to pay these expenses out of his personal account and keep the fund open or close the fund and default on the company's obligations, without negative effect on his personal account. The manager is able to consume, in continuous time, from his personal account and derives utility from this consumption. The manager's objective is to make investment decisions in both accounts and consume in order to maximize expected utility of future consumption. Initially we make the simplifying assumption that the fund

manager is given an initial endowment and that no money is ever withdrawn from the fund and that no new money ever comes in, as in Carpenter (2000), but consider an extension of the model to incorporate capital flows in and out of the fund in Section 4.5. We also assume that there are no transaction costs, thus allowing for continuous trading in between the fee collection times.

The fund manager has three investment vehicles: two (possibly correlated) risky assets and a bond, and the manager decides how to invest in these three assets. One of the risky assets in exclusively available to the manager's personal account, the other risky asset is exclusively available to the fund and the risk-free asset is available to both. Uncertainty is described by the triple $(\Omega, \mathcal{F}, \mathbb{P})$, where Ω is the set of possible outcomes, $\mathcal{F}$ is the σ-algebra detailing the set of all events, and $\mathbb{P}$ is the probability measure of each set in the σ-algebra. At time t the value of the fund is represented by X_t, the value of the manager's personal account is represented by Y_t, the two risky assets follow Geometric Brownian motions represented by $S_{1,t}$, for the fund, and $S_{2,t}$, for the personal account, and the bond is represented by B_t. The times at which the manager collects fees are denoted as $\{T_i\}_{i=1}^{\infty}$, where $T_i - T_{i-1} = \Delta T$. The fees collected at these times, F_i, are a function of the value of the fund at the time of collection and the high-water-mark.

We consider a fee structure common in hedge fund management. The components of the fee consist of management fees and performance fees. The management fee is represented by λ_m, so that at time T_i the dollars collected from the management fee is $\lambda_m \cdot X_{T_i}$. In addition to the management fee we

also consider the inclusion of a performance fee, which is collected based on the 'profits' over the last time period, where profits are calculated using a high-water-mark, meaning the fund must exceed its previous high in order to collect performance fees.

The percentage of profits charged in the performance fee is represented by λ_p, and the basis for the profit calculation is represented by H, so that the dollars charged from the performance fee is $\lambda_p \cdot \max(X_{T_i} - H, 0)$. In general we refer to H as a *water-mark*.

The dynamics of the assets are given by

$$\begin{aligned} dS_{1,t} &= \mu_1 S_{1,t} dt + \sigma_1 S_{1,t} dW_{1,t}, \\ dS_{2,t} &= \mu_2 S_{2,t} dt + \sigma_2 S_{2,t} dW_{2,t}, \\ \left\langle dW_{1,t} \middle| dW_{2,t} \right\rangle &= \rho dt \\ dB_t &= r B_t dt, \end{aligned}$$

where μ_1 and μ_2 are the expected returns of the risky assets available to the fund and the managers personal account respectively, σ_1 and σ_2 are the volatilities of the risky assets, ρ is the correlation between the two Brownian motions and r is the risk free rate. Given that the manager invests a fraction, ℓ_t, of the fund's value in the first risky asset and a fraction p_t of his personal wealth in the second risky asset and consumes at a rate c_t out of his personal

account at time t, the dynamics of X and Y are given by

$$\begin{aligned} dX_t &= [\ell_t(\mu_1 - r) + r]X_t dt + \sigma_1 \ell_t X_t dW_{1,t}, \quad T_i \leq t < T_{i+1}, && (4.1) \\ dY_t &= ([p_t(\mu_2 - r) + r]Y_t - c_t)dt + \sigma_2 p_t Y_t dW_{2,t}, \quad T_i \leq t < T_{i+1}, && (4.2) \\ X_{T_i} &= X_{T_i-} - F_i, && (4.3) \\ Y_{T_i} &= Y_{T_i-} + \phi(F_i), && (4.4) \end{aligned}$$

if the manager has not closed the fund yet. Equations (4.3) - (4.4) reflect the fact that the manager takes the fees out of the fund at time T_i and transfers some fraction of those fees, $\phi(F_i)$ which may be negative, into his personal account. If, however, the manager decides to shut down the fund at some time, T_{i^*}, then the manager no longer collects fees and Equation (4.2) governs the dynamics for all $t > T_{i^*}$ because shutting down is an irreversible decision.

In order to formalize F_i we must include H_t as a state variable. When profits are calculated using a high-water-mark the dynamics of H_t are given by

$$\begin{aligned} H_{T_i} &= \max(X_{T_i-}, H_{T_i-}), && (4.5) \\ \frac{dH_t}{dt} &= 0, \quad T_i \leq t < T_{i+1}. \end{aligned}$$

Figure 4.1 illustrates the dynamics of the high-water-mark provision. The solid green line represents the value of the fund through time and at time T_i the high-water-mark is given by the dashed blue line. At time T_{i+1} the fund value is below the high-water-mark so the manager does not collect a performance fee and the high-water-mark stays where it is. At time T_{i+2} the

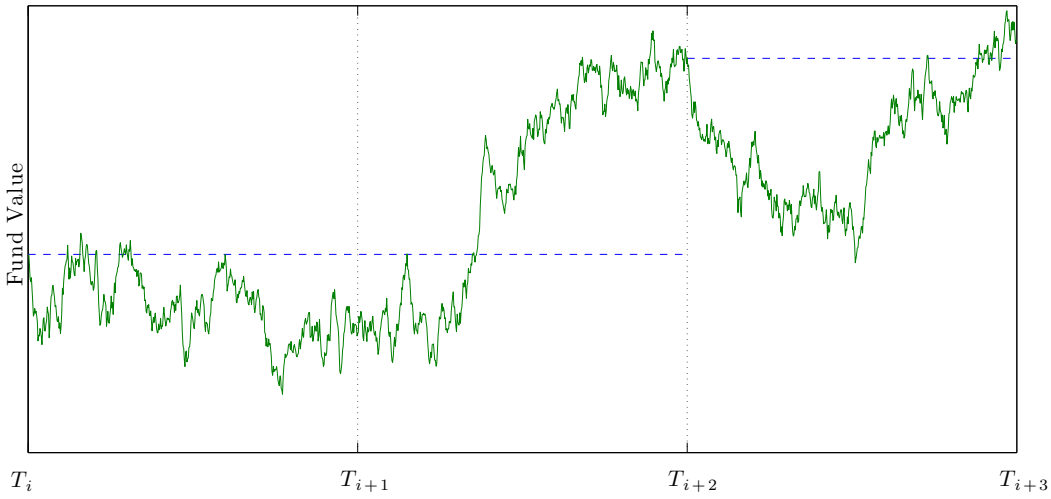

Figure 4.1: An illustration of the high-water-mark provision.

fund value is above the previous high-water-mark so the manager collects a performance fee proportional to the difference between the dashed blue line on the right and the dashed blue line on the left, and the high-water-mark resets to be the value of the fund at time T_{i+2} for future fee collection opportunities. We can see that between T_i and T_{i+1} the fund value gets above the high-water-mark but it finishes at T_{i+1} below the water-mark. Even though at one time the fund was above the water-mark it does not reset at T_{i+1} because the only times that matter for the high-water-mark are the T_i's. At time T_{i+3} the fund finishes above the high-water-mark from T_{i+2} and so the manager will collect a performance fee and the high-water-mark will reset.

Given these dynamics for H_t the fee charged at time T_i can be written

as

$$F_i = f(X_{T_i-}, H_{T_i-}) = \lambda_m \cdot X_{T_i-} + \lambda_p \cdot \max(X_{T_i-} - H_{T_i-}, 0). \tag{4.6}$$

In the case where there is no performance fee we have $\lambda_p = 0$ and H_t is no longer a state variable.

With the dynamics of the state variables we can now examine the manager's optimal investment problem. The manager wishes to maximize the discounted utility of future consumption. The manager has multiple control variables to help him achieve this goal: $c_t,\ p_t,\ \ell_t$ and T_{i^*}. In order to guarantee the manager is non-anticapative these control variables are required to be measurable functions with respect to $\mathcal{F}_t$, the filtration generated by $(W_{1,t}, W_{2,t})$. The set of all such measurable functions is denoted $\mathcal{M}_t$. The manager's optimization problem then becomes

$$V(x, y, h, t) = \max_{(c_s, p_s, \ell_s, T_{i^*}) \in \mathcal{M}_t} \mathbb{E}\left[\int_t^\infty e^{-\beta(s-t)} U(c_s) ds \middle| X_t = x, Y_t = y, H_t = h\right], \tag{4.7}$$

where $U(c_s)$ is the utility the manager gets from consuming at rate c_s and β is the manager's impatience parameter. We will assume the existence of a finite value function.

4.3 Characterizing and Finding the Optimal Solution

The formulation presented in the last section culminates in having to solve Equation (4.7). Unfortunately this formulation does not fall within a class that has standardized methods for computing the solution. The primary

reason for the complication comes from the fact that this problem has elements of both discrete and continuous formulations and cannot be meaningfully approximated entirely as a discrete time or a continuous time problem. If we had a terminal time and an objective at the terminal time, we could walk back in time using dynamic programming and solve the problem. On the other hand if we did not have a terminal time, usually we would be able to remove the time variable since the current time will not affect the decision making, only the other state variables will.

We solve this essentially in two steps. First we look at the continuous control between two discrete fee collection times and construct a mapping that maps the value function at the end of the period to the beginning of the period, under the optimal strategy. This mapping is obtained using the standard Bellman arguments in continuous time. With this mapping, we set this into the discrete setting, along with the fee collection structure and the shut-down decision and propose an iterative method that converges to the fixed point solution. The mapping is set up so that the continuous control can easily accommodate more general stochastic processes and frictions like transaction costs. However, we will focus on the model described in the previous section since our objective is to understand the implications of the fee structure and the multi-period nature of these money management contracts with high-water-marks.

We note that if $t > T_{i^*}$ or $y = 0$ (the manager has shut down or bankrupted the fund) then the manager no longer has to make decisions with

the fund's money. In this situation he only makes decisions in his personal account and faces the standard problem of optimal investment and consumption found in Merton (1969). Specifically if the manager has a constant relative risk averse (CRRA) utility function of the form

$$U(c) = \frac{c^{1-\gamma}}{1-\gamma}$$

the the manager's objective function has the solution

$$M(y) := V(x,y,h,t) = \frac{\gamma^\gamma}{1-\gamma}\left(\beta - \frac{1-\gamma}{2\gamma}\left(\frac{\mu_2 - r}{\sigma_2}\right)^2 - r(1-\gamma)\right)^{-\gamma} y^{1-\gamma}.$$

In the general utility case the solution is not always so nice, but it is still the solution to an ODE which we will assume has a solution represented by $M(y)$.

From the model described in Section 4.2 we follow the standard practice, as in Yong and Zhou (1999), and find that between the times that fees are collected the value function from Equation (4.7) must satisfy the Hamilton-Jacobi-Bellman (HJB) equation

$$\begin{aligned} \beta V &= V_t + \max_{p,\ell,c}\left\{\tfrac{1}{2}\ell^2\sigma_1^2x^2V_{xx} + \tfrac{1}{2}p^2\sigma_2^2y^2V_{yy} + \rho\sigma_1\sigma_2p\ell xyV_{xy}\right. \qquad (4.8)\\ &+ \left.[\ell(\mu_1 - r) + r]xV_x + ([p(\mu_2 - r) + r]y - c)V_y + U(c)\right\},\ T_i < t < T_{i+1}. \end{aligned}$$

Taking first order conditions we find that

$$\ell^* = \frac{(\mu_1 - r)\sigma_2V_xV_{yy} - \rho(\mu_2 - r)\sigma_1V_yV_{xy}}{\sigma_1^2\sigma_2x\left(\rho^2V_{xy}^2 - V_{xx}V_{yy}\right)}, \qquad (4.9)$$

$$p^* = \frac{(\mu_2 - r)\sigma_1V_yV_{xx} - \rho(\mu_1 - r)\sigma_2V_xV_{xy}}{\sigma_1\sigma_2^2y\left(\rho^2V_{xy}^2 - V_{xx}V_{yy}\right)}, \qquad (4.10)$$

$$c^* = \left(U'\right)^{-1}\left(V_y\right). \qquad (4.11)$$

These first order conditions hold between fee collections only if $V_{xx} < 0$ and $V_{yy} < 0$ (more precisely when the Hessian matrix is negative definite), meaning that V is concave. Due to the performance fee, however, V may not always be concave close to the water-mark, and the first order conditions will lead to minimization or a saddle-point rather than maximization. When V is convex maximizing over (ℓ, p) implies that the manager should take on infinite leverage, which is not feasible from a practical standpoint. In order to resolve this issue we place upper bounds, $\hat{\ell}$ and $\hat{p}$, on the amount of leverage, ℓ and p, that the manager can take so that whenever V is convex we use $\hat{\ell}$ or $\hat{p}$ in Equation (4.8). Specifically, if we have the set

$$\mathcal{G} = \{(p^* \wedge \hat{p}, \ell^* \wedge \hat{\ell}), (\hat{p}, \ell^* \wedge \hat{\ell}), (p^* \wedge \hat{p}, \hat{\ell}), (\hat{p}, \hat{\ell})\}$$

the Equation (4.8) can be rewritten as a discrete choice problem

$$\begin{aligned} \beta V &= V_t + \max_{(p,\ell)\in\mathcal{G}} \left\{ \tfrac{1}{2}\ell^2\sigma_1^2 x^2 V_{xx} + \tfrac{1}{2}p^2\sigma_2^2 y^2 V_{yy} + \rho\sigma_1\sigma_2 p\ell xy V_{xy} \right. \\ &+ \left. [\ell(\mu_1 - r) + r]xV_x + [p(\mu_2 - r) + r]y \right\} + U(c^*) - c^* V_y, \ T_i < t < T_{i+1}. \end{aligned} \tag{4.12}$$

We need not worry about c^* because the utility function, U, is concave by definition.

Figure 4.2 in Section 4.4 shows an example of a convexity in the value function from the performance fee. This derivation has been similar to Merton (1969), however in this case we must consider the extra income from managing the fund.

For a PDE of the form in Equation (4.12) to be well defined it must also have a terminal condition. Typically this terminal condition is exogenously

defined, however in this case we do not know what the terminal condition is. Due to the infinite horizon in this problem the value function at the T_i's must be the same and we can use this to define a terminal condition endogenously.

In order to find the appropriate terminal condition we define an operator, $\mathcal{A}$, that maps the value function at the end of a period to the beginning of the period, on a general class of functions which will be described later. To define this operator suppose there are functions g and ψ such that ψ satisfies Equation (4.12) with the terminal condition $\psi(x, y, h, T_i) = g(x, y, h)$ then the operator, $\mathcal{A}$, acting on g is defined by

$$(\mathcal{A}g)(x, y, h) = \psi(x, y, h, T_{i-1}). \tag{4.13}$$

Intuitively, the operator $\mathcal{A}$ takes a function, g, and evolves it backwards, using the HJB from Equation (4.12), ΔT amount of time, from T_i to T_{i-1}. We need this to examine the difference between a proposed value function at the different T_i's and to formalize the endogenous terminal condition for the HJB.

Defining the class of functions that can be operated on by $\mathcal{A}$ is not entirely straightforward. In order for there to be a classical solution to the PDE in Equation (4.12), we must have that g is twice differentiable with its second derivative not equal to zero. However, stochastic control problems are seldom that 'nice' and we will have to find the viscosity solution to Equation (4.12) and so we define $\mathcal{A}$ on a more broad class of distributions that possibly have finitely many places where the first derivatives, with respect to x and y, are discontinuous for each value of h.

In order to characterize the solution to Equation (4.7) we provide the following theorem.

Theorem 4.1. Suppose there is a function, v that satisfies Equation (4.12), weakly, as well as

$$\begin{aligned} v(x,y,h,T_i) &= \max\big\{(\mathcal{A}v)(x-f(x,h),y+\phi(f(x,h)),\max(x,h),T_i), \\ &\qquad M(y+\phi(f(x,h))),M(y)\big\} \end{aligned} \tag{4.14}$$

then v is the optimal value function in Equation (4.7).

The proof follows directly from Theorem C.1, which is stated and proved in the appendix.

The maximization in Equation (4.14) comes from the fact that the manager has the option to shut down the fund at the T_i's. The first option in the maximization represents the manager deciding to keep the fund open and continuing to collect fees in the future. The second option corresponds to the manager collecting fees this time but closing the fund afterwards. The third option corresponds to the manager closing down the fund and defaulting on its obligations. This may happen if $\phi(f) < 0$ which is possible if the fees collected aren't enough to cover fixed costs associated with the fund. When $\phi(f) < 0$ the manager has the option of paying the remaining costs out of his personal account and keeping the fund open, but he can also shut down.

In order to find a function that satisfies the conditions in Theorem 4.1 we develop an algorithm that, upon iteration, converges to the optimal value

function. First we find the value function at the times T_i and then with this we can find the value function between the T_i's using Equation (4.12).

To define this iterative algorithm let us first define $\hat{v}_0(x,h)$ as the expected future utility from collecting fees just one time and shutting down,

$$\hat{v}_0(x,y,h) = \max\{M(y+\phi(f(x,h))), M(y)\}. \tag{4.15}$$

The iterative steps are next defined as

$$\begin{aligned} v_j(x,y,h) &= (\mathcal{A}\hat{v}_j)(x,y,h), & (4.16)\\ \hat{v}_{j+1}(x,y,h) &= \max\{v_j(x-f(x,h), y+\phi(f(x,h)), \max(x,h)), & (4.17)\\ &\qquad M(y+\phi(f(x,h))), M(y)\big\}. \end{aligned}$$

Theorem 4.2. If the expected value in Equation (4.7) exists and is bounded then in the limit as j approaches infinity we have

$$\begin{aligned} \lim_{j\to\infty} \hat{v}_j(x,y,h) &= V(x,y,h,T_i-), & (4.18)\\ \lim_{j\to\infty} v_j(x,y,h) &= V(x,y,h,T_i), & (4.19) \end{aligned}$$

where convergence is pointwise.

The proof of this theorem follows directly from Theorem C.3 in the appendix.

Here the difference between Equations (4.18) and (4.19) comes from the definition of the value function in Equation (4.7). Time T_i- is infinitesimally before a fee is collected and so it is in the managers expected future utility,

however at time T_i the fee has been collected and so that fee is no longer expected in the future, because it was collected already.

Thus, if a solution to this problem exists then the algorithm in Equations (4.16) and (4.17) will find the value function at the times of fee collection. Then the converged solution, or an approximation there of, can be used to find the value function and the manager's optimal investment strategy at times between fee collections using Equations (4.9) - (4.12).

4.4 Analysis of Manager Risk Profile

When a money manager considers a one-time performance fee payout, it is understandable that when the fund value is low the money manager will take large risks to maximize his payout objectives. Several analytical results in the literature have given us good insights into the risk profile under such one-time performance fee payouts. While these analytical results offer clear insights on the nature of the results' dependence on various parameters, the fee structures and the models setup are also quite limited. Our objective in this section is to understand how risk profiles change when the manager's objective is in maximizing the rewards from a series of payouts rather than just one terminal payout, especially under high-water-marks.

We begin with a simpler setup comparing the manager's risk profiles under different fee structures under the one-time payout setup, as in Carpenter (2000), where the manager gains utility from fees collected at the end of one period without intermediate consumption. In this setup the manager's wealth

does not influence his behavior since he only gains utility from a one-time fee.

We specify the parameters of the model so that the expected return, $\mu_1 = 8\%$, the volatility, $\sigma_1 = 20\%$, the risk-free rate, $r = 2\%$, the impatience parameter, $\beta = 10\%$, the performance fee, $\lambda_p = 15\%$, the management fee, $\lambda_m = 1.5\%$ (per year), the manager has a CRRA utility function (as above) with $\gamma = 2$, and the maximum amount of risk the manager is allowed to take is $\hat{\ell} = 1,000\%$. From Merton (1969) we know that if the manager were managing this money for himself (rather than for the client) then he would optimally set

$$\ell^* = \frac{\mu - r}{\gamma\sigma^2} = 75\%,$$

which we will denote ℓ_M, and we will compare the risk exposures to this so we can understand the manager's relative risk taking profile.

In Carpenter (2000) the author considers a single period problem where the management collects a known base-line fee and the performance fee is charged on the final value of the fund. For the purposes of comparison we can consider the base-line fee collected by the manager to be a management fee that is collected on the initial value of the fund and is known before the problem begins. Between the beginning of the fund and fee collection the manager has the same opportunity set as in our paper and seeks to maximize the expected utility of the first fee collection; once the fee is collected the problem is over. In her paper, Carpenter finds an analytical solution to this problem and finds that the manager will always take on infinite leverage when the fund value is close to zero, and lower risk when the fund value is higher

than the benchmark.

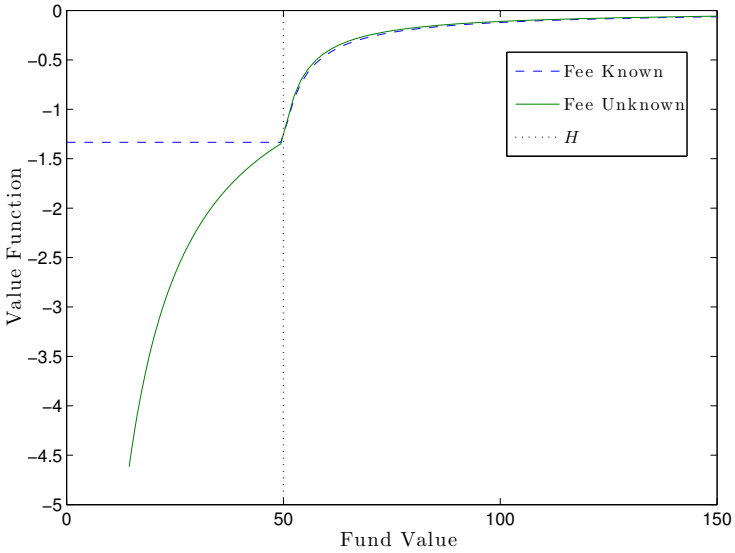

Figure 4.2: Terminal value function when the management fee is known ahead of time and when it depends on the final value of the fund. We can see that when the management fee is known ahead of time the utility is flat when the fund is below the water-mark because the performance fee does not get paid until the fund exceeds H. Alternatively, the utility function is increasing below the water-mark when the management fee is determined at the end because. When the management fee is determined at the end the manager may not want to take as much risk so that he doesn't forfeit the fee.

If, however, rather than setting the management fee at the beginning of the period, the fee is set at the end then we find that the manager drastically changes his risk taking behavior. Figure 4.2 plots the objective function in these two cases. The blue dashed line represents the objective function that the manager wants to maximize when the management fee is known at the beginning. Here we see that the objective is flat when the fund is less than

H because the manager will only get the management fee, which is known ahead of time, so that the manager has incentive to take on extra risk in this region since he has nothing to lose. Alternatively, the solid green line represents the manager's objective function when the management fee is computed as a function of the fund's terminal value. Here the objective is increasing everywhere (it goes to $-\infty$ as the fund value goes to zero because $\gamma > 1$) and so the manager does not have as much incentive to take on extra risk in this region.

In Figure 4.3 we illustrate the manager's behavior in these two scenarios: when the management fee is known ahead of time, and when it is not. We plot the optimal value of ℓ versus the fund value, 6 months before the fee is collected where $H = \$50$. In this figure the blue dashed line represents the optimal leverage when the management fee is determined at the beginning of the contract, as in Carpenter (2000), the solid green line represents the optimal leverage when the management fee is determined by the final value of the fund, the red dash-dotted line is the Merton portfolio (ℓ_M) and the dotted black line is the water-mark.

In the case where the management fee is determined at the beginning of the contract we can see, as expected, the manager takes on as much risk as possible when the fund value is low, relative to the benchmark, because he has nothing to lose in this region. However once the manager has exceeded the benchmark he drastically reduces his risk to help lock in the performance fee. We note, however, that he begins to reduce his risk when the fund value is still

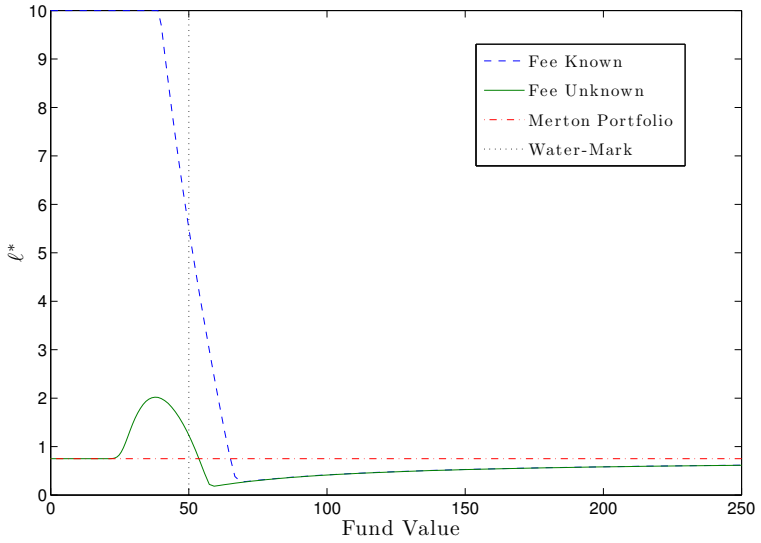

Figure 4.3: Optimal leverage when the management fee is known ahead of time and when it depends on the final value of the fund, 6 months before the fees are collected. The blue dashed line shows the optimal leverage in the risky asset when the management fee is known ahead of time. It shows that the manager should take on as much risk as possible when the fund value is low to attain the performance fee. The solid green line shows the optimal leverage when the management fee is determined by the final value of the fund. Here the manager takes on much less risk than in the alternative case. The red dash-dotted line shows the Merton portfolio, or the optimal leverage in the risky asset if the manager were investing his own money.

slightly below the water-mark. This is because there are still six months until the fee will be collected and so he has plenty of time for the fund value to go above the water-mark before the fee will be collected, and so he reduces his risk to help the positive trend of the risk-free asset guarantee the fund value goes above the benchmark. When the fund value is very large relative to the water-mark the manager asymptotes to the Merton portfolio because it seems

more and more likely that the performance fee is guaranteed.

In the case where the management fee is determined by the terminal value of the fund the manager no longer maxes out his risk for small fund values because by doing this he would risk losing his management fee, which is not a concern in Carpenter (2000). Instead, when the fund value is low the manager sets his optimal leverage close to the Merton portfolio, ℓ_M, because attaining a performance fee is not realistic and thus behaves as if the management fee is the only possibility. He then increases his leverage as he gets closer to the water-mark to increase the chance of getting the performance fee. After he goes above the water-mark the manager reduces his risk below ℓ_M to help lock-in the performance fee, and finally for large fund values the manager sets his leverage close to ℓ_M because losing the performance fee is not likely and so he begins to behave as if it is guaranteed. We can see that even by changing something as minor as the timing of the management fee the manager will drastically change his risk levels. By charging the management fee at the end of the contract there will be much less distortion in the manager's risk as compared to the Merton portfolio.

We next move on to an example following our more complex model setup where fees are transferred into the manager's personal account periodically and he consumes out of this account in continuous time. As we are primarily concerned with the management of the client's assets we assume that the manager invests 100% of his personal wealth in the risk-free asset at all times, but still consumes optimally. As this eliminated the dependence on

S_2 we set the remaining parameters to be $\mu_1 = 17\%,\ \sigma_1 = 25\%,\ \gamma = 2,\ \lambda_m = 1.5\%,\ \lambda_p = 15\%$ and we set $\phi(f) = \alpha(f - \kappa)$ where $\alpha = 75\%$ and $\kappa = 0.1$. Setting ϕ in this way means that every period the manager has to pay a fixed cost of 10¢ for rents and then he takes home 75% of whatever is leftover after paying the fixed cost.

Figure 4.4 plots the optimal portion of the fund invested in the risky asset as a function of the fund's value 6 months before the next fee will be collected, assuming the manager currently has $1 in personal wealth. The dashed line represents a manager who will definitely shut down the fund after the fee is collected (perhaps sub-optimally) and the solid line represents a manager who will make an optimal shut down decision and keep collecting fees in the future.

We can see that when the manager is definitely going to shut down the fund after one period (myopically) the manager behaves similar to the manager in Carpenter (2000). In this situation since the manager has his own personal wealth, if the fund value is low the manager really has nothing to lose, as in the case of Carpenter (2000), because if the fund goes bankrupt he still has his own money to consume. On the other hand, however, if the manager keeps the fund open the manager behaves quite differently. For extremely low fund values we see that the manager takes on large risk for the same reason as before, just not as drastically. When the fund value increases a bit we see that the manager takes on much less risk than the myopic manager because his ability to collect fees in the future could be diminished if he takes on too much

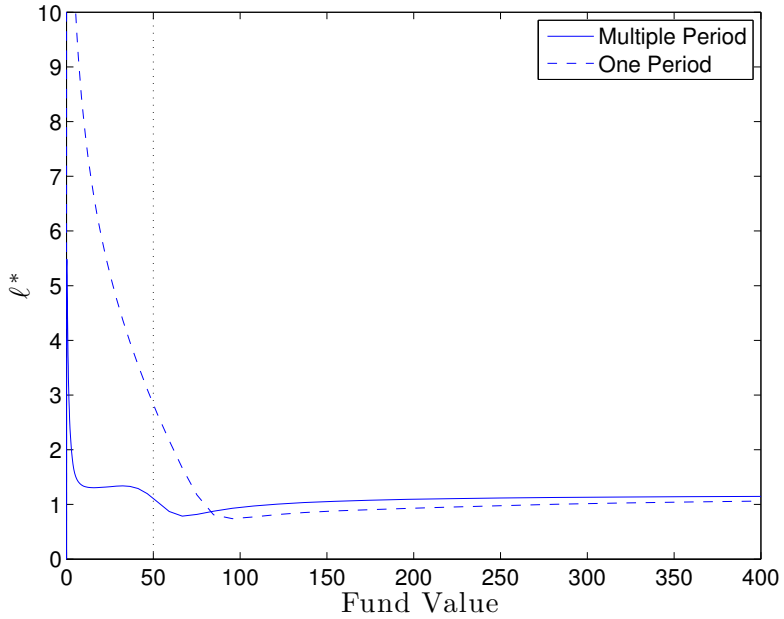

Figure 4.4: Optimal proportion of the fund invested in the risky asset as a function of the fund's value for a manager with a personal wealth of \$1, six months before the next fee will be collected. The dashed line represents a manager who will close down after one fee collection, and the solid line represents a manager who will keep playing the game.

risk; his upside is still present but his downside has been increased due to his ability to collect fees in the future. We can also see that around the current high-water-mark the manager alters his risk profile similar to the solid green line in Figure 4.3. As the fund value increases from zero the manager decreases his risk but as he gets closer to the water-mark he realizes that earning the performance fee is possible and so he increases his risk slightly. Then above the water-mark the manager decreases his risk again to lock-in the performance fee and finally when the fund value is high the manager asymptotes to some

stable level. Interestingly the forward looking manager takes on a little more risk than the myopic manager for large fund values. This is due to the fact that the water-mark will reset to a high level if the fund finishes at a high level, meaning that in the next period the performance fee will be harder to collect. Therefore the manager is willing to take on a little more risk and accepts the possibility of lowering the fund value because it could lead to easier fee collection in the future; a consideration not taken into account by the myopic manager.

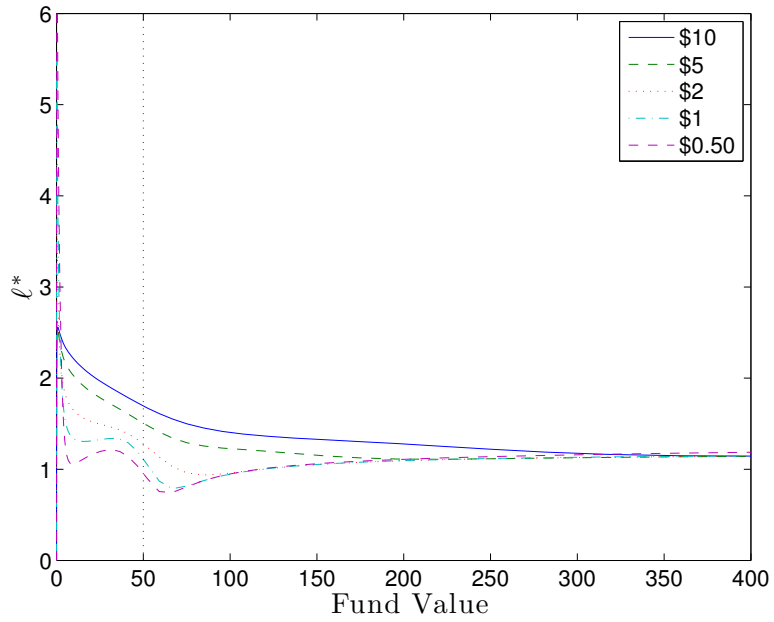

Figure 4.5: Optimal proportion of the fund invested in the risky asset as a function of the fund's value, 6 months before the next fee will be collected, for various values of manager wealth.

We are also interested in knowing how a manager's initial wealth affects

the risk that he takes with his clients' money. In Figure 4.5 we plot the optimal proportion of the fund's value to be invested in the risky asset six months before the next fee will be collected for several values of the manager's initial wealth. The solid line on top represents a manager whose personal wealth is 20% of the fund's value at the last fee collection, and is therefore relatively rich as compared to the assets he manages. The dashed line on the bottom represents a manager whose personal wealth is 1% of the fund's value at the last fee collection, and is therefore relatively poor as compared to the assets he manages. We can see that for the most part the richer managers take on more risk than the poorer managers. This is because the richer managers have much less to lose than the poorer managers, meaning that the rich managers are affectively "playing with house money." For the poorer managers the ultimate goal is to become rich and this is not possible if the fund blows up.

We also notice that the poorer managers alter their risk profile more drastically than the rich managers around the current high water mark. For a poor manager the additional performance fee can make a big difference in personal wealth. Alternatively a manager who is already rich doesn't benefit as much from the additional income and therefore doesn't change his risk profile by much.

4.5 Model Extension

The basic model set up in Section 4.2 is flexible enough to incorporate several extensions. This section considers such an extension; we consider the

setting where fund performance affects capital flows in and out of the fund. For example, if the fund is doing well investors may want to invest more money in the fund, or alternatively if the fund is performing poorly investors may want to take some money out of the fund. There have been empirical studies of capital flows in and out of funds, as in Chevalier and Ellison (1997), and generally speaking funds get new investments when they have positive returns and investors leave the fund when there are negative returns.

We model capital flows in and out of the fund with a multiplicative function, Q_i, that is observed only at fee collection times, T_i, corresponding to when the fund reports performance. If $Q_i > 1$ then money flows into the fund and if $Q_i < 1$ money leaves the fund. In general we assume that Q_i is a function of the fund's performance through the relationship between X_{T_i-} and H_{T_i-}; if $X_{T_i-} > H_{T_i-}$ then the fund has performed well recently and we expect money to come into the fund and vice versa. For the sake of accounting we assume that if $X_{T_i-} < H_{T_i-}$ then $Q_i \leq 1$. Without this assumption the problem becomes infinite dimensional and each individual investor's high-water-mark would have to be tracked. With this assumption, however, all investors' high-water-marks can be aggregated and the dimensionality of the problem remains unchanged.

With capital flows in and out of the fund the dynamics of the fund value and the high-water-mark change at the fee collection times, T_i, to

$$\begin{aligned} X_{T_i} &= Q_i(X_{T_i-}, H_{T_i-}) \cdot (X_{T_i-} - F_i), \\ H_{T_i} &= Q_i(X_{T_i-}, H_{T_i-}) \max(X_{T_i-}, H_{T_i-}). \end{aligned}$$

Here the Q in the new high-water-mark equation is simply a scaling factor that aggregates all investors' high-water-marks.

With these new dynamics the solution to Equation (4.7) no longer satisfies Equation (4.14), but rather must satisfy

$$\begin{aligned} v(x,y,h,T_i) &= \max\Big\{(\mathcal{A}v)(Q(x,h)(x-f(x,h)), y+\phi(f(x,h)), \\ &\qquad Q(x,h)\max(x,h), T_i), M(y+\phi(f(x,h))), M(y)\Big\}. \end{aligned}$$

With this we can appropriately modify the algorithm to find V so that

$$\begin{aligned} v_j(x,y,h) &= (\mathcal{A}\hat{v}_j)(x,y,h), \\ \hat{v}_{j+1}(x,y,h) &= \max\Big\{v_j(Q(x,h)(x-f(x,h)), y+\phi(f(x,h)), \\ &\qquad Q(x,h)\max(x,h)), M(y+\phi(f(x,h))), M(y)\Big\}. \end{aligned}$$

As a numerical example using the same parameters as in Section 4.4 we assume that Q_i's follow a piecewise linear function of returns, as in Chevalier and Ellison (1997) and Basak et al. (2007). In these papers the authors judge the returns of the fund relative to the market as a whole. Here the market is not included so we modify their functional form of Q to depend on the fund's return relative to the high-water mark; specifically

$$Q(x,h) = \begin{cases} Q_D, & \log\frac{x}{h} < \eta_D \\ Q_D + \zeta(\log\frac{x}{h} - \eta_D), & \eta_D \le \log\frac{x}{h} < \eta_U \\ Q_U \equiv Q_D + \zeta(\eta_U - \eta_D), & \eta_U \le \log\frac{x}{h} \end{cases}$$

and we set $Q_D = 0.75,\ Q_U = 1.35,\ \eta_D = -0.08,\ \eta_U = 0.112$ and $\zeta = \frac{Q_U - Q_D}{\eta_U - \eta_D} = 3.125$. Figure 4.6 plots Q as a function of the returns of the fund relative to the high-water-mark.

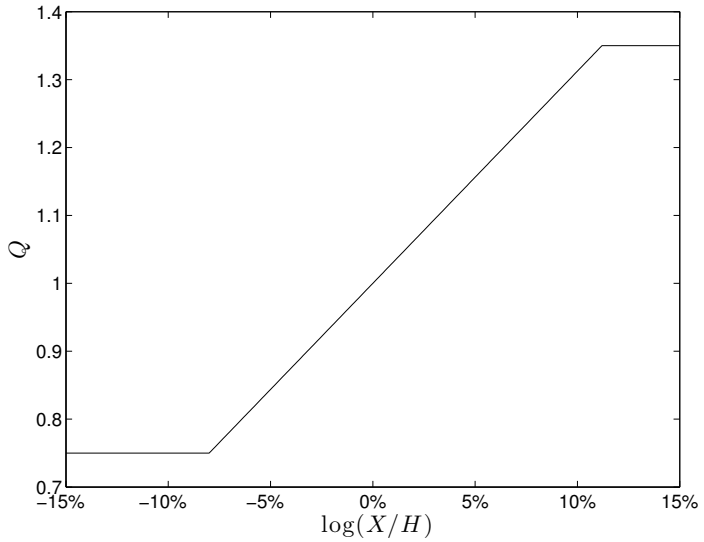

Figure 4.6: Q as a function of the fund's return relative to the high-water-mark. For fund losses relative to the water-mark money flows out of the fund because $Q < 1$ and for fund gains relative to the water-mark money flows into the fund because $Q > 1$. The potential gains from new investment are larger than the potential losses from poor performance because empirically it seems that investors are bit sticky with their old investments, see Chevalier and Ellison (1997).

In Figure 4.7 we plot the optimal percentage of the fund's value to be invested in the risky asset six months before the next fee collection opportunity under the assumption that at the end of each period money will flow in or out of the fund according to the Q function shown in Figure 4.6. We can see that in this situation the manager's risk profile is qualitatively similar to the case without capital flows, however everything is a little more extreme. When the fund is a bit below the water-mark the manager alters his risk profile, however he drops his risk very quickly as he gets closer to the water-mark.

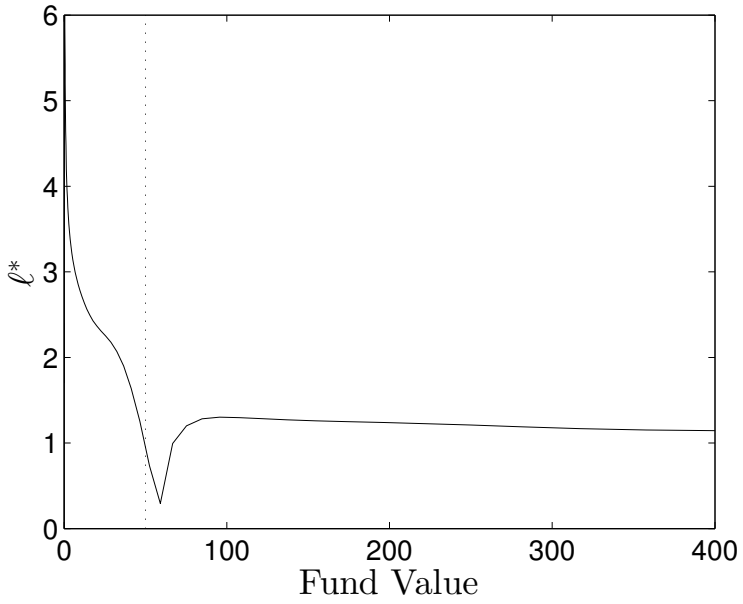

Figure 4.7: Optimal proportion of the fund's value invested in the risky asset six months prior to the next fee collection opportunity. At the end of each period money will flow in or out of the fund and presently the manager has \$1 in personal wealth.

The manager has a lot more to lose in this scenario because if he doesn't get above the water mark he knows that clients will withdraw their money, so getting positive returns is doubly important. Also when the fund is slightly above the water-mark the manager reduces his risk by much more than when money doesn't flow into the fund because it is even more important to stay above the water-mark now to avoid withdrawals. As the fund gets more above the water-mark the manager is willing to take on more risk. Here the manager sees a bright future of potential extra investment and wants to take the gamble to try to get even more money invested in the fund so next period he can collect

extra fees. If this gamble doesn't pay off he will quickly decrease his risk to avoid large losses. This more extreme behavior, relative to the case without capital flows, is fundamentally due to the extra convexity introduced to the problem by considering capital flows. As we saw earlier, the performance fee brings a convexity into the manager's objective and the addition of capital flows serves to intensify this convexity.

4.6 Conclusion

This chapter investigates the behavior of a money manager under several common fee structures. For this investigation we model the dynamics of stock and bond behavior and pose an optimization problem to be solved by the fund manager. We formulate this problem as a stochastic optimal control problem and then transform it into a Hamilton-Jacobi-Bellman equation that characterizes the optimal solution. We then present an algorithm that converges to this solution.

We find that the inclusion of a management fee that is determined by the terminal value of the fund can drastically change the risk taking behavior of a manager from the behavior found in Carpenter (2000). When the fund value is low, relative to the benchmark, the manager should not take on large leverage because he may put the management fee at risk.

We see that when fees are collected repeatedly using a high-water-mark the manager must weigh two opposing incentives. These two incentives are the very next fee that will collected and potentially resetting the water-mark which

will make future fee collections more difficult. When the manager optimally weighs these incentives his risk taking behavior can be drastically different than when the next fee is the only thing on his mind. We also investigate the effect that a manager's initial wealth has on the risk he takes with client money and the effect that capital flows has on manager risk taking behavior.

Going forward it would be interesting to study this problem in the presence of transaction costs to understand when the manager is more or less willing to pay transaction costs with respect to the timing of management and performance fee collections. We could also study this problem in the presence of heavy tails and diminishing returns commonly found in the hedge fund world.

Chapter 5

Concluding Remarks

This dissertation has focused on developing numerical methods to solve stochastic optimal control problems. Three classes of stochastic control models were considered and applied to financial problems. While the methods and techniques developed here were specific to the application areas considered in the previous chapters there are many other applications that could benefit from the numerical methods developed here. Additionally, more analysis could be considered for each problem as well.

In the first example we considered the optimal stopping problem of pricing American derivative securities. To solve this problem we derived differential equations that govern the evolution of the early exercise boundary and developed numerical methods that exploit these boundary evolution equations to price American options quickly and accurately. In the constant volatility setting we found that the modified integral method was the best method considered; to extend upon this it would be prudent to investigate integral equations for American options with stochastic volatility, as in Detemple and Tian (2002), and try to implement our boundary evolution equations in this setting. Following this application area it would be interesting to also examine

local volatility models. Local volatility models are nice because they can easily replicate the volatility smiles seen empirically in the options market, and they also maintain the low dimensionality of the classic Black-Scholes setting. To this end, it could be insightful to modify Equation (2.6) to incorporate local volatility models, such as the constant elasticity of variance model seen in Emanuel and MacBeth (1982). There are many other application areas for optimal stopping problems, such as real options and earliest detection problems, and investigating boundary evolution equations for these problems could be an interesting area of future work as well.

In the second example we considered a general impulse control model applied to the intervention problem faced by a nation's central bank. A key contribution of this chapter is the development of an efficient and systematic numerical method that can solve a very large class of impulse control problems. We formulate the bank's intervention problem as an impulse control because of the relative infrequency of interventions and the jumps resulting from intervention. Going forward we would like to consider the problem of calibrating the model and solving the inverse problem to determine the bank's objective function. This would be insightful so that we could have a better understanding of the bank's preferences and tolerances. Additionally we believe the bank's control problem could be more realistically modeled by considering extra factors such as inflation or payroll growth. In our work so far the only driving factor behind the bank's intervention is deviations in the short rate, when in reality inflation is a more reasonable driving factor for intervention.

Although the bank is more concerned with inflation than interest rates, the interest rate market is the main vehicle for intervention; the hope being that changes in the interest rate market affect inflation. We also believe that the intervention mechanism could be more realistically modeled. For example, in the United States the Federal Reserve meets every six weeks to set a "target rate" and then buys and sells repurchase agreements daily to reach its goals. This type of control could perhaps be more realistically modeled using the mechanism developed in Chapter 4.

Finally, we considered a new hybrid problem that has elements of discrete and continuous time control. Here we formulated a general class of problems and developed a numerical method to solve them. This hybrid control was applied to the problem faced by a money manager that discretely collects fees and continuously makes trading decisions. Going forward we are interested in considering the case where the fund's and the personal risky assets are negatively correlated. This will effectively allow the manager to hedge his position in the personal risky asset with the fund's assets. We still expect to see similar behavior around the high-water-mark but there may be more interesting behavior related to this hedge. The frequency with which fees are collected is also an interesting setting to examine. When a manager collects fees more frequently he is guaranteed to make more money through the performance fee but it would be interesting to see if he also reduces his leverage since he may not need as much risk to get the same reward. Given these competing objectives for the manager we would also like to look at this problem

from the point of view of the investor. Specifically, it would be interesting to model the investor's objectives and set up a competitive market with several possible money managers and then find the optimal fee structure for the fund given the investor's behavior.

Appendices

Appendix A

Boundary Evolution Equations for American Options

A.1 Proofs of Theorems

Proof. **Theorem 2.1.** First differentiate the boundary conditions with respect to time, which will be in terms of the time derivative of p. This will also lead to time derivatives of the exercise boundary, $c(\tau)$, which is indeed differentiable by Lemma 4.1 in Myneni (1992). Notice that the time derivative of p also satisfies Equation (2.1). The first boundary condition, (2.2) becomes

$$\frac{\partial p}{\partial x}\frac{\partial c}{\partial \tau} + \frac{\partial p}{\partial \tau} = -\frac{\partial c}{\partial \tau}$$

which is simplified using Equation (2.3) to

$$\frac{\partial p(c(\tau),\tau)}{\partial \tau} = 0. \tag{A.1}$$

Next take the time derivative of Equation (2.3) and find

$$\frac{\partial^2 p}{\partial x^2}\frac{\partial c}{\partial \tau} + \frac{\partial^2 p}{\partial x \partial \tau} = 0. \tag{A.2}$$

Now take the limit as $x \to c(\tau)$ from the right and substitute Equation (A.1) into Equation (2.1) and get

$$0 = \tfrac{1}{2}\sigma^2 c^2(\tau)\frac{\partial^2 p(c(\tau),\tau)}{\partial x^2} + bc\frac{\partial p(c(\tau),\tau)}{\partial x} - rp(c(\tau),\tau). \tag{A.3}$$

Next substitute Equations (2.2) and (2.3) into (A.3),

$$\frac{\partial^2 p(c(\tau),\tau)}{\partial x^2} = \frac{2qr - 2(r-b)c(\tau)}{\sigma^2 c^2(\tau)}. \tag{A.4}$$

Finally combine Equations (A.2) and (A.4) and rearrange terms to find the desired function, (2.6). □

Proof. **Theorem 2.2.** Similar to the derivation of Equation (A.1), in stochastic volatility we also have

$$\frac{\partial}{\partial \tau} p(c(y,\tau),y,\tau) = 0. \tag{A.5}$$

Next we differentiate (2.14) with respect to y and τ, and (2.15) with respect to y giving us

$$\begin{aligned}
\frac{\partial^2 p}{\partial x^2}\frac{\partial c}{\partial y} + \frac{\partial^2 p}{\partial x \partial y} &= 0, && \text{(A.6)}\\
\frac{\partial^2 p}{\partial x^2}\frac{\partial c}{\partial \tau} + \frac{\partial^2 p}{\partial x \partial \tau} &= 0, \quad \text{and} && \text{(A.7)}\\
\frac{\partial^2 p}{\partial x \partial y}\frac{\partial c}{\partial y} + \frac{\partial^2 p}{\partial y^2} &= 0. && \text{(A.8)}
\end{aligned}$$

Now combine (A.6) and (A.8) to see that

$$\frac{\partial^2 p}{\partial y^2} = \frac{\partial^2 p}{\partial x^2}\left(\frac{\partial c}{\partial y}\right)^2. \tag{A.9}$$

Next evaluate (2.12) at the boundary and substitute in (2.13), (2.14), (2.15), (A.6) and (A.9), which gives us

$$0 = \tfrac{1}{2} f(y)^2 c^2 \frac{\partial^2 p}{\partial x^2} - \rho\lambda(y) f(y) c \frac{\partial^2 p}{\partial x^2}\frac{\partial c}{\partial y} + \tfrac{1}{2}\lambda(y)^2 \left(\frac{\partial c}{\partial y}\right)^2 \frac{\partial^2 p}{\partial x^2} - rq. \tag{A.10}$$

Finally plug in (A.7) to Equation (A.10) and rearrange terms to obtain the desired result, (2.17). □

Appendix B

Impulse Control of Interest Rates

B.1 Proofs of Theorems and Lemmas

Unless otherwise specified, each expectation and Brownian motion in the appendix is taken with respect to the physical measure, P. We also specify the notation that $\mathbb{E}_r[\,\cdot\,] = \mathbb{E}\left[\,\cdot\,\middle|r_0 = r\right]$. The proofs of several of the theorems rely on the following lemma.

Lemma B.1. Suppose $F(r)$ is linear in $(-\infty, d]$ and in $[u, \infty)$ for some d and u such that $d < u$. If $F \in C^1(\mathbb{R}) \cap C^2(\mathbb{R} \setminus N_F)$ where N_F is a set of finitely many points, then for any admissible impulse control $\nu = (\tau_1, \xi_1; \cdots; \tau_i, \xi_i; \cdots)$ and $r \in \mathbb{R}$, we have

$$-F(r) = \mathbb{E}_r\left[\int_0^\infty e^{-\beta t}[\mathcal{A}F(r_{t-}) - \beta F(r_{t-})]dt + \sum_{i=1}^{\infty} e^{-\beta\tau_i}[F(r_{\tau_i}) - F(r_{\tau_i-})]\right]. \tag{B.1}$$

Proof. **Lemma B.1.** We first define some notation. For any admissible impulse control $\nu = (\tau_1, \xi_1; \cdots; \tau_i, \xi_i; \cdots)$, we define $\eta(t)$ as

$$\eta(t) = \sum_{i:\tau_i \le t} \xi_i. \tag{B.2}$$

Then $\eta(t)$ is an $\mathcal{F}_t$ measurable càdlàg process. As in (3.4), we have

$$r_t = r + \int_0^t \mu(r_s)ds + \int_0^t \sigma(r_s)dW_s + \eta(t), \tag{B.3}$$

which is the integral form of the dynamic of the state process under control ν.

Applying the extant second derivative Meyer-Itô's formula (c.f. page 221 of Protter (2005)) together with integration by parts, we have

$$\begin{aligned} e^{-\beta T}F(r_T) - F(r_{0-}) &= \int_0^T e^{-\beta t}F'(r_{t-})\cdot\sigma(r_{t-})dW(t) \\ &+ \int_0^T e^{-\beta t}[\mathcal{A}F(r_{t-}) - \beta F(r_{t-})]dt + \int_0^T e^{-\beta t}F'(r_{t-})d\eta(t) \\ &+ \sum_{t\le T:\eta(t)\neq\eta(t-)} e^{-\beta t}[F(r_t) - F(r_{t-}) - F'(r_{t-})\cdot(\eta(t)-\eta(t-))]. \end{aligned} \tag{B.4}$$

Note that $d\eta(t) = 0$ whenever $\eta(t) = \eta(t-)$ since ν is an impulse control. Also, $\eta(t) = \eta(t-)$ for every $t \notin \{\tau_i : i = 1, 2, \cdots\}$. Therefore,

$$\begin{aligned} \int_0^T e^{-\beta t}F'(r_{t-})d\eta(t) &= \sum_{t\le T:\eta(t)\neq\eta(t-)} e^{-\beta t}F'(r_{t-})\cdot(\eta(t)-\eta(t-)) \\ &= \sum_{i:\tau_i\le T} e^{-\beta\tau_i}F'(r_{\tau_i-})\cdot\xi_i, \end{aligned}$$

and (B.4) becomes

$$\begin{aligned} e^{-\beta T}F(r_T) - F(r) &= \int_0^T e^{-\beta t}F'(r_{t-})\cdot\sigma(r_{t-})dW(t) \\ &+ \int_0^T e^{-\beta t}[\mathcal{A}F(r_{t-}) - \beta F(r_{t-})]dt + \sum_{i:\tau_i\le T} e^{-\beta\tau_i}[F(r_{\tau_i}) - F(r_{\tau_i-})]. \end{aligned} \tag{B.5}$$

Taking expectation of both sides, the first term on the RHS of (B.5) vanishes since F' is bounded, and we have

$$\begin{aligned} e^{-\beta T}\mathbb{E}_r[F(r_T)] - F(r) = \mathbb{E}_r\Bigg[&\int_0^T e^{-\beta t}[\mathcal{A}F(r_{t-}) - \beta F(r_{t-})]dt \\ &+ \sum_{i:\tau_i\le T} e^{-\beta\tau_i}[F(r_{\tau_i}) - F(r_{\tau_i-})]\Bigg]. \end{aligned}$$

Taking the limit as $T \to \infty$, the LHS of above is $-F(r)$. The first term of the RHS, $\mathbb{E}_r[\int_0^T e^{-\beta t}[\mathcal{A}F(r_{t-}) - \beta F(r_{t-})]dt]$ goes to $\mathbb{E}_r[\int_0^\infty e^{-\beta t}[\mathcal{A}F(r_{t-}) - \beta F(r_{t-})]dt]$ as $T \to \infty$, thanks to the Fubini Theorem and the assumptions on F. The last term of RHS, $\sum_{i:\tau_i \le T} e^{-\beta\tau_i}[F(r_{\tau_i}) - F(r_{\tau_i-})]$ goes to $\sum_{i:\tau_i<\infty} e^{-\beta\tau_i}[F(r_{\tau_i}) - F(r_{\tau_i-})]$, due to the admissibility of ν and the assumptions on F. □

Proof. **Theorem 3.1 (Verification Theorem).** By definition, we have $v \ge V$. Thus we only need to prove that $v \le V$. Let ν be an arbitrary admissible impulse control. Applying Lemma B.1 to v, we have

$$-v(r) = \mathbb{E}_r\left[\int_0^\infty e^{-\beta t}[\mathcal{A}v(r_{t-}) - \beta v(r_{t-})]dt + \sum_{i=1}^\infty e^{-\beta\tau_i}[v(r_{\tau_i}) - v(r_{\tau_i-})]\right].$$

On the other hand, the cost function associated with ν is
$\mathcal{J}_r(\nu) = \mathbb{E}_r\Big[\int_0^\infty h(r_t)e^{-\beta t}dt + \sum_n G(\xi_n)e^{-\beta\tau_n}\Big]$. This leads to

$$\begin{aligned}\mathcal{J}_r(\nu) - v(r) &= \mathbb{E}_r\Big[\int_0^\infty e^{-\beta t}\mathcal{L}v(r_{t-})dt \\ &+ \sum_{i=1}^\infty e^{-\beta\tau_i}[G(\xi_i) + v(r_{\tau_i-} + \xi_i) - v(r_{\tau_i-})]\Big] \\ &\ge 0, \end{aligned} \tag{B.6}$$

where we define

$$\mathcal{L}v(\cdot) \equiv \mathcal{A}v(\cdot) - \beta\cdot v(\cdot) + h(\cdot). \tag{B.7}$$

The last inequality is because, v is a solution to the QVI. Therefore, $V(r) = \inf_{\nu\in\mathcal{A}}\mathcal{J}_r(\nu) \ge v(r)$. This leads to $v(r) = V(r)$. □

Proof. **Theorem 3.2 (The fixed boundary problem).** Applying the extant second derivative Meyer-Itô's formula and integration by part, we have

$$-v(r) = \mathbb{E}_r\Bigg[\int_0^\infty e^{-\beta t}[\mathcal{A}v(r_{t-}) - \beta v(r_{t-})]dt + \sum_{i=1}^{\infty} e^{-\beta\tau_i}[v(r_{\tau_i}) - v(r_{\tau_i-})]\Bigg] \ \forall r \in [d, u].$$

Thus, for any $r \in [d, u]$, we have

$$\begin{aligned}\mathcal{J}_r(\nu) - v(r) &= \mathbb{E}_r\Bigg[\int_0^\infty e^{-\beta t}\mathcal{L}v(r_{t-})dt \\ &\quad + \sum_{i=1}^{\infty} e^{-\beta\tau_i}[G(\xi_i) + v(r_{\tau_i-} + \xi_i) - v(r_{\tau_i-})]\Bigg] \qquad \text{(B.8)} \\ &= 0.\end{aligned}$$

The last equality above is due to definition of the $(d,\ D,\ U,\ u)$ policy and the fact that v solves the differential equation problem (3.11)-(3.13). □

Proof. **Theorem 3.3.** 1. Let $w(r) = V_n(r) - \bar{V}_n(r)$, then we have

$$\begin{aligned}\mathcal{A}w(r) - \beta w(r) &= 0,\ r \in (d_{n+1}, u_{n+1}) \qquad \text{(B.9)} \\ w(d_{n+1}) &= V_n(d_{n+1}) - \bar{V}_n(d_{n+1}) = V_n(d_n) - \bar{V}_n(d_{n+1}) \\ &\quad + V_n(d_{n+1}) - V_n(d_n) \\ &= V_n(D_n) - \bar{V}_n(D_n) + [V_n(d_{n+1}) + k \cdot d_{n+1}] \\ &\quad - [V_n(d_n) + k \cdot d_n] \\ &= w(D_n) + \int_{d_n}^{d_{n+1}} (V_n'(s) + k)ds \geq w(D_n). \qquad \text{(B.10)}\end{aligned}$$

The final inequality in (B.10) is because $V_n'(r) + k \geq 0$ in $[d_n, d_{n+1}]$. Similarly, we have $w(u_{n+1}) \geq w(U_n)$. Therefore, $\exists t_0 \in (d_{n+1}, u_{n+1})$ such that $\forall r \in$

$[d_{n+1}, u_{n+1}], w(t_0) \leq w(r)$. At t_0, we have $w'(t_0) = 0$ and $w''(t_0) \geq 0$. This, together with Equation (B.9), yields

$$w(t_0) = \frac{1}{\beta} \cdot \frac{\sigma^2(t_0)}{2} w''(t_0) \geq 0, \tag{B.11}$$

and this implies that for any $r \in [d_{n+1}, u_{n+1}]$,$w(r) \geq w(t_0) \geq 0$.

Also, by Equation (B.10), we know that

$$\begin{aligned} V_n(d_{n+1}) - \bar{V}_n(d_{n+1}) = w(d_{n+1}) &= w(D_n) + [V_n(d_{n+1}) + k \cdot d_{n+1}] \\ &\quad -[V_n(d_n) + k \cdot d_n] \\ &\geq [V_n(d_{n+1}) + k \cdot d_{n+1}] - [V_n(d_n) + k \cdot d_n] \end{aligned}$$

or equivalently, $\bar{V}_n(d_{n+1}) \leq V_n(d_n) - k \cdot (d_{n+1} - d_n)$. Thus any $r \in [d_n, d_{n+1}]$, we have

$$\begin{aligned} \bar{V}_n(r) = \bar{V}_n(d_{n+1}) + k \cdot (d_{n+1} - r) &\leq V_n(d_n) - k \cdot (r - d_n) \\ &= V_n(r) - \int_{d_n}^{r} [k + V_n'(s)] ds \leq V_n(r). \end{aligned}$$

Similarly, we have $\bar{V}_n(r) \leq V_n(r)$ in $[u_{n+1}, u_n]$. In $(-\infty, d_n]$ and $[u_n, +\infty)$, it is trivial to see that $\bar{V}_n(r) \leq V_n(r)$ since both cost functions are linear with the same slope in those regions.

2. To prove that $\bar{V}_n'(d_{n+1}+) + k \geq 0$, we only need to show that $w'(d_{n+1}+) \leq 0$. Assume the contrary, then we have $w'(d_{n+1}+) > 0$. This, together with $w(d_{n+1}) \geq w(D_n)$, implies that $\exists t_1 \in (d_{n+1}, D_n)$ such that $w(t_1) = \max_{r \in [d_{n+1}, D_n]} w(r)$, and $w(t_1) > w(d_{n+1})$. This leads to

$$\beta w(t_1) = \frac{1}{2}\sigma^2(t_1) w''(t_1) + (a + b \cdot t_1) w'(t_1) = \frac{1}{2}\sigma^2(t_1) w''(t_1) \leq 0, \tag{B.12}$$

which contradicts that $w(t_1) > w(d_{n+1}) \geq 0$. Thus $w'(d_{n+1}+) \leq 0$, which implies $\bar{V}_n'(d_{n+1}) + k \geq V_n'(d_{n+1}) + k \geq 0$. Similarly, it is easy to show that $-\bar{V}_n'(u_{n+1}) + l \geq 0$.

3. Assume the contrary, that is $D_{n+1} > U_{n+1}$.

Case 1: $\bar{V}_n(D_{n+1}) \leq \bar{V}_n(U_{n+1})$.This leads to $\bar{V}_n(D_{n+1}) - l \cdot D_{n+1} \leq \bar{V}_n(U_{n+1}) - l \cdot D_{n+1} < \bar{V}_n(U_{n+1}) - l \cdot U_{n+1}$, which contradicts the definition of U_{n+1}.

Case 2: $\bar{V}_n(D_{n+1}) > \bar{V}_n(U_{n+1})$. We have $\bar{V}_n(D_{n+1}) + k \cdot D_{n+1} > \bar{V}_n(U_{n+1}) + k \cdot D_{n+1} > \bar{V}_n(U_{n+1}) + k \cdot U_{n+1}$, which contradicts the definition of D_{n+1}.

Thus both cases lead to $D_{n+1} \leq U_{n+1}$.

4 and 5. Let $\bar{w}(r) = \bar{V}_n(r) - V_{n+1}(r)$, then, $\mathcal{A}\bar{w}(r) - \beta\bar{w}(r) = 0$ in $[d_{n+1}, u_{n+1}]$. Also, we have

$$\begin{aligned}
\bar{w}(d_{n+1}) &= \bar{V}_n(d_{n+1}) - V_{n+1}(d_{n+1}) \\
&= \bar{V}_n(D_n) + k \cdot D_n - [V_{n+1}(D_{n+1}) + k \cdot D_{n+1}] \\
&= \{[\bar{V}_n(D_n) + k \cdot D_n] - [\bar{V}_n(D_{n+1}) + k \cdot D_{n+1}]\} \\
&\quad +[\bar{V}_n(D_{n+1}) - V_{n+1}(D_{n+1})] \\
&\geq \bar{V}_n(D_{n+1}) - V_{n+1}(D_{n+1}) = \bar{w}(D_{n+1}).
\end{aligned}$$

The inequality is because $\bar{V}_n(D_n) + k \cdot D_n \geq \bar{V}_n(D_{n+1}) + k \cdot D_{n+1}$, according to the definition of D_{n+1}.

Similarly, we have $\bar{w}(u_{n+1}) \geq \bar{w}(U_{n+1})$. Following exactly the same argument

in the proof for claim 1 and 2, we know that $\bar{w}(u_{n+1}) \geq 0$, and $\bar{w}'(d_{n+1}) \leq 0$, and $\bar{w}'(u_{n+1}) \geq 0$. This implies, $V_{n+1}(r) \leq \bar{V}_n(r)$ for any $r \in [d_{n+1}, u_{n+1}]$, $V'_{n+1}(d_{n+1}) + k \geq 0$ and $-V'_{n+1}(u_{n+1}) + l \geq 0$. In $(-\infty, d_{n+1}]$, $V_{n+1}(r) \leq \bar{V}_n(r)$ since both functions are linear with the same slope. So is the case in $[u_{n+1}, +\infty)$.

□

Proof. **Theorem 3.4.** We first focus on the case when $\beta - \mu'(r) \geq 0 \; \forall r$. Due to the Theorem 3.1, to prove that $v(r)$ is the value function, it suffices to show that $v(r)$ satisfies the QVI (3.10), since the rest of the requirements in Theorem 3.1 are automatically satisfied. We prove this Theorem by establishing the following,

(i) $\mathcal{A}v(r) - \beta v(r) + h(r) \geq 0$ a.e. $r \in \mathbb{R}$.

(ii) $\mathcal{Q}v(r) \geq 0$ for all $r \in \mathbb{R}$.

(iii) $\mathcal{Q}V(r) \cdot [\mathcal{A}V(r) - \beta \cdot V(r) + h(r)] = 0 \; \forall \; r$.

Now, to prove i, we first define $f(r) = v'(r)$. Since (d, D, U, u) is the policy obtained at convergence, and v is its associated cost function, there exists $\epsilon_1 > 0$ such that

$$\begin{cases} v'(r) + k < 0, & \forall r \in (d, d + \epsilon_1] \\ -v'(r) + l < 0, & \forall r \in [u - \epsilon_1, u). \end{cases} \tag{B.13}$$

Also, we have

$$\begin{cases} D = \arg\min_{r\in(d,u)} \{v(r) + k \cdot r\} & (\text{implying } v'(D) = -k) \\ U = \arg\min_{r\in(d,u)} \{v(r) - l \cdot r\} & (\text{implying } v'(U) = l). \end{cases} \tag{B.14}$$

The reason is, if any of (B.13)–(B.14) does not hold, the scheme could further update (d, D, U, u) to improve v, which contradicts to the assumption that (d, D, U, u) and v are the policy and the associated cost function obtained at convergence. The assumption that v is C^1 leads to $v'(d) + k = 0$ and $-v'(u)+l = 0$, and this together with (B.13) implies $f'(d+) = v''(d+) < 0$ and $f'(u-) = v''(u-) < 0$. Since $f'(d+) = v''(d+) < 0$ and $f(d) = f(D) = -k$, we know that $\exists\ \bar{r}_1 \in (d, D)$ which minimizes f over the closed interval $[d, D]$. We define

$$\begin{aligned} r_1 &= \min_{r>d}\{r \text{ is a local minimizer of } f\} \\ r_2 &= \max_{r<D}\{r \text{ is a local minimizer of } f\}. \end{aligned}$$

And from (3.11), we know that

$$\frac{1}{2}\sigma^2(r)v''(r) = -\mu(r) \cdot v'(r) + \beta \cdot v(r) - h(r), \forall r \in (d, u). \tag{B.15}$$

The RHS of (B.15) is $C^1(\mathbb{R} - N_h)$, and thus the LHS is also $C^1(\mathbb{R} - N_h)$. Taking left Derivative of (B.15), we get

$$\frac{1}{2}\sigma^2(r)v'''(r-) + \sigma'(r)\sigma(r)v''(r) = -\mu(r) \cdot v''(r) + (\beta - \mu'(r)) \cdot v'(r) - h'(r-), \quad \forall r \in (d, u),$$

or equivalently,

$$\frac{1}{2}\sigma^2(r)f''(r-)+(\sigma'(r)\sigma(r)+\mu(r))\cdot f'(r) = (\beta-\mu'(r))\cdot f(r)-h'(r-), \forall r \in (d, u).$$

Let $r = r_2$, we have

$$\begin{aligned}
\frac{1}{2}\sigma^2(r_2)f''(r_2-) &= (\beta - \mu'(r_2)) \cdot f(r_2) - h'(r_2-) \\
&\leq (\beta - \mu'(r_2)) \cdot f(D) - h'(r_2-) \\
&= -(\beta - \mu'(r_2)) \cdot k - h'(r_2-).
\end{aligned}$$

The last inequality above is because $f(r_2) \leq f(D)$ and $\beta - \mu'(r) \geq 0$ $\forall r$. This can be easily seen from the definition of r_2 together with the fact that $f'(D) = v''(D) \geq 0$. Since $f''(r_2-) \geq 0$, we know that $h'(r_2-)+(\beta-\mu'(r_2))\cdot k \leq 0$. By the assumption on $h(r)$, we have $h'(r-) + (\beta - \mu'(r)) \cdot k \leq 0$, $\forall r < r_2$. Therefore, $\forall r \in (-\infty, d)$, we have

$$\begin{aligned}
\mathcal{L}v(r) &= \frac{1}{2}\sigma^2(r)v''(r) + \mu(r) \cdot v'(r) - \beta \cdot v(r) + h(r) \\
&= 0 - \mu(r) \cdot k - \beta \cdot [v(d) + k \cdot (d - r)] + h(r) \\
&= [0 - \mu(d) \cdot k - \beta \cdot v(d) + h(d)] - \beta k \cdot (d - r) + \mu(d) \cdot k - \mu(r) \cdot k \\
&\quad + h(r) - h(d) \\
&= [0 - \mu(d) \cdot k - \beta \cdot v(d) + h(d)] \\
&\quad - [(\beta \cdot (d - r) - \mu(d) + \mu(r)) \cdot k + h(d) - h(r)] \\
&> \frac{1}{2}\sigma^2 v''(d+) + \mu(d) \cdot v'(d) - \beta \cdot v(d) + h(d) \\
&\quad - \int_r^d [(\beta - \mu'(s)) \cdot k + h'(s)]ds \\
&\geq \mathcal{L}v(d+) = 0.
\end{aligned}$$

The inequality in the above is because $\frac{1}{2}\sigma^2 v''(d+) < 0$ and $(\beta - \mu'(s)) \cdot k + h'(s) \leq 0$ for any $s \in (r, d)$.

Similarly, we define

$$\begin{aligned} r_3 &= \min_{r>U}\{r \text{ is a local maximizer of } f\} \\ r_4 &= \max_{r<u}\{r \text{ is a local maximizer of } f\}. \end{aligned}$$

Then, we have $(\beta-\mu'(r))\cdot l-h'(r) \leq 0$, $\forall r > r_3$. By similar arguments, we can prove that $\mathcal{L}v(r) > 0$, $\forall r > u$. Therefore, $\mathcal{A}v(r) - \beta v(r) + h(r) = \mathcal{L}v(r) \geq 0$, *a.e.* $r \in \mathbb{R}$.

Next we will prove ii. We define the notation: $\mathcal{I}v(r) \equiv \inf_{\xi>0}\left\{v(r+\xi)+K+k\xi\right\}$ which represents the value of *increasing* the short rate. Similarly we define $\mathcal{D}v(r) \equiv \inf_{\xi>0}\left\{v(r-\xi)+L+l\cdot\xi\right\}$, which represents the value of placing a control to *decrease* the short rate. We will finish the proof of ii by showing the following:

(I) $\mathcal{I}v(r) - v(r) \geq 0$ for all $r \in \mathbb{R}$.

  (a) $\mathcal{I}v(r) - v(r) = 0$ for $r \in (-\infty, d]$.

  (b) $\mathcal{I}v(r) - v(r) > 0$ for $r \in [u, \infty)$.

  (c) $\mathcal{I}v(r) - v(r) > 0$ for $r \in (d, D]$.

  (d) $\mathcal{I}v(r) - v(r) > 0$ for $r \in [U, u)$.

  (e) $\mathcal{I}v(r) - v(r) > 0$ for $r \in (D, U)$.

(II) $\mathcal{D}v(r) - v(r) \geq 0$ for all $r \in \mathbb{R}$.

  (a) $\mathcal{D}v(r) - v(r) = 0$ for $r \in [u, \infty)$.

(b) $\mathcal{D}v(r) - v(r) > 0$ for $r \in (-\infty, d]$.

(c) $\mathcal{D}v(r) - v(r) > 0$ for $r \in [U, u)$.

(d) $\mathcal{D}v(r) - v(r) > 0$ for $r \in (d, D]$.

(e) $\mathcal{D}v(r) - v(r) > 0$ for $r \in (D, U)$.

Note that $d < D < U < u$, and D minimizes $v(r) + k \cdot r$ over $[d, u]$, and thus, minimizes it over $\mathbb{R}$. This is because $v'(r) + k \equiv 0$ for all $r < d$, and $v'(r) + k > 0$ for all $r > u$. Therefore, (I.Ia) is easy to verify. Considering $r \geq u$, it is easy to see that

$$\begin{aligned} \mathcal{I}v(r) - v(r) &= \inf_{\eta > r, \eta \in \mathbb{R}} \Big\{ v(\eta) + K + k \cdot (\eta - r) \Big\} - v(r) \\ &= \inf_{\eta > r, \eta \in \mathbb{R}} \Big\{ v(r) + l \cdot (\eta - r) + K + k \cdot (\eta - r) \Big\} - v(r) \\ &\geq K > 0. \end{aligned}$$

Thus (I.Ib) is proved. To prove (I.Ic), we claim that $v'(r) + k \leq 0$ for any $r \in [d, D]$. If $r_1 = r_2$, then the claim is easy to verify. If $r_1 < r_2$, and assuming the contrary, there will be an $\hat{r} \in (r_1, r_2)$ which is a local maximizer of $v'(r) \equiv f(r)$ such that $v'(\hat{r}) > -k$. Using $f(r)$ to denote $v'(r)$, and we have

$$\begin{aligned} h'(\hat{r}-) &= (\beta - \mu'(\hat{r})) \cdot f(\hat{r}) - \frac{1}{2}\sigma^2(\hat{r}) f''(\hat{r}-) \\ &> (\beta - \mu'(\hat{r})) \cdot (-k). \end{aligned}$$

However, since $h'(r_2-) + (\beta - \mu'(r_2)) \cdot k \leq 0$ and $\hat{r} < r_2$, we should have $h'(\hat{r}-) + (\beta - \mu'(\hat{r})) \cdot k \leq 0$ which leads to a contradiction. So, we have that

$v'(r) + k \leq 0$ for $r \in [d, D]$. Similarly, we have $-v'(r) + l \leq 0$ for $r \in [U, u]$. Then, considering $\mathcal{I}v(r) - v(r)$ for any $r \in (d, D)$, we have

$$\begin{aligned}
\mathcal{I}v(r) - v(r) &= v(D) + K + k \cdot (D - r) - v(r) \\
&= v(D) + K + k \cdot (D - d) - v(d) + v(d) - v(r) + k \cdot (d - r) \\
&= 0 - \int_d^r [v'(s) + k] ds \\
&> 0.
\end{aligned}$$

The inequality is due to the fact that $v'(s) + k \leq 0$ over the interval of integration. At $r = D$, we have

$$\begin{aligned}
\mathcal{I}v(D) - v(D) &= \inf_{\xi > D, \xi \in \mathbb{R}} \{v(\xi) + K + k \cdot (\xi - D)\} - v(D) \\
&\geq \inf_{\xi \geq D, \xi \in \mathbb{R}} \{v(\xi) + K + k \cdot (\xi - D)\} - v(D) \\
&= v(D) + K + k \cdot 0 - v(D) \\
&> 0
\end{aligned}$$

This proves (I.Ic). Now, (I.Id) is trivial since, when proving (I.Ic) we showed that $v'(r) \geq l > 0$ for $r \in [U, u]$, which yields

$$\begin{aligned}
\mathcal{I}v(r) - v(r) &= \inf_{\xi > r, \xi \in \mathbb{R}} \{v(\xi) + K + k \cdot (\xi - r)\} - v(r) \\
&= \inf_{\xi > r, , \xi \in \mathbb{R}} \{\int_r^\xi [v'(s) + k] ds\} + K \\
&\geq K.
\end{aligned}$$

To prove (I.Ie), we claim that $v'(r) + k \geq 0$ for all $r \in (D, U)$. (Note that we only need to consider the case where $k, l \geq 0$ and $k + l > 0$, since if

$k = l = 0$, then the assumption in the theorem implies $D = U$, and hence the (I.Ie) is automatically true.) To prove this claim, we first define r_5 as

$$r_5 = \inf\{r > D : \ v'(r) + k \neq 0\}.$$

Since $v'(U) = l > -k$, we know that $r_5 < U$. Then, either there exists some $\epsilon > 0$ such that $v'(y) + k > 0$ for all $y \in (r_5, r_5 + \epsilon)$, or there exists some $\epsilon > 0$ such that $v'(y) + k < 0$ for all $y \in (r_5, r_5 + \epsilon)$. Due to the fact that D is the minimizer of $v(r) + k \cdot r$ over $[d, u]$, and $d < D < U < u$, we know that, only the first case could be true; otherwise, $v(y) + k \cdot r < v(D) + k \cdot D$ for any $y \in (r_5, r_5 + \epsilon)$, which is a contradiction. Therefore, we can define r_6 as

$$r_6 = \min\{r > D : \ r \text{ is a local maximizer of } v'(r)\}.$$

Due to the above reasoning, $v'(r_6) > -k$. Now, if the claim were false, there should be some point $r_7 \in (r_6, U)$ such that $v'(r_7) < -k$ and r_7 is a local minimizer of $v'(r)$. These lead to the following

$$\begin{aligned} h'(r_6-) &= (\beta - \mu'(r_6))f(r_6) - \frac{1}{2}\sigma^2(r_6)f''(r_6-) > -(\beta - \mu'(r_6)) \cdot k \\ h'(r_7-) &= (\beta - \mu'(r_7))f(r_7) - \frac{1}{2}\sigma^2(r_7)f''(r_7-) < -(\beta - \mu'(r_7)) \cdot k, \end{aligned}$$

and this contradicts the assumption on $h(r)$ since $r_6 < r_7$. The claim is proved. Combining this with the result we proved above, we know that $v'(r) + k \geq 0$

if $r > D$, which implies that for every $r > D$, we have

$$\begin{aligned}
\mathcal{I}v(r) - v(r) &= \inf_{\xi > r, \xi \in \mathbb{R}} \{v(\xi) + K + k \cdot (\xi - r)\} - v(r) \\
&= \inf_{\xi > r, \xi \in \mathbb{R}} \{v(\xi) + k \cdot (\xi - r) - v(r)\} + K \\
&= \inf_{\xi > r, \xi \in \mathbb{R}} \{\int_r^{\xi} [v'(s) + k] ds\} + K \\
&\geq K \\
&> 0,
\end{aligned}$$

proving (I.Ie).

The proof of (II.IIa)–(II.IIe) is similar to those of (I.Ia)–(I.Ie).

Lastly, we need to prove iii. Note that $\mathcal{A}v(r) - \beta v(r) + h(r) = 0$ in (d, u) due to the assumptions on v, therefore $\mathcal{Q}v(r)[\mathcal{A}v(r) - \beta v(r) + h(r)] = 0$ in this region. Also note that $\mathcal{Q}v(r) = \min\{\mathcal{I}v(r) - v(r), \mathcal{D}v(r) - v(r)\}$. (I.Ia) and (II.IIb) yields $\mathcal{Q}v(r) = \mathcal{I}v(r) - v(r) = 0 \ \forall r \leq d$; similarly from (I.Ib) and (II.IIa) we have $\mathcal{Q}v(r) = \mathcal{D}v(r) - v(r) = 0$ in $\forall r \geq u$. Thus $\mathcal{Q}v(r)[\mathcal{A}v(r) - \beta v(r) + h(r)] = 0 \ \forall r$. □

We next focus on the case when $\beta - \mu'(r) < 0$ for some r. Similar to the case when $\beta - \mu'(r) \geq 0 \ \forall r$, we only need to show that $v(r)$ satisfies the QVI (3.10).

First, we want to prove that $\mathcal{A}v(r) - \beta v(r) + h(r) \geq 0$ a.e. $r \in \mathbb{R}$. Based on the same reasoning as that in the proof of Theorem 3.4, we have (B.13)–(B.14) hold as well as $v''(d+) < 0$ and $v''(u-) < 0$. Therefore, $\forall r \in (-\infty, d)$,

we have

$$\begin{aligned}
\mathcal{L}v(r) &= \frac{1}{2}\sigma^2(r)v''(r) + \mu(r)\cdot v'(r) - \beta\cdot v(r) + h(r) \\
&= 0 - \mu(r)\cdot k - \beta\cdot[v(d) + k\cdot(d-r)] + h(r) \\
&= [0 - \mu(d)\cdot k - \beta\cdot v(d) + h(d)] - \beta k\cdot(d-r) + \mu(d)\cdot k - \mu(r)\cdot k \\
&\quad + h(r) - h(d) \\
&= [0 - \mu(d)\cdot k - \beta\cdot v(d) + h(d)] \\
&\quad -[(\beta\cdot(d-r) - \mu(d) + \mu(r))\cdot k + h(d) - h(r)] \\
&> \frac{1}{2}\sigma^2 v''(d+) + \mu(d)\cdot v'(d) - \beta\cdot v(d) + h(d) \\
&\quad - \int_r^d [(\beta - \mu'(s))\cdot k + h'(s)]ds \\
&\geq \mathcal{L}v(d+) = 0.
\end{aligned}$$

The inequality in the above is because $(\beta - \mu'(s))\cdot k + h'(s) \leq 0$ for any $s \in (r, d)$.

Similarly, we can prove that $\mathcal{L}v(r) > 0$, $\forall r > u$. Therefore, $\mathcal{A}v(r) - \beta v(r) + h(r) = \mathcal{L}v(r) \geq 0$, *a.e.* r

Next we will prove that $\mathcal{Q}v(r) \geq 0$ for all r. Specifically we will show the following, which are the counterpart of those in the proof of Theorem 3.4

(I) $\mathcal{I}v(r) \equiv \inf_{\xi>0}\left\{v(r+\xi) + K + k\xi\right\} \geq v(r)$ for all r.

(a) $\mathcal{I}v(r) - v(r) = 0$ for $r \leq d$.

(b) $\mathcal{I}v(r) - v(r) > 0$ for $r \geq u$.

(c) $\mathcal{I}v(r) - v(r) > 0$ for $r \in (d, D]$.

(d) $\mathcal{I}v(r) - v(r) > 0$ for $r \in [U, u)$.

(e) $\mathcal{I}v(r) - v(r) > 0$ for $r \in (D, U)$.

(II) $\mathcal{D}v(r) \equiv \inf_{\xi>0} \left\{v(r-\xi) + L + l \cdot \xi\right\} \geq v(r)$ for all $r \in \mathbb{R}$.

(a) $\mathcal{D}v(r) - v(r) = 0$ for $r \geq u$.

(b) $\mathcal{D}v(r) - v(r) > 0$ for $r \leq d$.

(c) $\mathcal{D}v(r) - v(r) > 0$ for $r \in [U, u)$.

(d) $\mathcal{D}v(r) - v(r) > 0$ for $r \in (d, D]$.

(e) $\mathcal{D}v(r) - v(r) > 0$ for $r \in (D, U)$.

Note that D minimizes $v(r) + k \cdot r$ over $[d, u]$, and thus, minimizes it over all possible r. This is because $v'(r) + k \equiv 0$ for all $r < d$, and $v'(r) + k > 0$ for all $r > u$. Therefore, for $r \leq d$ $\inf_{\xi>0} \left\{v(r+\xi)+K+k\xi\right\} = v(D)+K+k(D-r) = v(r)$, implying (I.Ia).

For $r \geq u$, $v'(r) = l \geq 0$, verifying (I.Ib) since $\inf_{\eta>r,\eta\in\mathbb{R}} \Big\{v(\eta) + K + k \cdot (\eta - r)\Big\} - v(r) \geq K > 0$.

Note that we have $v'(r) + k \leq 0$ for any $r \in [d, D]$ from the assumption of the Theorem. Then we have $\mathcal{I}v(r) - v(r) = v(D) + K + k \cdot (D - d) - v(d) + v(d) - v(r) + k \cdot (d - r) = 0 - \int_d^r [v'(s) + k] ds > 0$ for r in $(d, D]$, proving (I.Ic).

(I.Id) and (I.Ie) are trivial since $v'(r) + k \geq 0$ for $r > D$, which yields $\mathcal{I}v(r) - v(r) = \inf_{\xi>r}\{v(\xi)+K+k\cdot(\xi-r)\} - v(r) = \inf_{\xi>r}\{\int_r^\xi [v'(s)+k] ds\} + K \geq K$.

The proof of (II.IIa)–(II.IIe) is similar to those of (I.Ia)–(I.Ie).

Finally, $\mathcal{A}v(r) - \beta v(r) + h(r) = 0$ in (d, u) due to the assumption on v; (I.Ia) and (II.IIb) yields $\mathcal{Q}v(r) = \mathcal{I}v(r) - v(r) = 0\ \forall r \leq d$; (I.Ib) and (II.IIa) yields $\mathcal{Q}v(r) = \mathcal{D}v(r) - v(r) = 0$ in $\forall r \geq u$. Thus $\mathcal{Q}v(r)[\mathcal{A}v(r) - \beta v(r) + h(r)] = 0\ \forall r$. Therefore v satisfies the QVI, and this finishes the proof of the theorem.

To prove $\epsilon-$Optimality Theorem, we first establish the following lemma.

Lemma B.2. Suppose $v(r)$ is the cost function associated with an admissible impulse control characterized by $d < D \leq U < u$, which implies that $v(r)$ solves (3.11)–(3.14). Further assume that $\sigma^2(\cdot) > 0$, $v'(d+) + k \geq 0$, $-v'(u-) + l \geq 0$ and $v(r)$ satisfies the following conditions for some $\epsilon_1,\ \epsilon_2,\ \epsilon_3 > 0$

$$\begin{cases} \mathcal{A}v(r) - \beta \cdot v(r) + h(r) & \geq -\epsilon_1 \text{ a.e. } r \\ \inf_{\xi>0} \left\{ v(r+\xi) + K + k \cdot \xi \right\} - v(r) & \geq -\epsilon_2 \\ \inf_{\xi>0} \left\{ v(r-\xi) + L\ + l \cdot \xi \right\} - v(r) & \geq -\epsilon_3 \end{cases}$$

Then, $\forall \bar{\epsilon} > 0$, $\exists \bar{v} \in C^1$ such that $v(r) - \bar{\epsilon} \leq \bar{v}(r) \leq v(r)$, and it is linear outside some finite interval $(\bar{d}, \bar{u})$. Also, it is C^2 except on a few points, and it satisfies the following conditions

$$\begin{cases} \mathcal{A}\bar{v}(r) - \beta \cdot \bar{v}(r) + h(r) & \geq -(\epsilon_1 + \bar{\epsilon}) \text{ a.e. } r \\ \inf_{\xi>0} \left\{ \bar{v}(r+\xi) + K + k \cdot \xi \right\} - \bar{v}(r) & \geq -(\epsilon_2 + \bar{\epsilon}) \\ \inf_{\xi>0} \left\{ \bar{v}(r-\xi) + L\ + l \cdot \xi \right\} - \bar{v}(r) & \geq -(\epsilon_3 + \bar{\epsilon}) \end{cases}$$

Proof. **Lemma B.2.** If $v'(d+) + k = 0$ and $-v'(u-) + l = 0$, then we are done by setting $\bar{v} = v$. If at the case where at least one of them is positive, say, $v'(d+) + k = \Delta$ for some $\Delta > 0$, then let $\bar{v}(r) = v(r)$ in $[d, u]$ and define $\bar{v}(r)$

in the following way for $r \leq d$:

$$\bar{v}(r) = \begin{cases} A_2 r^2 + A_1 r + A_0 & \forall r \in [\bar{d}, d] \\ \bar{v}(\bar{d}) + k(\bar{d} - r) & \forall r < \bar{d} \end{cases} \tag{B.16}$$

in which $\bar{d} = d - \delta$, and δ is a positive constant whose value will be specified later. Here A_0, A_1 and A_2 are some constants whose value are specified in the way to make $\bar{v}$ be C^1, therefore, we need

$$\bar{v}(d) = A_2 \cdot d^2 + A_1 \cdot d + A_0 = v(d), \tag{B.17}$$

$$\bar{v}'(d-) = 2A_2 \cdot d + A_1 = \bar{v}(d+) = v'(d+) = \Delta - k, \tag{B.18}$$

$$\bar{v}'(\bar{d}-) = 2A_2 \cdot \bar{d} + A_1 = -k = \bar{v}'(\bar{d}+). \tag{B.19}$$

Solving (B.17)–(B.19), we have

$$A_2 = \frac{1}{2}\frac{\Delta}{\delta}, \quad A_1 = \Delta - k - \frac{\Delta \cdot d}{\delta}, \quad A_0 = v(d) - (\Delta - k) \cdot d + \frac{1}{2}\frac{\Delta}{\delta} \cdot d^2. \tag{B.20}$$

It is easy to verify that $\max_{r \leq u}\{v(r) - \bar{v}(r)\} = v(\bar{d}) - \bar{v}(\bar{d}) = \frac{1}{2}\frac{\Delta}{\delta} > 0$ and $v(r) \geq \bar{v}(r)\ \forall r \leq u$. When setting δ small enough, we have $v(r) - \bar{\epsilon} \leq \bar{v}(r) \leq v(r)\ \forall r \leq u$. Similarly, if $-v'(u-) + l$ is strictly positive, we set $\bar{v}(r) = B_2 r^2 + B_1 r + B_0$ in $[u, \bar{u}]$ and extend it linearly with slope l for $r \geq \bar{u} \equiv u + \delta$. Choosing δ small enough we will have $v(r) - \bar{\epsilon} \leq \bar{v}(r) \leq v(r)\ \forall r$. We omit this construction for $r \geq u$.

Now we look at $\mathcal{I}\bar{v}(r) \equiv \inf_{\xi > 0}\left\{\bar{v}(r + \xi) + K + k\xi\right\}$. Since

$$\bar{v}(r + \xi) + K + k\xi - \bar{v}(r) \geq v(r + \xi) - \frac{\Delta}{2}\delta + K + k\xi - v(r),$$

we have $\inf_{\xi > 0}\left\{\bar{v}(r + \xi) + K + k \cdot \xi\right\} - \bar{v}(r) \geq -(\epsilon_2 + \bar{\epsilon})$ when δ is small enough. Similarly we have $\inf_{\xi > 0}\left\{\bar{v}(r - \xi) + L\ + l \cdot \xi\right\} - \bar{v}(r) \geq -(\epsilon_3 + \bar{\epsilon})$.

Now we look at $\bar{v}(r) - \beta \cdot \bar{v}(r) + h(r)$. In $(\bar{d}, d)$ using (B.20) we have

$$\begin{aligned}\mathcal{A}\bar{v}(r) - \beta \cdot \bar{v}(r) + h(r) &= \frac{\sigma^2(r)}{2}\frac{\Delta}{\delta} + \mu(r) \cdot (-k + \frac{r - \bar{d}}{\delta}\Delta) - \beta\bar{v}(r) + h(r) \\ &\geq [\frac{\sigma^2(r)}{2}\frac{\Delta}{\delta} + \mu(r)\frac{r - \bar{d}}{\delta}\Delta] \\ &\quad +\mu(r) \cdot (-k) - \beta v(r) + h(r) \qquad \text{(B.21)}\end{aligned}$$

Since $\mu(r)$ is bounded in $[\bar{d}, d]$, and $0 \leq \frac{r-\bar{d}}{\delta} \leq 1$, for small enough δ we have

$$\begin{aligned}\mathcal{A}\bar{v}(r) - \beta \cdot \bar{v}(r) + h(r) &\geq 0 + (-k)\mu(r) - \beta v(r) + h(r) - \bar{\epsilon} \\ &= \mathcal{A}v(r) - \beta v(r) + h(r) - \bar{\epsilon} \geq -(\epsilon_1 + \bar{\epsilon}).\end{aligned}$$

For $r < \bar{d}$, $\bar{v}''(r) = v(r) = 0$, $\bar{v}'(r) = \bar{v}'(r) = -k$, implying $\mathcal{A}\bar{v}(r) = \mathcal{A}v(r)$. This, together with $\bar{v}(r) \leq v(r)$, yields $\mathcal{A}\bar{v}(r) - \beta \cdot \bar{v}(r) + h(r) \geq \mathcal{A}v(r) - \beta v(r) + h(r) \geq -\epsilon_1 \geq -(\epsilon_1 + \bar{\epsilon})$.

Similarly, we can have$\mathcal{A}\bar{v}(r) - \beta \cdot \bar{v}(r) + h(r) \geq -(\epsilon_1 + \bar{\epsilon})$ for $r \in (u, \bar{u})$ and for $r > \bar{u}$. Lastly, $\bar{v}(r)$ is C^2 except on $\{d, u, \bar{d}, \bar{u}\}$, finishing the proof of the Lemma. □

Proof. **Theorem 3.5 ($\epsilon-$Optimality Theorem).** Take any admissible impulse control policy $\nu = (\tau_1, \xi_1; \cdots; \tau_i, \xi_i; \cdots)$. For any given $\bar{\epsilon} > 0$, we apply Lemma B.2 to construct $\bar{v}$from $v(r)$. Applying Lemma B.1

$$-\bar{v}(r) = \mathbb{E}_r\left[\int_0^\infty e^{-\beta t}[\mathcal{A}\bar{v}(r_{t-}) - \beta\bar{v}(r_{t-})]dt + \sum_{i=1}^{\infty} e^{-\beta\tau_i}[\bar{v}(r_{\tau_i}) - \bar{v}(r_{\tau_i-})]\right],$$

This leads to

$$\begin{aligned}
\mathcal{J}_r(\nu) - \bar{v}(r) &= \mathbb{E}_r\left[\int_0^\infty e^{-\beta t}\mathcal{A}\bar{v}(r_{t-}) - \beta\cdot\bar{v}(r_{t-}) + h(r_{t-})dt\right] \\
&\quad + \mathbb{E}_r\left[\sum_{n:\xi_n>0} e^{-\beta\tau_n}[K + k\xi_n + \bar{v}(r_{\tau_n-}+\xi_n) - \bar{v}(r_{\tau_n-})]\right] \\
&\quad + \mathbb{E}_r\left[\sum_{n:\xi_n<0} e^{-\beta\tau_n}[L - l\xi_n + \bar{v}(r_{\tau_n-}+\xi_n) - \bar{v}(r_{\tau_n-}))]\right] \\
&\geq \int_0^\infty (-\epsilon_1 - \bar{\epsilon})e^{-\beta t}dt \\
&\quad + \mathbb{E}_r\left[\sum_{n:\xi_n>0} e^{-\beta\tau_n}(-\epsilon_2 - \bar{\epsilon}) + \sum_{n:\xi_n<0} e^{-\beta\tau_n}(-\epsilon_3 - \bar{\epsilon})\right] \quad \text{(B.22)} \\
&\geq -\frac{\epsilon_1 + \bar{\epsilon}}{\beta} - (\epsilon_2 + \bar{\epsilon})\frac{\mathcal{J}_r(\nu)}{K} - (\epsilon_3 + \bar{\epsilon})\frac{\mathcal{J}_r(\nu)}{L}.
\end{aligned}$$

The last inequality is because

$$\mathcal{J}_r(\nu) \geq \mathbb{E}_r\left[\sum_n G(\xi_n)e^{-\beta\tau_n}\right] \geq K\cdot\mathbb{E}_r\left[\sum_{n:\xi_n>0} e^{-\beta\tau_n}\right] + L\cdot\mathbb{E}_r\left[\sum_{n:\xi_n<0} e^{-\beta\tau_n}\right]. \quad \text{(B.23)}$$

This leads to $(1 + \frac{\epsilon_2+\bar{\epsilon}}{K} + \frac{\epsilon_3+\bar{\epsilon}}{L})\cdot\mathcal{J}_r(\nu) + \frac{\epsilon_1+\bar{\epsilon}}{\beta} \geq \bar{v}(r) \geq v(r) - \bar{\epsilon}$. Re-arranging the terms we have

$$v(r) \leq (1 + \frac{\epsilon_2 + \bar{\epsilon}}{K} + \frac{\epsilon_3 + \bar{\epsilon}}{L})\cdot\mathcal{J}_r(\nu) + \frac{\epsilon_1 + \bar{\epsilon}}{\beta} + \bar{\epsilon}$$

Since this holds for any given $\bar{\epsilon} > 0$, taking the limit $\bar{\epsilon} \to 0+$ we have

$$v(r) \leq (1 + \frac{\epsilon_2}{K} + \frac{\epsilon_3}{L})\cdot\mathcal{J}_r(\nu) + \frac{\epsilon_1}{\beta}.$$

This is true for any admissible impulse control ν, and thus is true for the optimal one. □

Proof. **Corollary 3.1.** In the proof of Theorem 3.5, take $\epsilon_1 = \epsilon_2 = \epsilon_3 \equiv \epsilon$. From (B.23) we have

$$\mathcal{J}_r(\nu) \geq K \cdot \mathbb{E}_r \left[\sum_{n:\xi_n>0} e^{-\beta\tau_n} \right] + L \cdot \mathbb{E}_r \left[\sum_{n:\xi_n<0} e^{-\beta\tau_n} \right] \geq \bar{K} \cdot \mathbb{E}_r \left[\sum_{n} e^{-\beta\tau_n} \right], \tag{B.24}$$

in which $\bar{K} \equiv \min\{K, L\}$. Combining this with (B.22) yields

$$v(r) \leq (1 + \frac{\epsilon + \bar{\epsilon}}{\bar{K}}) \cdot \mathcal{J}_r(\nu) + \frac{\epsilon + \bar{\epsilon}}{\beta} + \bar{\epsilon}$$

Taking the limit $\bar{\epsilon} \to 0+$ leads to $v(r) \leq (1 + \frac{\epsilon}{\bar{K}}) \cdot \mathcal{J}_r(\nu) + \frac{\epsilon}{\beta}$. This holds for any admissible impulse control, and in particular, holds for the optimal one. Therefore

$$v(r) \leq (1 + \frac{\epsilon}{\bar{K}}) \cdot V(r) + \frac{\epsilon}{\beta}.$$

□

Proof. **Theorem 3.6 (Bond Price Theorem).** This proof closely follows the derivation in Vasicek (1977). We begin with the fact that the price of a bond is a function of time and the current short rate, and so we can use Itô's lemma to find the dynamics of the bond price. Given that $d < r_t < u$, the bond price dynamics are

$$dB_t = B_t \cdot \pi(t, T, r_t)dt - B_t \cdot s(t, T, r_t)dW_t^P, \tag{B.25}$$

$$\pi(t, T, r) = \frac{1}{B(t, T, r)} \left[\frac{\partial B}{\partial t} + \mu(r)\frac{\partial B}{\partial r} + \frac{1}{2}\sigma^2(r)\frac{\partial^2 B}{\partial r^2} \right], \tag{B.26}$$

$$s(t, T, r) = -\frac{1}{B(t, T, r)}\sigma(r)\frac{\partial B}{\partial r}. \tag{B.27}$$

Now consider a portfolio consisting, at time t, of a short amount θ_1 of a bond that expires at T_1 and a long amount θ_2 of a bond that expires at T_2. The total value of this portfolio is then $\Theta = \theta_2 - \theta_1$, and its dynamics are

$$d\Theta_t = (\theta_2 \pi(t, T_2, r_t) - \theta_1 \pi(t, T_1, r_t))dt - (\theta_2 s(t, T_2, r_t) - \theta_1 s(t, T_1, r_t))dW_t^P, \tag{B.28}$$

if $d < r_t < u$. Now pick the weights proportional to the variance of the two bonds, so that

$$\theta_1 = \Theta \frac{s(t, T_2, r)}{s(t, T_1, r) - s(t, T_2, r)}, \tag{B.29}$$

$$\theta_2 = \Theta \frac{s(t, T_1, r)}{s(t, T_1, r) - s(t, T_2, r)}. \tag{B.30}$$

After plugging these weights into Equation (B.28) we find that

$$d\Theta_t = \Theta \frac{\pi(t, T_2, r_t)s(t, T_1, r_t) - \pi(t, T_1, r_t)s(t, T_2, r_t)}{s(t, T_1, r_t) - s(t, T_2, r_t)} dt, \tag{B.31}$$

which does not include a Brownian motion term, and thus is riskless over the next instant. To prevent arbitrage we must have that Θ yields the same return as an investment in the short rate, by definition, and we have

$$\frac{\pi(t, T_2, r_t)s(t, T_1, r_t) - \pi(t, T_1, r_t)s(t, T_2, r_t)}{s(t, T_1, r_t) - s(t, T_2, r_t)} = r_t, \tag{B.32}$$

which can be rearranged to the equivalent

$$\frac{\pi(t, T_1, r_t) - r_t}{s(t, T_1, r_t)} = \frac{\pi(t, T_2, r_t) - r_t}{s(t, T_2, r_t)}, \tag{B.33}$$

if $d < r_t < u$. We derived Equation (B.33) for general expiration dates, and thus this quantity must be independent of the bond's tenor. We therefore

denote

$$q(t,r) = \frac{\pi(t,T,r) - r_t}{s(t,T,r)}, \tag{B.34}$$

and call this the market price of risk, since π and s represent the mean and volatility of instantaneous returns on a bond. We then plug the definitions of $\pi(t,T,r)$ and $s(t,T,r)$, from Equations (B.26) and (B.27), into Equation (B.34) and we recover Equation (3.23) for $d < r_t < u$. The only thing left are the boundary conditions, Equations (3.24) – (3.26).

To see that these boundary conditions hold we must consider a path of r_t that reaches d or u. This, of course, is impossible because r_t is right continuous with left limits, but we can consider a limiting case without any theoretical issues. We know that if the short rate were to reach either of these points it would immediately jump to D or U, respectively almost surely, due to the central bank's control. Given that a trader can know the entire price function, with respect to r_t, if the price at d and D were not equal there would be an opportunity for arbitrage. The same is true for u and U. Therefore these boundary conditions must hold at all times. □

Appendix C

Money Management with Performance Fees

C.1 Optimization Problem

We consider a minimum discounted cost infinite horizon problem in multiple dimensions. The controller has some preferences for the state vector, X_t, and continuous control, represented by $h(X_t, c_t) \geq 0$, as well as the discrete control, represented by $K(\xi) \geq 0$, with $K(0) = 0$. Putting this all together with a discount parameter, β, the controller wishes to minimize the value function, V, such that

$$V(x,t) = \min_{c,\xi} \mathbb{E}\left[\int_t^\infty e^{-\beta(s-t)} h(X_s, c_s) ds + \sum_{j:T_j>t} e^{-\beta(T_j-t)} K(\xi_j) \middle| X_t = x \right]. \tag{C.1}$$

Here, even though this is an infinite horizon problem, time is still important because the time until the next discrete control should affect the controller's decisions about the continuous control.

In order to solve this optimization problem we must rely on a dynamic programming Bellman operator. To find this operator we evaluate Equation (C.1) at $t = T_i-$ and rewrite it, taking advantage of the fact that $X_{T_i} =$

$X_{T_i-} + \xi_i$, as

$$\begin{aligned} V(x, T_i-) &= \min_{c,\xi} \mathbb{E}\Bigg[\int_{T_i}^{T_{i+1}} e^{-\beta(s-T_i)} h(X_s, c_s) ds + K(\xi_i) \\ &\quad + e^{-\beta(T_{i+1}-T_i)} \Bigg(\int_{T_{i+1}}^{\infty} e^{-\beta(s-T_{i+1})} h(X_s, c_s) ds \\ &\quad + \sum_{j=i+1}^{\infty} e^{-\beta(T_j - T_{i+1})} K(\xi_j) \Bigg) \Bigg| X_{T_i-} = x \Bigg], \end{aligned} \tag{C.2}$$

Assuming continuity of the value function at T_i (with probability 1) we find that

$$V(x, T_i-) = \min_{\xi_i} \{ V(x + \xi_i, T_i) + K(\xi_i) \}. \tag{C.3}$$

We note however that the second line of Equation (C.2) is, in fact, the discounted value function evaluated at $t = T_{i+1}-$ so that

$$\begin{aligned} V(x, T_i-) &= \min_{\xi_i} \Bigg\{ \min_{c} \mathbb{E}\Bigg[\int_{T_i}^{T_{i+1}} e^{-\beta(s-T_i)} h(X_s, c_s) ds \\ &\quad + e^{-\beta(T_{i+1}-T_i)} V(X_{T_{i+1}-}, T_{i+1}-) \Bigg| X_{T_i-} = x \Bigg] + K(\xi_i) \Bigg\} \end{aligned} \tag{C.4}$$

For our purposes we will define an operator, $\mathcal{A}$, that takes a function over $\mathbb{R}^n$ and returns another function over $\mathbb{R}^n$ such that

$$\begin{aligned} \mathcal{A}f(x) &= \min_{c} \mathbb{E}\Bigg[\int_{T_i}^{T_{i+1}} e^{-\beta(s-T_i)} h(X_s, c_s) ds \\ &\quad + e^{-\beta(T_{i+1}-T_i)} f(X_{T_{i+1}-}) \Bigg| X_{T_i} = x \Bigg] \end{aligned} \tag{C.5}$$

In general, $\mathcal{A}f$ takes the form of the solution to a terminal value partial integro-differential equation problem, or PIDE. We assume this equation can be solved and that for the specific forms of X_t and h verification can also be proved.

We can therefore combine Equations (C.4) and (C.5) to find, excusing the abuse of notation[1], that

$$V(x, T_i-) = \min_{\xi_i}\{\mathcal{A}V(x + \xi_i, T_{i+1}-) + K(\xi_i)\} \tag{C.6}$$

However, since T_i and T_{i+1} are both opportunities to use the discrete control we must have that

$$V(x, T_i-) = \min_{\xi_i}\{\mathcal{A}V(x + \xi_i, T_i-) + K(\xi_i)\} \tag{C.7}$$

where the difference between Equations (C.6) and (C.7) is that in (C.7) we have V at T_i- on both sides of the equal sign. With this we can also find that

$$V(x, T_i) = \mathcal{A}V(x, T_i-). \tag{C.8}$$

If, however, we have that the optimal $\xi_i = 0$ then we also have that $V(x, T_i) = V(x, T_i-)$.

Equation (C.7) will help us find an algorithm to find V at the T_i's, however we use Equation (C.6) to show that any function that satisfies this relationship, for all i, must be the solution to the original optimization problem in Equation (C.2).

Theorem C.1. Any function that satisfies Equation (C.6) for all i is the optimal solution to Equation (C.2).

[1]The abuse of notation is that $\mathcal{A}f(x)$ should actually be written as $(\mathcal{A}f(\cdot))(x)$ so that $\mathcal{A}V(x,t)$ should be interpreted as $(\mathcal{A}V(\cdot,t))(x)$.

Proof. Suppose we have a function $v(x,t)$ that satisfies Equation (C.6) for all i then

$$\begin{aligned} v(x,T_i-) &= \min_{\xi_i}\left\{\min_{c}\mathbb{E}\Big[\int_{T_i}^{T_{i+1}} e^{-\beta(s-T_i)}h(X_s,c_s)ds \right. \\ &\quad \left. +e^{-\beta(T_{i+1}-T_i)}v(X_{T_{i+1}-},T_{i+1}-)\Big|X_{T_i-}=x\Big]+K(\xi_i)\right\}. \end{aligned} \tag{C.9}$$

However since v also satisfies this equation at time $T_{i+1}-$ we can substitute Equation (C.9) into itself on the right hand side of the equal sign and use the law of iterated expectations to find that

$$\begin{aligned} v(x,T_i-) &= \min_{\xi_i,\xi_{i+1}}\left\{\min_{c}\mathbb{E}\Big[\int_{T_i}^{T_{i+2}} e^{-\beta(s-T_i)}h(X_s,c_s)ds \right. \\ &\quad +e^{-\beta(T_{i+2}-T_i)}v(X_{T_{i+2}-},T_{i+2}-) \\ &\quad \left. +e^{-\beta(T_{i+1}-T_i)}K(\xi_{i+1})\Big|X_{T_i-}=x\Big]+K(\xi_i)\right\}. \end{aligned} \tag{C.10}$$

Upon iteration we find that

$$\begin{aligned} v(x,T_i-) &= \min_{c,\xi_{i,\ldots,i+m}}\mathbb{E}\Big[\int_{T_i}^{T_{i+m}} e^{-\beta(s-T_i)}h(X_s,c_s)ds \\ &\quad +\sum_{j=0}^{m} e^{-\beta(T_{i+j}-T_i)}K(\xi_{i+j}) \\ &\quad +e^{-\beta(T_{i+m}-T_i)}v(X_{T_{i+m}-},T_{i+m}-)\Big|X_{T_i-}=x\Big] \end{aligned} \tag{C.11}$$

Taking the limit as $m\to\infty$, under relatively mild growth conditions on v, we find that the last term inside the expectation in Equation (C.11) vanishes and, indeed, this is equal to the original optimization problem in Equation (C.2). Therefore any function that satisfies Equation (C.6) for all i must be the solution to Equation (C.2). □

C.2 Algorithm

We now present an iterative algorithm to find the optimal value function at times $\{T_i\}$ and show that this algorithm converges to the true solution. After that we present a result on the convergence rate.

Let us first define $\hat{v}_0(x, \Theta)$ as the solution to the infinite horizon problem with only continuous control, that is, without the opportunity to issue discrete control. In this way

$$\hat{v}_0(x) = \min_c \mathbb{E}\left[\int_0^\infty e^{-\beta s} h(X_s, c_s) ds \middle| X_0 = x\right]. \tag{C.12}$$

This is a time homogeneous problem and can typically be solved using a partial integro-differential equation, such as an HJB equation.

We now define our iterative steps as

$$v_j(x) = \min_\xi \left\{\hat{v}_j(x+\xi) + K(\xi)\right\}, \tag{C.13}$$

$$\hat{v}_{j+1}(x) = \mathcal{A} v_j(x). \tag{C.14}$$

We would like to show that in the limit we have that

$$\lim_{j\to\infty} v_j(x) = V(x, T_i-). \tag{C.15}$$

In order to prove this we must first show that Equation (C.15) converges, pointwise, to some function, then we must show that the converged value satisfies Equation (C.7) and is therefore the optimal solution.

Theorem C.2. Equation (C.15) converges pointwise.

Proof. To do this first we have to show that v_j is non-increasing in j for every x. Let us consider $v_0(x)$; suppose at time 0- the state is at x, $\hat{v}_0(x)$ corresponds to the minimum expected cost if we can never change X_t discretely in the future. Therefore, by the definition of Equation (C.13), $v_0(x)$ corresponds to the optimal value function if the controller is given one opportunity to change X and so $v_0(x) \leq \hat{v}_0(x)\ \forall x$.

This also means that $v_1(x)$ corresponds to the minimal value function if the controller is given the opportunity to change X at time 0, plus one additional time in the future, T_1. Therefore $v_1(x) \leq v_0(x)\ \forall x$, because the controller has the option to not control at T_1 which would exactly correspond to v_0, since it is free to not control, $K(0) = 0$. However with this additional opportunity to control, at T_1, the controller can do no worse than without this opportunity. Iterating Equations (C.13)-(C.14) and applying the definition of $\mathcal{A}$ we can see that $v_j(x)$ corresponds to the situation where the controller is given the opportunity to control at times $0, T_1, T_2, ..., T_j$. This means that for every j we have $v_j(x) \leq v_{j-1}(x)$ because the controller is given one more opportunity to control, at T_j, and he can do no worse than if he is given one less opportunity to control. This shows that $v_j(x)$ is decreasing in j. Furthermore, $v_j(x) \geq 0\ \forall(j, x)$ since we assumed that h and K are non-negative. Putting this together, for every x we have a non-increasing sequence that is bounded below; therefore this sequence must converge by the monotone convergence

theorem. Stating this mathematically we can write

$$v_{j-1}(x) = \min_{c,\xi_{0,\ldots,j-1}} \mathbb{E}\Bigg[\int_0^{T_{j+1}} e^{-\beta s} h(X_s, c_s) ds + e^{-\beta T_{j+1}} \hat{v}_0(X_{T_{j+1}}) + \sum_{k=0}^{j-1} e^{-\beta T_k} K(\xi_k) \Big| X_{0-} = x \Bigg], \quad \text{(C.16)}$$

$$v_j(x) = \min_{c,\xi_{0,\ldots,j}} \mathbb{E}\Bigg[\int_0^{T_{j+1}} e^{-\beta s} h(X_s, c_s) ds + e^{-\beta T_{j+1}} \hat{v}_0(X_{T_{j+1}}) + \sum_{k=0}^{j} e^{-\beta T_k} K(\xi_k) \Big| X_{0-} = x \Bigg], . \quad \text{(C.17)}$$

Here the only difference between Equations (C.16) and (C.17) is that Equation (C.17) has one more optimization variable than (C.16), and therefore $v_j(x, \Theta) \leq v_{j-1}(x, \Theta)$. □

Since we have proved that the v_j converge we now need to show that Equation (C.7) is satisfied.

Theorem C.3. Suppose that $v^*(x) = \lim_{j\to\infty} v_j(x)$, then $v^*(x)$ corresponds to the optimal value function $V(x, T_i-)$.

Proof. Since $v^*(x, \Theta)$ is the converged function from Equations (C.13)-(C.14), by the definition of the iterative steps we have that

$$v^*(x) = \min_{\xi} \left\{ \mathcal{A} v^*(x + \xi) + K(\xi) \right\}.$$

This is exactly Equation (C.7) and in Section C.1 we proved that any function that satisfies this relationship must be the optimal value function at the T_i's, therefore we have $v^*(x) = V(x, T_i-)$. □

Bibliography

AitSahlia, F., Carr, P., 1997. American options: A comparison of numerical methods. In: Rogers, L., Talay, D. (Eds.), Numerical Methods in Finance. Cambridge University Press.

Balduzzi, P., Bertola, G., Foresi, S., 1997. A model of target changes and the term structure of interest rates. Journal of Monetary Economics 39, 223–249.

Basak, S., Pavlova, A., Shapiro, A., 2007. Optimal asset allocation and risk shifting in money management. Review of Financial Studies 20 (5), 1583–1621.

Bensoussan, A., Lions, J. L., 1973. Nouvelle formulation de problèmes de contrôle impulsionnel et applications. C.R. Acad. Sci. Paris 276, 1189–1192.

Black, F., Karasinski, P., 1991. Bond and option pricing when short rates are lognormal. Financial Analysts Journal 47, 52–59.

Black, F., Scholes, M., 1973. The pricing of options and corporate liabilities. J. Political Economy 81, 637–654.

Brennan, M., Schwartz, E., 1977. The valuation of American put options. J. Finance 32, 449–642.

Broadie, M., Detemple, J., 1996. American option valuation: New bounds, approximations, and a comparison of existing methods. The Review of Financial Studies 9 (4), 1211–1250.

Broadie, M., Detemple, J., 1997. Recent advances in numerical methods for pricing derivative securities. In: Rogers, L., Talay, D. (Eds.), Numerical Methods in Finance. Cambridge University Press.

Broadie, M., Detemple, J., Ghysels, E., Torres, O., 2000. American options with stochastic dividends and volatility: A nonparametric investigation. Journal of Econometrics 94, 53–92.

Broadie, M., Glasserman, P., 1997. Pricing American-style securities by simulation. J. Economic Dynamics and Control 21, 1323–1352.

Bunch, D., Johnson, H., 2002. The american put option and its critical stock price. J. Finance 55 (3), 219–237.

Cadenillas, A., Lakner, P., Pinedo, M., 2010. Optimal control of a mean-reverting inventory. Operations Research 58 (6), 1697–1710.

Cadenillas, A., Zapatero, F., 1999. Optimal central bank intervention in the foreign exchange market. Journal of Economic Theory 87 (1), 218–242.

Cadenillas, A., Zapatero, F., 2000. Classical and impulse stochastic control of the exchange rate using interest rates and reserves. Mathematical Finance 10, 141–147.

Carpenter, J., 2000. Does option compensation increase managerial risk appetite? The Journal of Finance 55 (5), 2311–2331.

Carr, P., Jarrow, R., Myneni, R., 1992. Alternative characterizations of American put options. Mathematical Finance 2, 87–106.

Chan, K., Karolyi, G., Longstaff, F., Sanders, A., 1992. An empirical comparison of alternative models of the short term interest rate. The Journal of Finance 47, 1209–1227.

Chapman, D., Pearson, N., 2000. Is the short rate drift actually nonlinear? The Journal of Finance 55, 355–388.

Chen, S., Merriman, B., Osher, S., Smereka, P., 1997. A simple level set method for solving stefan problems. J. Computational Physics 135.

Chen, X., Chadam, J., 2007. A mathematical analysis of the optimal exercise boundary for American put options. SIAM J. Math. Anal. 38 (5), 1613–1641.

Chevalier, J., Ellison, G., 1997. Risk taking by mutual funds as a response to incentives. Journal of Political Economy 105 (6), 1167–1200.

Chockalingam, A., Muthuraman, K., 2011. American options under stochastic volatility. Operations Research 59, 793–809.

Clarke, N., Parrott, K., 1999. Multigrid for American option pricing with stochastic volatility. Applied Mathematical Finance 6, 177–195.

Constantinides, G. M., Richard, S. F., 1978. Existence of optimal simple policies for discounted-cost inventory and cash management in continuous time. Operations Research 26 (4), 620–636.

Courant, R., Friedrichs, K., Lewy, H., 1967. On the partial difference equations of mathematical physics. IBM Journal of Research and Development 11 (2), 215–234.

Cox, J., Ingersoll, J., Ross, S., 1996. A theory of the term structure of interest rates. Econometrica 53, 385–407.

Cox, J., Ross, S., Rubinstein, M., 1979. Option pricing: A simplified approach. J. Financial Economics 7, 229–263.

Crank, J., Nicolson, P., 1947. A practical method for numerical evaluation of solutions of partial differential equations of the heat-conduction type. Proc. Camp. Phil. Soc. 43, 50–67.

Dai, J., Yao, D., 2012a. Brownian inventory models with convex holding cost: Part 1 average-optimal controls. In Revision for Stochastic Systems.

Dai, J., Yao, D., 2012b. Brownian inventory models with convex holding cost: Part 2 discount-optimal controls. In Revision for Stochastic Systems.

Detemple, J., Tian, W., 2002. The valuation of American options for a class of diffusion processes. Management Science 48 (7), 917–937.

Emanuel, D., MacBeth, J., 1982. Further results of the constant elasticity of variance call option pricing model. Journal of Financial and Quantitative Analysis 4, 533–553.

Evans, J., Kuske, R., Keller, J., 2002. American options on assets with dividends near expiry. Mathematical Finance 12 (3), 219–237.

Feng, H., Muthuraman, K., 2010. A computational method for stochastic impulse control problems. Mathematics of Operations Research 35 (4), 830–850.

Fouque, J., Papanicolaou, G., Sircar, K., 2000. Derivatives in Financial Markets with Stochastic Volatility. Cambridge University Press, Cambridge.

Freund, W., Guttentag, J., 1969. Defensive and dynamic open market operations, discounting, and the Federal Reserve system's crisis-prevention responsibilities. The Journal of Finance 24 (2), 249–263.

Gatheral, J., 2006. The Volatility Surface: A Practitioner's Guide. Wiley, Hoboken.

Goetzmann, W., Ingersoll, J., Ross, S., 2003. High-water marks and hedge fund management contracts. The Journal of Finance 58 (4), 1685–1717.

Goodman, J., Ostrov, D., 2002. On the early exercise boundary of the American put option. SIAM J. Applied Mathematics 62, 1823–1835.

Grinblatt, M., Titman, S., 1989. Adverse risk incentives and the design of performance-based contracts. Management Science 35 (7), 807–822.

Harrison, J. M., Sellke, T., Taylor, A., 1983. Impulse control of brownian motion. Mathematics of Operations Research 8 (3), 454–466.

Hayes, E., 2006. PhD thesis. Courant Institute of Mathematical Sciences, New York University.

Heston, S., 1993. A closed-form solution for options with stochastic volatility with applications to bond and currency options. Rev. Financial Studies 6, 327–343.

Huang, J., Subrahmanyam, M., Yu, G., 1996. Pricing and hedging American options: A recursive integration method. Rev. Financial Studies 9, 277–300.

Hull, J., White, A., 1987. The pricing of options on assets with stochastic volatilities. J. Finance 42, 281–300.

Ikonen, S., Toivanen, J., 2007. Componentwise splitting methods for pricing American options under stochastic volatility. International Journal of Theoretical and Applied Finance 10, 331–361.

Ikonen, S., Toivanen, J., 2008. Efficient numerical methods for pricing American options under stochastic volatility. Numerical Methods for Partial Differential Equations 24, 104–126.

Iserles, A., 2008. A First Course in the Numerical Analysis of Differential Equations. Cambridge Univ. Press, Cambridge.

Jacka, S., 1991. Optimal stopping and the American put. Mathematical Finance 1, 1–14.

Karatzas, I., Shreve, S., 1998. Methods of Mathematical Finance. Springer, New York.

Kim, I., 1990. The analytic valuation of American options. Rev. Financial Studies 3, 547–772.

Korn, R., 1997. Optimal impulse control when control actions have random consequences. Mathematics of Operations Research 22 (3), 639–667.

Kushner, H., 1976. Approximations and computational methods for optimal stopping and stochastic impulsive control problems. Applied Mathematics and Optimization 3 (2/3), 81–99.

Lawrence, P., Salsa, S., 2009. Regularity of the free boundary of an american option on several assets. Comm. Pure Appl. Math. 62, 969–994.

Lohmann, S., 1992. Optimal commitment in monetary policy: Credibility versus flexibility. The American Economic Review 82 (1), 273–286.

Longstaff, F., Schwartz, E., 2001. Valuing American options by simulation: Simple least-squares approach. Rev. Financial Studies 14, 113–147.

McKinsey, Company, ., 2011. Mapping global capital markets 2011.

Merton, R., 1992. Continuous-Time Finance. Blackwell, Oxford.

Merton, R. C., 1969. Lifetime portfolio selection under uncertainty: The continuous time case. The Review of Economics and Statistics 51, 247–257.

Mitchell, D., Feng, H., Muthuraman, K., 2014a. Impulse control of interest rates. Operations Research, Forthcoming.

Mitchell, D., Goodman, J., Muthuraman, K., 2014b. Boundary evolution equations for American options. Mathematical Finance, Forthcoming.

Muthuraman, K., 2008. A moving boundary approach to American option pricing. J. Economic Dynamics and Control 32, 3520–3537.

Myneni, R., 1992. The pricing of the American option. Annals of Applied Probability 2 (1), 1–23.

Nielsen, B., Skavhaug, O., Tveito, A., 2002. Penalty and front-fixing methods for the numerical solution of American option problems. J. Computational Finance 5, 69–97.

Panageas, S., Westerfield, M., 2009. High-water marks: High risk appetites? convex compensation, long horizons, and portfolio choice. The Journal of Finance 64 (1), 1–36.

Peskir, G., Shiryaev, A., 2006. Optimal Stopping and Free-Boundary Problems. Birkhäuser Verlag, Basel.

Piazzesi, M., 2005. Bond yields and the federal reserve. Journal of Political Economy 113, 311–344.

Protter, P., 2005. Stochastic Integration and Differential Equations. 2nd Ed., Version 2.1. Springer.

Ross, S., 1973. The economic theory of agency: The principal's problem. The American Economic Review 63 (2), 134–139.

Ross, S., 2004. Compensation, incentives, and the duality of risk aversion and riskiness. The Journal of Finance 59 (1), 207–225.

Rudebusch, G., 1995. Federal reserve interest rate targeting, rational expectations, and the term structure. Journal of Monetary Economics 35, 245–274.

Scott, L., 1987. Option pricing when the variance changes randomly: Theory, estimation, and an application. J. Financial and Quantitative Analysis 22, 419–438.

Shreve, S., 2004. Stochastic Calculus for Finance II. Springer.

Stamicar, R., Sevcovic, D., Chadam, J., 1999. The early exercise boundary for the American put near expiry: Numerical approximations. Canad. Appl. Math. Quart. 7 (4), 427–444.

Stein, E., Stein, J., 1991. Stock price distributions with stochastic volatility: An analytic approach. Review of Financial Studies 4, 727–752.

Sulem, A., 1986. A solvable one-dimensional model of a diffusion inventory system. Mathematics of Operations Research 11 (1), 125–133.

Thompson, J., Warsi, Z., Mastin, C., 1985. Numerical Grid Generation: Foundations and Applications. Elsevier Science, New York.

Tilley, J., 1993. Valuing American options in a path simulation model. Transactions of the Society of Actuaries 45, 83–104.

van Moerbeke, P., 1975. On optimal stopping and free boundary problems. Arch. Rat. Mech. Anal. 60 (2), 101–148.

Vasicek, O., 1977. An equilibrium characterization of the term structure. Journal of Financial Economics 5, 177–188.

Wilmott, P., 1998. Derivatives. Wiley, Chichester.

Wu, L., Kwok, Y., 1997. A front-fixing finite difference method for the valuation of American options. J. Financial Engineering 6, 83–97.

Yong, J., Zhou, X., 1999. Stochastic Controls, Hamiltonian Systems and HJB Equations. Springer.